# AN IMPROVED ELECTROMAGNETISM-LIKE MECHANISM ALGORITHM FOR THE OPTIMIZATION OF MAXIMUM POWER POINT TRACKING

**TAN JIAN DING**

**THESIS SUBMITTED IN FULFILMENT OF THE REQUIREMENTS FOR THE DEGREE OF DOCTOR OF PHILOSOPHY**

**FACULTY OF ENGINEERING**
**UNIVERSITY OF MALAYA**
**KUALA LUMPUR**

**2017**

**UNIVERSITY OF MALAYA**
**ORIGINAL LITERARY WORK DECLARATION**

Name of Candidate: **TAN JIAN DING**

Matric No: **KHA 110009**

Name of Degree: **DOCTOR OF PHILOSOPHY**

Title of Project Paper/Research Report/Dissertation/Thesis ("this Work"):

**"AN IMPROVED ELECTROMAGNETISM-LIKE MECHANISM ALGORITHM FOR THE OPTIMIZATION OF MAXIMUM POWER POINT TRACKING"**

Field of Study: **AUTOMATION, CONTROL, AND ROBOTIC**

I do solemnly and sincerely declare that:

(1) I am the sole author/writer of this Work;
(2) This Work is original;
(3) Any use of any work in which copyright exists was done by way of fair dealing and for permitted purposes and any excerpt or extract from, or reference to or reproduction of any copyright work has been disclosed expressly and sufficiently and the title of the Work and its authorship have been acknowledged in this Work;
(4) I do not have any actual knowledge nor do I ought reasonably to know that the making of this work constitutes an infringement of any copyright work;
(5) I hereby assign all and every rights in the copyright to this Work to the University of Malaya ("UM"), who henceforth shall be owner of the copyright in this Work and that any reproduction or use in any form or by any means whatsoever is prohibited without the written consent of UM having been first had and obtained;
(6) I am fully aware that if in the course of making this Work I have infringed any copyright whether intentionally or otherwise, I may be subject to legal action or any other action as may be determined by UM.

Candidate's Signature Date:

Subscribed and solemnly declared before,

Witness's Signature Date:

Name:

Designation:

## ABSTRACT

The Electromagnetism-Like Mechanism algorithm (EM) is a meta-heuristic algorithm designed to search for global optimum solutions using bounded variables. The search mechanism of EM mimics the attraction and repulsion behaviours in the electromagnetism theory. Despite its notable performance in solving various types of optimization problems so far, literature study shows that in general, EM is good at solutions exploration but shows insufficiency in its solutions exploitation ability. Based on this motivation, this study aimed to improve the EM by enhancing this algorithm with stronger exploitation mechanisms. This research can generally be divided into several phases. The first phase of the research was on the investigation of the relationship between the search step size and the convergence performance. The conventional EM was tested to search under two different extremes of step sizes separately, marked as EM with Large Search Steps (EMLSS) and EM with Small Search Step (EMSSS) respectively. Experiments on ten test functions showed that the EMSSS performed much detailed searches in all dimensions and yielded outcome with higher accuracies. The trade-off, however, was that the convergence processes were comparatively slower than the EMLSS. The second phase of the research focused on enhancing the EM. Two major breakthroughs were achieved. The first successful modification was recorded by introducing a Split, Probe and Compare (SPC) feature into the EM (SPC-EM). The SPC-EM applied a dynamic strategy to regulate the search steps during the local search. The search scheme began with relatively bigger steps. The algorithm then systematically tuned the step sizes based on a specially designed nonlinear equation. This ensured accuracies of the final solutions returned, in the meanwhile not slowing down the whole convergence process by probing around too finely at the beginning of the search. The modified algorithm was tested out in the established test suite. The results indicated that SPC-EM outperformed the conventional EM and other algorithms in the benchmarking.

The second successful approach involved a more sophisticated modification, named as the Experiential Learning EM (ELEM). As the name suggests, the ELEM is enhanced with the ability to learn from previous search experience, from which a better projection can be generated for the coming iterations. The ELEM adapts a guided displacement mechanism with gradient information analysis and backtracking memory. A trail memory is generated as iterations go on, allowing the algorithm to backtrack previous search results and improvement rates. The experimental results showed that ELEM achieved solutions with relatively higher accuracies and precisions. The convergence performance of the ELEM showed significant superiority compared to that of a conventional EM and other algorithms in the benchmarking, including SPC-EM. In the final phase, the ELEM was implemented in the simulation to track the maximum power point (MPP) of a PV solar energy harvesting system with three serially connected PV panels. Simulations showed that the ELEM was successful in tracking the MPPs under uniform irradiance, non-uniform irradiance, and rapid changing shading conditions. With all the result indications in this research, it can be concluded that the enhanced EM proposed in this study showed improvements in solving numerical and engineering optimization problems.

## ABSTRAK

Algoritma Mimikan-Elektromagnetisme (ME) adalah sejenis algoritma carian meta-heuristik yang dicipta untuk mendapatkan nilai jawapan pengoptimuman global dengan menggunakan pembolehubah- pembolehubah tersempadan. Tatacara carian ME dihasilkan dengan memimik cara tarikan dan tolakan antara zarah-zarah dalam teori elektromagnetisme. Kajian kesusasteraan menunjukan bahawa ME mencatatkan prestasi yang memberangsangkan dalam menyelesaikan pelbagai jenis masalah pengoptimuman. Secara umumnya, ME menunjukkan kebolehan tinggi dalam proses penerokaan. Namun, keupayaannya dalam carian terperinci pula adalah sangat tidak memadai. Penyelidikan ini diadakan dengan motivasi untuk meningkatkan lagi prestasi keseluruhan ME dengan memantapkan lagi keupayaan carian terperincinya. Secara keseluruhannya, objektif dan pencapaian penyelidikan ini dapat dibahagikan kepada beberapa fasa. Dalam fasa yang pertama, siasatan telah dijalankan untuk mengenalpasti kaitan antara prestasi carian dengan sais langkah yang digunakan. Algoritma asli ME telah diuji secara berasingan dengan menggunakan dua sais langkah yang amat berbeza. ME bersais Langkah Besar ditandakan sebagai MELB manakala ME bersais Langkah Kecil pula ditandakan sebagai MELK. Kedua-dua algorithma ini diuji dengan menggunakan 10 masalah ujian yang kerap digunakan oleh penyelidik-penyelidik lain dalam kajian kesasteraan. Hasil eksperimen menunjukkan bahawa MELK berjaya mencapai jawapan yang lebih tepat. Sais langkah MELK yang kecil membolehkannya untuk melakukan carian yang lebih terperinci dalam semua dimensi. Namun, ini telah melambatkan proses cariannya berbanding MELB. Fasa kedua penyelidikan ini memberi fokus kepada kerja pemantapan ME. Dua kejayaan dicatatkan dalam usaha menambahkaikkan ME. Kejayaan pertama dicapai dengan menyerapkan tatacara yang dikenali sebagai Belah, Siasat, dan Banding (BSB) ke dalam ME (BSB-ME). BSB-ME menggunakan stratergi dinamik untuk menyelaraskan sais langkah dalam seksyen carian terperincinya, bermula dengan sais

langkah besar, dan kemudiannya dilaraskan dengan sistematik berdasarkan suatu persamaan tidak-berkadar-terus yang telah dibina khas untuk tujuan ini. Cara ini dapat memastikan jawapan yang lebih tepat boleh dijumpai tanpa perlu melengahkan masa dengan membuat carian yang terlalu terperinci pada awal proses. Algorithma yang diubahsuai ini telah diuji dengan menggunakan set ujian yang dibina sebelum ini. Perbandingan hasil eksperimen menunjukkan bahawa prestasi BSB-ME adalah lebih mantap berbanding dengan algoritma-algoritma lain yang terlibat sama dalam perbandingan tersebut. Kejayaan kedua dalam usaha penambahbaikan algorithma ME tercapai dengan cara memasukkan suatu tatacara yang lebih komplex. Tatacara ini diberi nama ME Berpandukan Pengalaman (MEBP). MEBP ini berkebolehan untuk mempelajari pengalaman daripada iterasi-iterasi carian sebelum. Berpandukan pengalaman yang dipelajari, tatacara ini dapat memberikan anggaran parameter yang lebih baik untuk iterasi carian yang akan datang. MEBP menggerakkan zarah-zarah berpandukan analisa informasi kecerunan dan memori jejakan kembali. Setiap carian meninggalkan kesan yang membolehkan algorithma tersebut untuk merujuk kembali kepada jawapan sebelum dan kadar kemajuan yang tercatat. Keputusan eksperimen menunjukkan bahawa MEBP berjaya mencapai jawapan yang lebih tepat berbanding ME asli dan algoritma-algoritma yang lain, termasuklah BSB-ME. Dalam fasa terakhir penyelidikan, MEBP diuji dalam simulasi untuk mengoptimasikan kuasa yang dihasilkan oleh sebuah sistem tenaga solar Photovoltaic. Keputusan eksperimen menunjukkan bahawa MEBP berjaya menjejaki titik-titik kuasa maksima sistem tersebut dalam keadaan sinaran cahaya seragam, sinaran cahaya tidak seragam, dan juga dalam keadaan berbayang yang berubah-ubah bentuk. Berdasarkan keputusan-keputusan yang ditunjukkan dalam kesemua eksperimen ini, dapat disimpulkan bahawa tatacara penambahbaikan ME yang dicadangkan dalam kajian ini menunjukkan kemajuan dari segi prestasi dalam menangani masalah optimasi berangka dan kejuruteraan.

## ACKNOWLEDGEMENT

I would like to express the deepest appreciation to my supervisor, Associate Professor Dr. Mahidzal Dahari, whose door is always open for me. Without his endless encouragement, help, and guidance from the get go, this study would not have materialized. Words will never be enough to express my gratitude to him for his encouragement, motivation and advice. He has been a wonderful mentor for me.

My intellectual debt in the field of artificial intelligence and optimization techniques is to Associate Professor Ir. Dr. Johnny Koh from UNITEN. I have greatly benefited from the illuminating discussions with him on many of the technical issues and solutions. My deepest heartfelt appreciation goes to him for all the facilities support and all the insightful comments and suggestions throughout the study.

I owe my warmest appreciation to Ms Koay Ying Ying for all her selfless help and support throughout my research process. She has been extraordinarily tolerant and supportive. Her warm encouragement and meticulous help were invaluable. I would also like to express my gratitude to the MyBrain15 Unit under the Scholarship Division of Malaysian Ministry of Education for their financial support throughout my PhD study.

To my life coach, my father: you made this possible. My forever interested, encouraging and always enthusiastic mother. Thank you for always believing in me. I owe it all to you. Many thanks for all the support and prayers. I am grateful to my siblings who have provided me through moral support in my life. I am also grateful to my friends who have accompanied and supported me along the way.

Thanks for all your encouragement!

## TABLE OF CONTENTS

## LIST OF TABLES

## LIST OF FIGURES

## LIST OF SYMBOLS AND ABBREVIATIONS

| | |
|---|---|
| ACO | : Ant Colony Optimization |
| AI | : Artificial Intelligence |
| AIS | : Artificial Immune System |
| ANN | : Artificial Neural Network |
| BB | : Branch-and-Bound Algorithm |
| COP | : Combinatorial Optimization Problem |
| DE | : Differential Evolution |
| ELEM | : Experiential-Learning Electromagnetism-like Mechanism Algorithm |
| EM | : Electromagnetism-like Mechanism Algorithm |
| EMLSS | : Electromagnetism-like Mechanism Algorithm with Larger Search Step |
| EMSSS | : Electromagnetism-like Mechanism Algorithm with Smaller Search Step |
| EPP | : Estimated Perturb–Perturb |
| FAD | : Feasible and Dominance |
| FL | : Fuzzy Logic |
| FLC | : Fuzzy Logic Controller |
| GA | : Genetic Algorithm |

GS : Guided Search

HC : Hill Climbing

IC : Incremental Conductance

I-V : Current-Voltage

$l_k$ : Lower Bound

*LSIte* : Local Search Iteration Number

MPP : Maximum Power Point

MPPT : Maximum Power Point Tracking

NTVE : Nonlinear Time-Varying Evolution

*OSIte* : Overall Search Iteration Number

P&O : Perturb and Observe

PBSA : Population Based Search Algorithm

PSC : Partial Shading Condition

PSO : Particle Swarm Optimization

PV : Photovoltaic

P-V : Power-Voltage

PVGC : Photovoltaic Grid-Connected Systems

$q^i$ : Particle Charge

SA : Simulated Annealing

SAPV : Stand Alone Photovoltaic System

SC : Soft Computing

| | |
|---|---|
| SOC | : State of Charge |
| SPC | : Split, Probe, and Compare |
| SPC-EM | : Electromagnetism-like Mechanism Algorithm with Split, Probe, and Compare |
| TS | : Tabu Search |
| UG | : Utility Grid |
| $u_k$ | : Upper Bound |
| WES | : Wind Energy System |
| $\alpha$ | : Gain Factor |
| $\beta$ | : Penalty Factor |

## LIST OF APPENDICES

# CHAPTER 1: INTRODUCTION

Ever since the creation of Genetic Algorithm (GA) in the early 1960's (Mitchell, 1999), the development of optimization algorithms have been evolving towards mechanisms with better exploration of global optima points. The general idea of a global optimization is to search for the ultimate best set of parameters within a feasible range to achieve an objective under a certain set of constraints without being trapped in local optimums. Throughout the years, the study of global optimization has proven to be imperative in many spectrums of practical science and engineering applications (Floudas & Gounaris, 2009). It is essential to achieve the global optima in many of these applications, as opposed to a local solution. Researchers around the globe have been coming up with numerous meta-heuristic search techniques to solve complex optimization problems and ways to improve them. Many of these techniques are population-based, such as genetic algorithm (GA), swarm optimization (Bratton & Kennedy, 2007), ant colony optimization (Neto & Filho, 2013), differential evolution (DE) (Storn & Price, 1997), and simulated annealing algorithm (Shojaee et. al., 2010) just to name a few.

The electromagnetism-like mechanism algorithm (EM) is a meta-heuristic search technique first introduced by Birbil and Fang (2003). Inspired by the attraction and repulsion mechanism of electromagnetic charges, this algorithm is designed to solve unconstrained nonlinear optimization problems in a continuous domain. EM has been widely employed as an optimization tool in various fields due to its capability to yield well-diversified results and solve complicated optimization problems. Examples include

multi-objective inventory optimization (Tsou & Kao, 2007), machine tools path planning problems (Kuo et. al., 2015), flowshop scheduling problems (Naderi, 2010), robot manipulator problems (Yin et. al., 2011), and many more. Similar to many other global optimization algorithms, the search mechanism of EM can generally be segmented into its exploration and exploitation partitions. The exploration segment of EM pushes the particles to search for a better variety of possible solutions globally by moving the particles in accordance with the superposition theorem. The exploitation segment, on the other hand, involves a random line search procedure which gather the information around the neighbourhood of a particular solution.

The implementation of optimization algorithms and AI techniques has gained significant popularity among researchers in the field of renewable energy worldwide over the past few decades. Among the renewable energy sources, solar energy proves to be one of the best options due to the sustainability of the mechanisms and minimal environmental damage (Gholamalizadeh & Kim, 2014). The literature study indicates that the photovoltaic (PV) systems contributed approximately 14,000 MW of power generation in 2010. This number is predicted to grow to 70,000 MW by the year 2020 (Seyedmahmoudian et. al., 2016). With the rapid hike in the demand of this clean energy, researchers around the world are now gathering their attention into ways to boost the energy conversion efficiency of the harvesting system. Research shows that the performance of a PV system can be affected by many factors, such as the efficiency of the materials used, integration setup and many more. However, it is found that the most economical way of improving the power generation system is by boosting it with a maximum power point tracking (MPPT) mechanism (Salam et. al., 2013).

## 1.1 Research Motivations and Problem Statement

Generally speaking, the performance of an optimization algorithm can be influenced by many factors. Among others is the search step setting. The size of the search steps employed in an optimization algorithm can show huge impact in the result accuracy and the general convergence performance of the algorithm itself (Yua et. al., 2015). Yet, in a conventional EM, the particle search is based on random step size and the iterations are terminated immediately upon achieving any comparatively better objective value (Birbil & Fang, 2003). The random search step size method is clearly not acceptable as it may jeopardize the balance between the efficiency of the convergence and the accuracy of the solution returned. A more systematic and dynamic search step size setting is essential to ensure the accuracy of the solution without compromising the convergence efficiency of the EM.

In term of solar energy harvesting, despite recent improvements in many PV utilization-related aspects such as cell efficiency, cost reduction, and structural integration to buildings (Zahedi, 2006), the inefficiency of PV energy conversion systems still proves to be a major obstacle to the extensive employment of PV power generation systems (Seyedmahmoudian, 2016). This impediment can be rectified by providing the system with the ability to accurately track the maximum power point. Therefore, this research is also motivated to develop a strong optimization algorithm to be implemented as a mean of MPPT to harvest the maximum output energy from PV arrays.

## 1.2 Research Objectives

The main objective of this research is to develop an enhanced electromagnetism-like mechanism algorithm with a higher performance in terms of the solution accuracy and convergence efficiency. The enhanced electromagnetism-like mechanism algorithm is to be implemented in the simulation to track the maximum power point (MPP) of a photovoltaic solar energy harvesting system. The sub-objectives of the research are as outlined below:

1 To investigate the effect of the search step size setting on the convergence behaviour and overall performance of the electromagnetism-like mechanism algorithm.

2 To develop a local search scheme with a dynamic tuning mechanism for the electromagnetism-like mechanism algorithm.

3 To modify and enhance the electromagnetism-like mechanism algorithm with an experience-based search strategy.

4 To develop a maximum power point tracking scheme for a photovoltaic solar energy harvesting system adopting the advantages of the enhanced electromagnetism-like mechanism algorithm.

## 1.3 Significance of the Study

The contribution of this study is fourfold and can be summarized along the following lines. First, this study offers a clear exposure on the correlations between the size of the search steps employed in an optimization algorithm and the impact on the convergence performance of the algorithm. Employing larger and smaller search steps both demonstrated different advantages and shortcomings. Secondly, a regulated search step strategy is proposed in the local search phase of the EM. By dynamically tuning the search steps as iterations go, this strategy has significantly improved the output accuracy and the convergence performance of the EM. Thirdly, an experience-based EM is proposed. This experience-base EM is modified with the ability to analyse previous search experience and projects the adjustments on the scale and direction of the following search iterations. This unique strategy enhances the EM with a powerful solution exploitation capacity. Integrating with the strong global solutions exploration ability of the EM, the modified algorithm strikes a good balance in providing well diversified solutions with high final output accuracies. The experience-based search scheme can also be introduced into other global optimization algorithms to enhance the convergence performance. Finally, the enhanced EM contributes as a mean of an MPPT mechanism in a PV solar energy harvesting system. In time to come, this modified and improved EM can be implemented as a strong tool in solving global optimization problems in many other fields.

## 1.4 Research Scopes

This research covers the improvement of the EM in terms of the output accuracy and the efficiency of the convergence performance in comparison to a standard EM. The performances of the algorithms were validated and demonstrated in a test suite of 10 common numerical optimization test problems, which included Rastrigin, Rosenbrock, Ackley, Shubert, Booth, Beale, Himelblau, Schaffer, Six-hump Camel, and De Jong's Sphere test. The Rosenbrock, Rastrigin, Ackley, Sphere, and Shubert tests were set to be conducted in a 10 dimensional hypercube.

The efficiency of the convergence process was evaluated based on the number of iterations it took to reach its best achievable solution. All the algorithms and simulations were developed and conducted using Microsoft Visual Basic.Net 2008 software with a 1.6GHz Intel Core i5 CPU with 4GB-RAM, in WIN-7OS. For the ease of analysis, 10 particles were employed for all the variants of EM. The enhanced EM was implemented in the MPPT simulation of a PV solar harvesting system in VB.Net software. Simulations were carried out to evaluate the performance of the algorithm in tracking the global MPP of an array with serially connected PV panels under uniform solar irradiance and changing partial shading patterns.

## 1.5 Organization of the Thesis

The outline of this thesis can be divided into 5 major chapters. In Chapter 2, a comprehensive review on related literature is carried out. Previous research and recent developments by researchers around the world are studied and reported. Chapter 3 offers the methodologies on the research and experiments done in this study. The flow of the algorithms, the search mechanisms, the proposed modifications, and the designs of the experiments are discussed in details in this chapter. The simulation and computational experiment results of the algorithms are then benchmarked, compared and discussed in Chapter 4. Some explanations and discussions are included as well. In Chapter 5, an overall conclusion is drawn.

# CHAPTER 2: LITERATURE REVIEW

Soft computing emerged as a computer science discipline in the mid-1950s. In the early stage, Herbert Simon, Allen Newell and Cliff Shaw conducted experiments in writing programs to imitate human thought processes (Krishnamoorthy & Rajeev, 1996). The experiments resulted in a program called Logic Theorist, which consisted of rules of already proved axioms. When a new logical expression was given to it, it would search through all possible operations to discover a proof of the new expression, using heuristics. The Logic Theorist was capable of solving quickly 38 out of 52 problems with proofs that Whitehead and Russell had devised (Newell et. al., 1963). At the same time, Shannon came out with a paper on the possibility of computers playing chess (Shannon, 1950). Though the works of Newell et al. (1963) and Shannon (1950) demonstrated the concept of intelligent computer programs, the year 1956 is considered the start of Artificial Intelligence (AI). In this year, the first conference on AI was organized by John McCarthy, Marvin Minsky, Nathaniel Rochester and Claude Shannon's at Dartmouth College in New Hampshire. This conference was the first effort recorded in the field of machine intelligence. It was at that conference that John McCarthy, the developer of LISP programming language, proposed the term AI.

This chapter offers a thorough study of the literature related to the research. The initial part of the chapter reviews on the some of the most well established optimization algorithms in the literature. This is then followed up by a more specific study on the EM algorithm, its implementations and its modifications. A study on the test functions used in the research is also reported. The chapter then continues with the study on some of the

state-of-the-art artificial intelligence techniques used in solar energy harvesting systems, specifically in the scope of maximum power point tracking of the PV systems.

Artificial intelligence (AI) is a term that in its broadest sense would indicate the ability of a machine or artefact to perform the same kind of functions that characterize human thought. The term AI has also been applied to computer systems and programs capable of performing tasks more complex than straightforward programming, although still far from the realm of actual thought. According to Barr and Feigenbaum (1981) AI is the part of computer science concerned with the design of intelligent computer systems, i.e. systems that exhibit the characteristics associated with intelligence in human behaviour—understanding, language, learning, reasoning, optimizing, solving problems and so on (Kalogirou, 2003, 2007). A system capable of planning and executing the right task at the right time is generally called rational (Russel & Norvig, 1995). Thus, AI alternatively may be stated as a subject dealing with computational models that can think and act rationally (Luger & Stubblefield, 1993, Winston, 1994, Schalkoff et. al., 1992). AI has been used in many applications, resolving different types of complex problems (Charniak & McDermot, 1985, Chen, 2000, Nilsson, 1998, Zimmermann et. al., 2001). Over the year, the research and development in this field has produced a number of powerful tools, many of which are of practical use in engineering to solve categorization, prediction, and optimization problems normally requiring human intelligence.

## 2.1 Optimization Algorithms

Optimization techniques first came about in conjunction with problems linked with the logistics of personnel and transportation management. Typically, the problems were modelled in terms of finding the minimum cost configuration subject to all constraints be satisfied, where both the cost and the constraints were linear functions of the decision variables. Diverse mathematical programming methods (Nocedal & Wright, 2000), such as fast steepest, conjugate gradient method, quasiNewton methods, sequential quadratic programming, were first extensively investigated. However, increasing evidences have shown that these traditional mathematical optimization methods are generally inefficient or not efficient enough to deal with many real-world optimization problems characterized by being multimodal, non-continuous and non-differential (Wu et. al., 2013). In response to this challenge, many population-based search algorithms (PBSAs) have been presented and demonstrated to be competitive alternative algorithms. Among them, the most classical, popular, and well-established is the genetic algorithm (GA) (Forrest, 1993, Goldberg & Holland, 1988).

### 2.1.1 Genetic Algorithm

The genetic algorithm is one of the most popular technique there is in the field of AI for the purpose of optimization. The GA was envisaged by Holland (1975) in the 1970s as a stochastic algorithm that mimics the natural process of biological evolution (Rich & Knight, 1996). The GA is inspired by the way living organisms are adapted to the harsh

realities of life in a hostile world by evolution and inheritance. The algorithm imitates in the process, the evolution of population by selecting only fit individuals for reproduction. Therefore, a GA is an optimum search technique based on the concepts of natural selection and survival of the fittest. It works with a fixed-size population of possible solutions of a problem, known as individuals, which are evolving in time. Problem states in a GA are denoted by chromosomes, which are usually represented by numbers or binary strings. A GA utilizes three principal genetic operators: selection, crossover and mutation (Kalogirou, 2003, Konar, 1999, Deyi & Yi, 2007). The algorithm normally starts by creating an initial population of chromosomes in the space using a random number generator. This space, referred to as the search space, comprises all possible solutions to the optimization problem at hand. At every evolutionary step, also known as a generation, the individuals in the current population are decoded and evaluated according to a fitness function set for a given problem. These fitness values of the chromosomes are used in the selection of chromosomes for subsequent operations. The expected number of times an individual is chosen is approximately proportional to its relative performance in the population.

Crossover is performed between two selected individuals by exchanging part of their genomes to form new individuals. The mutation operator is introduced to prevent premature convergence. Every member of a population has a certain fitness value associated with it, which represents the degree of correctness of that particular solution or the quality of solution it represents (Kalogirou, 2003, Kalogirou, 2007). After the cross-over and mutation operations, a new population is obtained and the cycle is repeated with the evaluation of that population (Holland, 1975, Goldberg, 1989, Davis, 1991). Figure 2.1 shows the flow of the GA in the basic form.

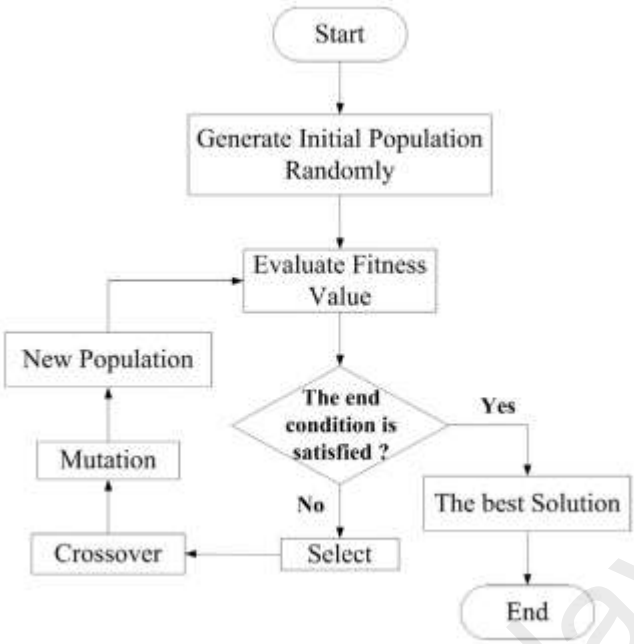


Figure 2.1: The flow of genetic algorithm in its most basic form.

Genetic optimization, including continuous optimization and discrete optimization, or constrained optimization and unconstrained optimization, is frequently involved across all branches of engineering, applied sciences, and sciences. Some examples of those applications include configuring transmission systems (Pham & Yang, 1993), generating hardware description language programs for high-level specification of the function of programmable logic devices (Seals & Whapshott, 1994), designing the knowledge base of fuzzy logic controllers (Pham & Karaboga, 1994), planning collision-free paths for mobile and redundant robots (Ashiru et. al. , 1995, Wilde & Shellwa, 1997, Nearchou & Aspragathos, 1997), scheduling the operations of a job shop (Cho et. al. , 1996, Drake & Choudhry, 1997), and many more.

The problem of finding the global optima of a function with large numbers of local minima arises in many applications. The methods that were first used in global optimization were deterministic techniques, mostly based on the divide-and-conquer principle. One typical algorithm which embodies such principle is the Branch-and-Bound

algorithm (BB) (Papadimitriou & Steiglitz, 1998). Because of the nature of the algorithm, where the sub-problems are produced by branching a problem entity, for instance variable, into its possible instances, the BB algorithm applies very well to cases where problem entities are discrete in nature. Thus, the first applications of BB to global optimization problems were devoted to discrete problems such as the Travelling Salesman Problem. Over the years, optimization algorithms have evolved into many new approaches with different features, such as the swarm-based optimization.

### 2.1.2 Particle Swarm Optimization

Particle swarm optimization (PSO) algorithm is a population based stochastic optimization technique developed by Eberhart and Kennedy in 1995 (1995). Inspired by the information circulation and social behaviour observed in bird flocks and fish schools, this algorithm is a global optimization algorithm which is particularly suited to solve problems where the optimal solution is a point in a multidimensional space of the parameter. Inspiration from the natural analogues, i.e. schooling or flocking, translates to the property that agents or particles are characterized not only by a position, but also a velocity. The particles move around in the search space. The social interaction in a PSO is direct, as the movement of each particle is not only influenced by its best solution found so far, but it is also directed towards the best position found by other particles, be they a subset of particles or the whole swarm. The pseudocode of a standard PSO is as shown in Table 2.1. The flow of a standard PSO is as shown in Figure 2.2.

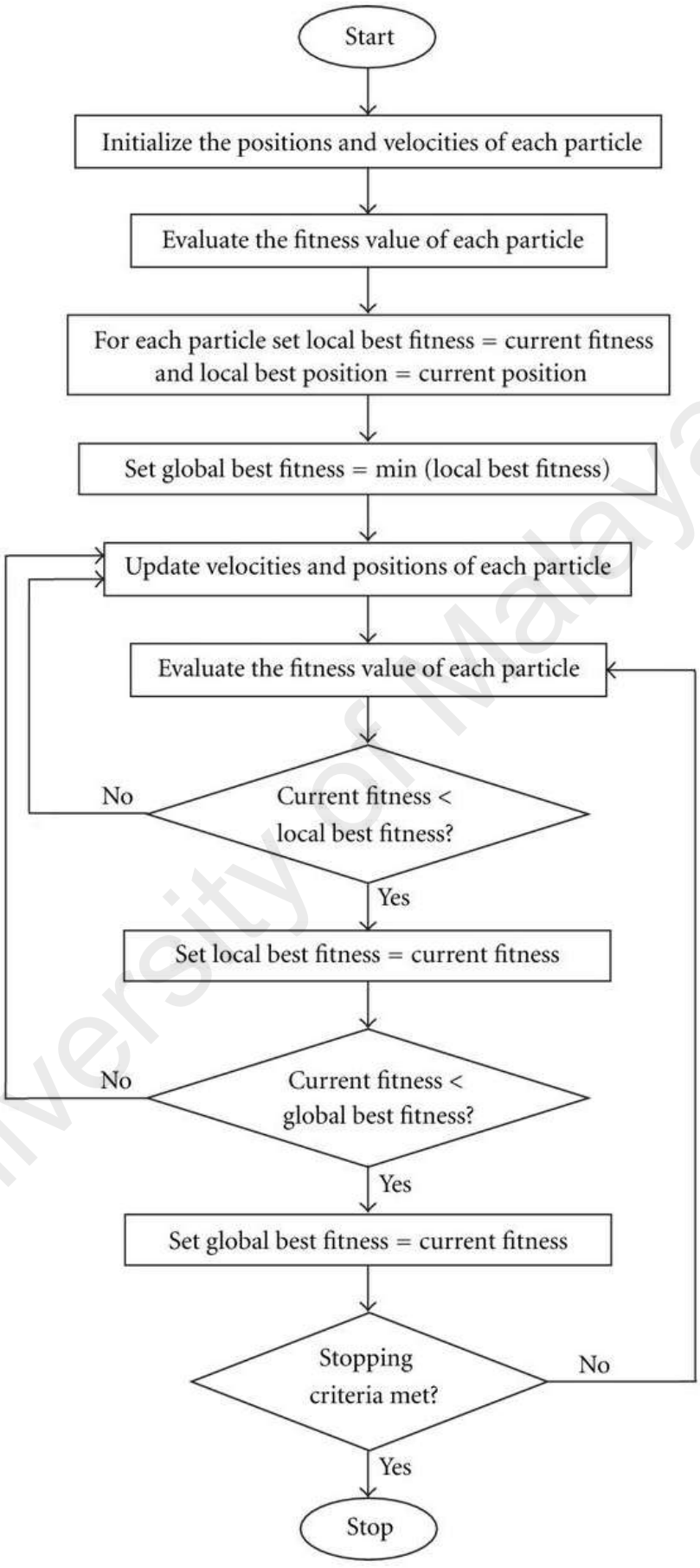


Figure 2.2: The flow of a PSO algorithm.

Table 2.1: PSO pseudocode.

| **Particle Swarm Optimization** |
|---|
| **Start** |
| Input PSO parameters and problem parameters |
| Randomly initialise particles and compute objective values, personal bests and swarm best. |
| **While stopping condition is not met** |
| Update velocities and positions of all particles by flight equations |
| Bound velocities to their limits |
| Bound decision variables to their specified ranges. |
| Compute objective values for all particles |
| Update personal bests |
| Update swarm best |
| **End While** |
| Display optimal decision vector and optimal objective |
| **End** |

Due to its meta-heuristic nature, which allows obtaining solutions also for non-differentiable problems which may be irregular, noisy or dynamically changing with time, PSO algorithm has found a wide range of application in many domains of computer science and applied mathematics, such as for the calculation of neural network weights (Meissner et. al., 2006, Mohammadi & Mirabedini, 2014), time series analysis (Hadavandi, 2010), business optimization (Yang et. al., 2011) and many others.

### 2.1.3 Ant Colony Optimization

Another well-known swarm-based optimization algorithm is the Ant Colony Optimization (ACO) (Dorigo & Stützle, 2004). Ant colony optimization is a probabilistic optimization technique, which is applicable where the task may be expressed as that of finding the best path along a graph (Dorigo, 1992, Dorigo & Stützle, 2004). Its inspiration

stems from the wandering behaviour of ants seeking a path between their colony and a source of food. In an ACO, the artificial ants iteratively build solutions to the problem at hand by moving from a candidate state to another and it selects the successive step, among all the possible ones based on the combination of two factors: the "attractiveness" of the move. Usually, it is inversely related to the distance to the destination point and the "pheromone trail". The "attractiveness" is a meta-heuristic parameter determining the desirability of the state transition while the "pheromone trail" indirectly provides the social interaction among the agents.

Indeed, analogously to what happens in the behaviour of real ants, which, along their wander in search of food, deposit pheromones on the ground, so that future members of the colony will choose with higher probability paths that are marked by stronger concentrations of these substances, the fitness, also known as optimality, of a solution found by an artificial ant will be accompanied by an increase of the pheromone trail associated to that direction. Many other swarm-based optimization algorithms can be found in the literature, such as firefly algorithm, artificial bee colony, bat algorithm, krill algorithm, and many more (Yang, 2014). Indeed, unlike what happens with other nature-inspired algorithms, evolution is based on cooperation and competition among individuals through generations (iterations): the flow of information among particles, which can be limited to a local neighbourhood or extended to the whole swarm is an essential characteristic of the algorithm.

### 2.1.4 Tabu Search

The Tabu search (TS) is a meta-heuristic search algorithm that incorporates adaptive memory and responsive exploration to avoid of local optima traps. The use of adaptive memory enables TS to learn and create a more flexible search strategy. TS differs from other stochastic optimization techniques by maintaining lists of previous solutions using a memory set. These lists help to guide the search process. The TS uses the lists to generate a sequence of progressively improving solutions through repetitive modification of current solutions. A neighbourhood search approach is used to explore the search space to escape local optima.

The memory in TS allows the algorithm to drive forward to discover regions that harbour one or more possible solutions, which can be better than the current best. A set of coordinated strategies such as intensification and diversification employed in TS allow the algorithm to explore the search space more thoroughly, thus helping to avoid becoming stuck in local optima. TS originally developed by Glover and Laguna (1997) has now become an established search procedure. The TS has been successfully applied to solve a wide spectrum of optimization problems, such as synthesis problems in chemical engineering and system modelling (Lin & Miller, 2004, Chelouah & Siarry, 2005, Aytekin, 2008).

### 2.1.5 Artificial Immune System

The artificial immune system algorithm (AIS) is designed based on human body's defence process against viruses (Burke & Kendall, 2005). Similar to the GA, the AIS is a population-based algorithm. The operators in the AIS include duplication, mutation and selection. Starting from a randomly generated population, the solutions are reproduced with different rates. Considering the objective function, the better and more suitable solutions are duplicated in a relatively higher rate. The solutions are then mutated in different rates. Solutions with lower fitness values are mutated in a higher rate. Finally, the selection operator is applied to the whole population to produce a stronger group of solutions. The AIS is more intelligent than the GA due to the guided mutation and duplication operators. However, the setting of the mutation and duplication rates proved to be a challenge for AIS in practical applications. The details of the algorithm is well described by Kilic & Nguyen (2010). Several examples of AIS applications are shown in (Carrano et. al., 2007, Muhtazaruddin et.al., 2014, Junjie et. al., 2012). Often, hybrid meta-heuristics combine a certain global strategy with a local search, which iteratively tries to change the current solution to a better one, placed in some neighbourhood of the current solution. Some of these modified algorithms target to solve some specific optimization problems. Bean (1994) introduced a random-key approach for real-coded GA for solving sequencing problem. Subsequently, numerous researchers show that this concept is robust and can be applied for the solution of different kinds of COPs (Mendes, Goncalves, & Resende, 2005; Norman & Bean, 1999, 2000; Snyder & Daskin, 2006). Other applications of the random-key approach are in solving single machine scheduling problems and permutation flowshop problems using PSO by (Tasgetiren, Sevkli, Liang, & Gencyilmaz, 2004, 2007).

## 2.2 Electromagnetism-Like Mechanism Algorithm

The electromagnetism method (EM) is a population-based meta-heuristic algorithm introduced by Birbil and Fang (2003). This algorithm is designed to solve unconstrained nonlinear optimization problems in a continuous domain. Unlike traditional meta-heuristics, where the population members exchange materials or information between each other, in EM, each particle is influenced by all other particles within its population (Yurtkuran & Emel, 2010). Guided by the electromagnetism theory, the EM imitates the attraction-repulsion mechanism of electromagnetic charges in order to move sample points towards global optimality using bounded variables. In the algorithm, all solutions are considered as charged particles in the search space. The charge of each point relates to the objective function value, which is the subject of optimization. Better solutions possess stronger charges and each point has an impact on others through charge. Particles with better objective yields will apply attracting forces while particles with worse objective values will apply repulsion forces onto other particles (Wu et. al., 2014). The exact value of the impact is given by Coulomb's Law. This means that the power of the connection between two points will be proportional to the product of charges and reciprocal to the distance between them. Bigger difference in objective values generates higher magnitude of attraction or repulsion force between the particles. In other words, the points with a higher charge will force the movement of other points in their direction more strongly. Besides that, the best EM point will stay unchanged. The particles are then moved based on superposition theorem. Figure 2.3 shows an example of the total force, $F_a$ applied on $Q_a$ by the repulsive force from $Q_b$ and attractive force from $Q_c$.

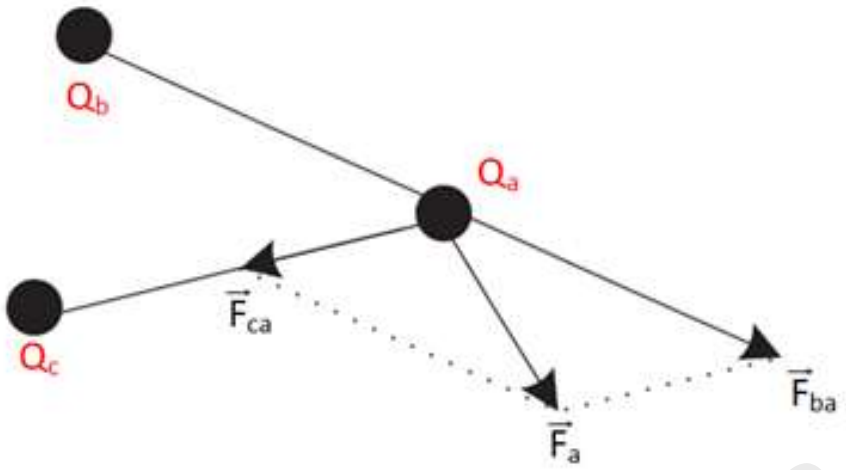


Figure 2.3: Total force exerted on $Q_a$ by $Q_b$ and $Q_c$

### 2.2.1 EM Scheme

Similar to many other global optimization algorithms, the search mechanism of EM can generally be divided into its exploration and exploitation segments. The exploration segment of EM searches globally for a better variety of possible solutions by moving the particles in accordance with the superposition theorem. The exploitation segment, on the other hand, involves a random line search procedure which gather the information around the neighbourhood of a particular solution. There are five critical operations in EM, namely the initialization, the local search, the charge calculation, the force calculation, and the movement of particles.

#### 2.2.1.1 Initialization

In the initialization stage of EM, the feasible ranges of all the tuning parameters (upper bound, $u_k$ and lower bound, $l_k$) are defined. Then, $m$ sample of initial particles are randomly picked from the feasible solution domain, each represents an $N$ dimensional hyper-solid. Each value of dimension in each particle is assumed to be uniformly distributed inside the upper and lower bound (Dutta et. al., 2013). Immediately after the randomization of the solutions, the particles are evaluated based on the objective function of the optimization problem. In a maximization problem, the solution with the highest function value is identified as the best particle, while in the case of a minimization problem, particle with the lowest function value is marked as the best.

#### 2.2.1.2 Local Search

This step in EM is important to gather local information in the neighbourhood of a particle. The original local search procedure in a conventional EM employs a random line search within the feasible range of a solution. This simple line search involves a particle being tuned along its dimensions one by one, restricted by a maximum feasible random step length of $\lambda \in (0, 1)$ (Zhang et. al., 2013). For each of the iterations, a new random step length is generated. The overall local search procedure is immediately terminated upon achieving any better objective value. This procedure is further discussed in details in Chapter 3.

### 2.2.1.3 Charge Calculation

The total force vector exerted onto each particle is calculated based on the Coulomb's Law (Lee et. al., 2012). The charge of each particle is evaluated by its current objective value compared to the best particle in the iteration. The computed charge of a particle, $q^i$ , when compared to that of other particles, will determine if it is a repulsive or attractive force to the respective particles. The calculation of $q^i$ is shown in equation (2.1)

$$q^i = exp\left(-n\frac{f(x^i)-f(x^{best})}{\sum_{k=1}^{m}\left(f(x^k)-f(x^{best})\right)}\right), \forall i \qquad (2.1)$$

where *n* refers the total dimension of the particle and *m* denotes the population size. $f(x^{best})$ represents the objective value of the best particle.

### 2.2.1.4 Force Calculation

With the charges calculated for all particles, the force generated by one particle onto another can be computed. According to the electromagnetic theory, the force of a particle onto another is inversely proportional to the square of the distance between the two particles and directly proportional to the product of their charges (Lee & Lee, 2012). The force vector for a particle can be determined using equation (2.2).

$$F^i = \sum_{j\neq i}^{m}\begin{Bmatrix}(x^j-x^i)\frac{q^iq^j}{||x^j-x^i||^2} & if \quad f(x^j)<f(x^i)\\ (x^i-x^j)\frac{q^iq^j}{||x^j-x^i||^2} & if \quad f(x^j)\geq f(x^i)\end{Bmatrix}, \forall i \qquad (2.2)$$

where $f(x^j) < f(x^i)$ denotes attraction and $f(x^j) \geq f(x^i)$ refers to repulsion.

#### 2.2.1.5 Particle Movement

The movement stage in EM involves relocation of all particles but the best to a new location in space. The calculation for the movement of a particle is as shown in equations (2.3), where $\lambda$ represents the global particle movement step length. It is a random value between 0 and 1, assumed to be uniformly distributed between the upper boundary ($u_k$) and the lower boundary ($l_k$).

$$x_k^i \leftarrow x_k^i + \lambda F_k^i ( u_k - x_k^i ) \qquad ; F_k^i \geq 0$$

$$x_k^i \leftarrow x_k^i + \lambda F_k^i ( x_k^i - l_k) \qquad ; F_k^i < 0 \qquad (2.3)$$

Holding the absolute power of attraction towards all other particles, the best particle of the iteration does not move (Cuevas et. al., 2012).

## 2.3 Implementations of EM

EM has been widely employed as an optimization tool in various fields due to its capability to yield well diversified results and solve complicated global optimization problems (Naderi et. al., 2010). Though EM algorithm is initially designed for solving continuous optimization problems with bounded variables, the algorithm has been extended by a few authors to solve discrete optimization problems. Some recent successful applications of the EM include the unicost set covering problem (Naji-Azimi et. al., 2010), the uncapacitated multiple allocation hub location problem (Filipovi, 2011), automatic detection of circular shapes embedded into cluttered and noisy images (Cuevas

et. al., 2012) and feature selection problem (Su & Lin, 2011). In handling scheduling problems, an EM algorithm with discrete variables is discussed in Davoudpour and Molana (2008) for flow shop scheduling with deteriorating jobs. Another discrete Electromagnetism-like Mechanism algorithm is proposed by Liu and Gao (2010) for the distributed permutation flow shop scheduling problem. Debels et al. (2006) integrated a scatter search with EM for the solution of resource constraint project scheduling problems. Naderi, Zandieh, and Shirazi (2009) present an EM algorithm for the flexible flow shop scheduling problem with sequence-dependent setup times and transportation times with the objective of minimizing the total weighted tardiness. A similar approach is discussed in Naderi, Tavakkoli-Moghaddam, and Khalili (2010) for the flow shop problem with stage-skipping in order to minimize the makespan and the total weighted tardiness. The EM has also been used by Meanhout and Vanhoucke (2007) for the nurse scheduling problem and by Chang et al (2009) to solve a single machine scheduling problem. Because the EM algorithm was originally developed for the continuous search space, the papers discussed above made some adaptations for using the algorithm in the discrete domain. Those adaptations are mostly made by applying a random key representation to limit the required modifications of the original algorithm. A minority of the authors make the translation to a binary 0/1-representation (Bonyadi & Li, 2012; Javadian et al., 2009; Naji-Azimi et al., 2010) or maintain the permutation representation (Davoudpour & Molana, 2008; Liu & Gao, 2010). The choice of such representation schemes led to a modified version of the EM algorithm to allow the electromagnetic operators to work in discrete spaces. Moreover, most authors consider hybridizations of the EM algorithm with another meta-heuristic in order to benefit from the advantages of the individual approaches.

Table 2.2: Implementations of EM in solving optimization problems.

| Authors | Year | EM Implementation |
|---|---|---|
| Naji-Azimi, Toth, & Galli | 2010 | Set covering problems |
| Lee & Chang | 2010 | PID controller optimization |
| Yurtkuran & Emel | 2010 | Vehicle routing problems |
| Javadian, Alikhani, & Tavakkoli-Moghaddam | 2008 | Traveling salesman problems |
| Tsou & Kao | 2007 | Multi-objective inventory optimization |
| Yin et al & Abed et al | 2011, 2013 | Kinematic problems for robot manipulators |
| Muhsen et. al | 2015 | Sustainable energy harvesting optimization |
| Bonyadi & Li | 2012 | Knapsack problems |
| Birbil & Feyzioglu | 2003 | Fuzzy relation equations solving |
| Wu, Yang, & Wei | 2004 | Artificial neural network training |
| Wu, Yang, & Hung | 2005 | Obtain fuzzy if–then rules |
| Naji-Azimi et. al. | 2010 | Unicost set covering problem |
| Filipovi | 2011 | Uncapacitated multiple allocation hub location problem |
| Cuevas et. al. | 2012 | Automatic detection of circular shapes embedded into cluttered and noisy images |
| Su & Lin | 2011 | Feature selection problem |
| Davoudpour and Molana | 2008 | Flow shop scheduling with deteriorating jobs |
| Liu and Gao | 2010 | Distributed permutation flow shop scheduling problem |
| Naderi, Zandieh, & Shirazi | 2009 | Flexible flow shop scheduling problem |
| Naderi, Tavakkoli-Moghaddam, & Khalili | 2010 | |
| Meanhout & Vanhoucke | 2007 | Nurse scheduling problem |
| Chang et al | 2009 | Single machine scheduling problem |

Literature also shows that EM has proven to be effective in solving COPs. Examples include set covering problems (Naji-Azimi, Toth, & Galli, 2010), PID controller optimization (Lee & Chang, 2010), vehicle routing problems (Yurtkuran & Emel, 2010), traveling salesman problems (Javadian, Alikhani, & Tavakkoli-Moghaddam, 2008), multi-objective inventory optimization (Tsou & Kao, 2007), kinematic problems for robot manipulators (Yin et al, 2011, Abed et al, 2013), sustainable energy harvesting optimization (Muhsen et. al., 2015), and knapsack problems (Bonyadi & Li, 2012). The EMs are also implemented to optimize other AI algorithms, such as

fuzzy relation equations solving (Birbil & Feyzioglu, 2003), artificial neural network training for textile retail operations (Wu, Yang, & Wei, 2004), and also to obtain fuzzy if–then rules (Wu, Yang, & Hung, 2005). Table 2.2 summarizes the implementations of EM in solving various optimization problems.

## 2.4 EM Modifications

The EM algorithm considers each particle to be an electrical charge. Subsequently, movement based on attraction and repulsion is introduced by Coulomb's law. Obviously, it has the advantages of multiple search, global optimization, and simultaneously evaluates many points in the search space, which in turn make it more likely to find a better solution (Birbil & Fang, 2003, Lee & Chang, 2008, Tsou & Kao, 2007). Several modifications have been suggested in the literature on either the local or global search segment of the EM. Gol-Alikhani, Javadian, and Tavakkoli-Moghaddam (2009) presented a novel hybrid approach based on EM embedded with a well-known local search, called Solis and Wets, for continuous optimization problems. They compared related results with two algorithms known as the original and revised EM.

Chen et. al., (2007) and Chang et. al., (2009) proposed a hybrid Electromagnetism-like Mechanism algorithm to solve the single machine earliness/tardiness problem. They hybridized the EM algorithm with the concepts of a genetic algorithm using a random-key representation. The results indicated that hybridizing can provide a better solution diversity as well as a good convergence ability. The same problem is discussed in

Javadian, Golalikhani, and Tavakkoli-Moghaddam (2009), who present a discrete binary version of the EM algorithm, using a binary representation.

Tavakkoli-Moghaddam, Khalili, and Nasiri (2009) presented a hybridization of a simulated annealing (SA) and an EM algorithm for a job shop scheduling problem to minimize the total weighted tardiness. By hybridizing both meta-heuristics, the authors intended to overcome the limitations of both individual approaches. The SA provided a good initial solution, which the EM algorithm tried to improve. The same approach is studied by Jamili, Shafia, and Tavakkoli-Moghaddam (2011), who proposed a hybrid EM-SA algorithm for the periodic job shop scheduling problem. Roshanaei et al. (2009) used the EM algorithm with random key representation to solve the job shop scheduling problem with sequence-dependent setup times in order to minimize the makespan. Mirabi, Ghomi, Jolai, and Zandieh (2008) discussed a hybrid EM approach with simulated annealing for flow shop scheduling with sequence-dependent setup times with the objective of minimizing the makespan.

Three papers presented modified EMs for constrained optimization problems by Rocha and Fernandes (2008a, 2008b, 2009a). The first one presented the use of the feasible and dominance (FAD) rules in EM algorithm (Rocha & Fernandes, 2008a). The second one incorporated the elite-based local search in EM algorithm for engineering optimization problems and the FAD rules were used again (Rocha & Fernandes, 2008b). A self-adaptive penalty approach for dealing with constraints within EM algorithm was proposed in the third paper (Rocha & Fernandes, 2009a).

Debels et al. (2006) integrated a scatter search with EM for the solution of resource constraint project scheduling problems. Their experimental results showed that the hybrid method of incorporating EM type analysis outperformed other methods in the benchmarking. Rocha and Fernandes (2008c, 2009b) modified the calculation of the charge and introduced a pattern-search-based local search. They also proposed a modification of calculation of total force vector (Rocha & Fernandes, 2009c). Many of the proposed combinations and modifications mentioned above have proven to be able to provide highly competitive results in their respective fields of applications. Table 2.3 summarizes the modifications carried out onto the EM throughout the years.

Table 2.3: Modification attempts on EM.

| Authors | Year | EM Modifications |
|---|---|---|
| Gol-Alikhani, Javadian, and Tavakkoli-Moghaddam | 2009 | Hybrid EM embedded with Solis and Wets. |
| Chen, Chang, Chan, and Mani | 2007 2009 | Hybrid EM with genetic algorithm using a random-key representation. |
| Chang, Chen, and Fan | | |
| Javadian, Golalikhani, and Tavakkoli-Moghaddam | 2009 | Discrete binary version of the EM algorithm. |
| Mirabi, Ghomi, Jolai, and Zandieh | 2008 | Hybrid EM with simulated annealing. |
| Tavakkoli-Moghaddam, Khalili, and Nasiri | 2009 | Hybrid EM with simulated annealing. |
| Jamili, Shafia, and Tavakkoli-Moghaddam | 2011 | Hybrid EM with simulated annealing. |
| Roshanaei et al. | 2009 | EM with random key representation. |
| Rocha and Fernandes | 2008, 2009 | FAD rules in EM, pattern-search based local search. |
| Debels et al. | 2006 | EM with scatter search. |

## 2.5 The Test Suite

In the field of soft computing and optimization, researchers always come up with different search mechanisms and analogical hypothesis. The introduction of many algorithms and the need for their computational comparison led to the development of standardized collections of benchmark problems. Over the decades, a rich literature on the test functions has been developed with the aim to test the convergence performance of the algorithms in different aspects. Such collections of test problems in local and global optimization can be found in the handbook by Floudas et al. (1999), the benchmark suite compiled by Shcherbina et al. (2003), as well as in other publications (Casado et al. (2003); Ali et al. (2005)). Often, confusing results limited to the test problems were reported in the literature in such a way that the same algorithm working for a set of functions may not work for any other set of functions. The IEEE Congress on Evolutionary Computation also introduced benchmark functions to be publicly available to the researchers for evaluating their algorithms. For unimodal functions, the convergence rates of the algorithm are more interesting than the final results of optimization. In contrast, for multimodal functions because of having lots of local optima, the ability of finding the optimum solution or a good near global optimum are more important than the convergence rate of the algorithm. After an extensive study, some of the most commonly used benchmark test functions are discussed in details in the subsections below.

### 2.5.1 Ackley Test Function

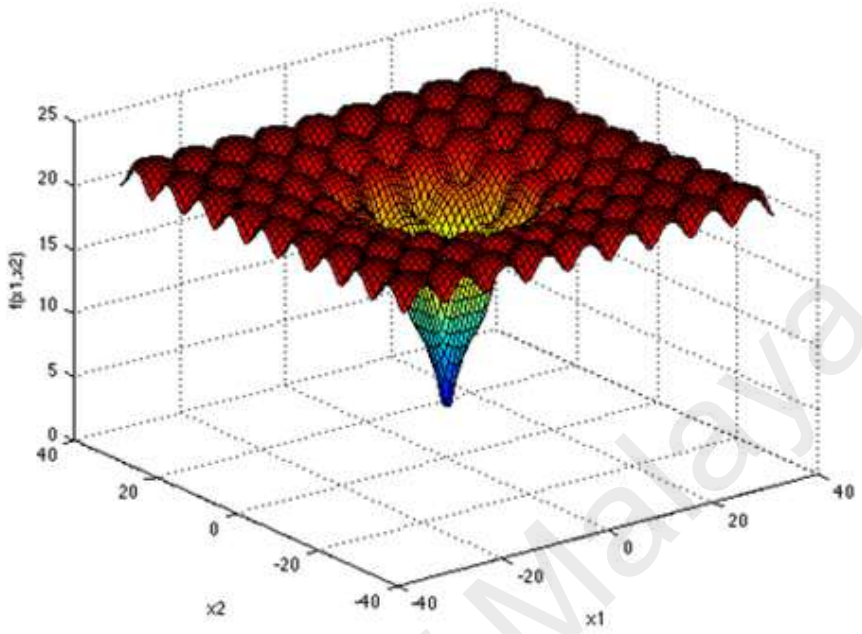


Figure 2.4: 2-dimensional Ackley test function

$$f(x) = -20\exp\left(-0.2\sqrt{\frac{1}{d}\sum_{i=1}^{d} x_i^2}\right) - \exp\left(\frac{1}{d}\sum_{i=1}^{d}\cos(2\pi x_i)\right) + 20 + e \qquad (2.4)$$

The Ackley function is a multi-model test function for minimization with multiple local optima. It has one global minima of 0 located at (0, … 0). The function poses a risk for optimization algorithms, particularly hill climbing type algorithms, to be trapped in one of its many local minima. The model of the test function is as shown in equation (2.4). The dimension can be set to any value, depending on the need of the test. Figure 2.4 shows an example plot of the function in 2 dimensions. This test function is usually evaluated on a hypercube from the range of -32.768 to 32.768 (Zhu & Kwong, 2010).

### 2.5.2 Beale Test Function

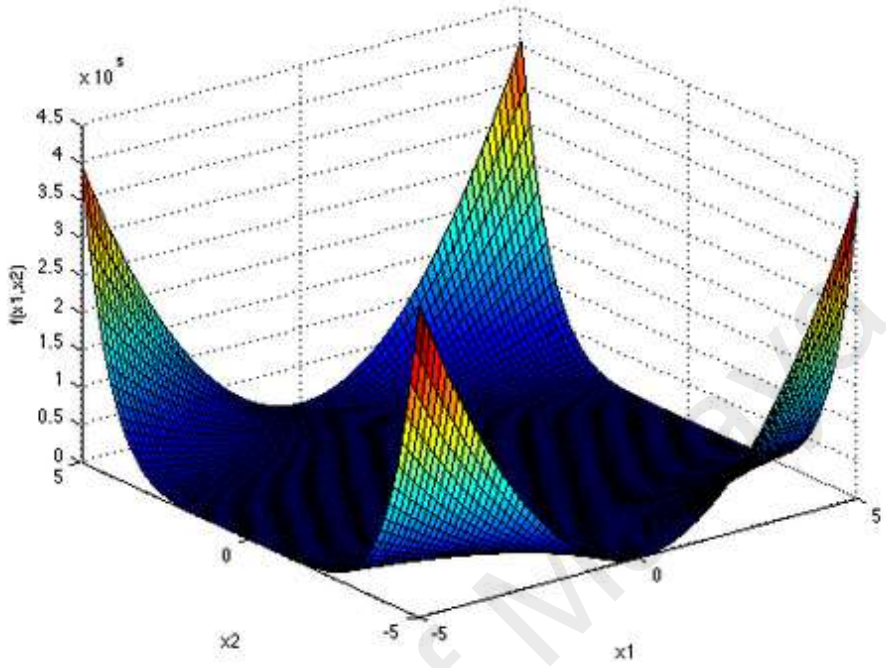


Figure 2.5: Beale test function

$$f(x) = (1.5 - x_1 + x_1x_2)^2 + (2.25 - x_1 + x_1x_2^2)^2 + (2.625 - x_1 + x_1x_2^3)^2 \qquad (2.5)$$

The Beale function is a multi-model test function for minimization with multiple local optima. It has one global minima of 0 located at (3, 0.5). Equation (2.5) shows the model of the test function. This is a two-dimensional test function. It can be observed from Figure 2.5 that this function comes with sharp peaks at the corners of the input domain. This test function is usually evaluated on a square from the range of -4.5 to 4.5 (Liang et. al., 2014).

### 2.5.3 Booth Test Function

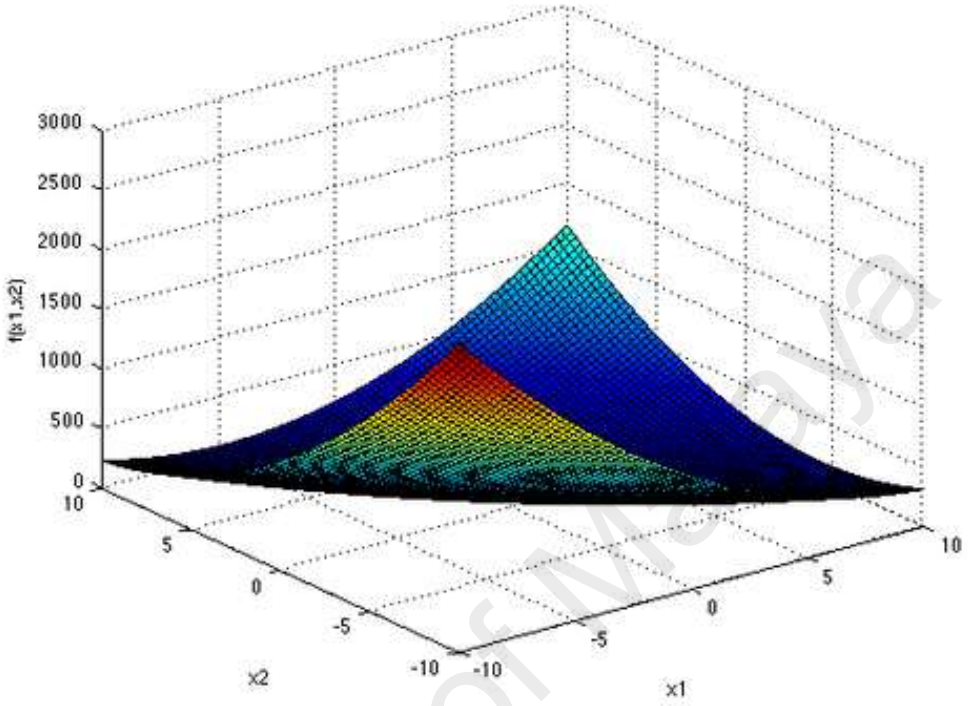


Figure 2.6: Booth test function

$$f(x) = (x_1 + 2x_2 - 7)^2 + (2x_1 + x_2 - 5)^2 \quad (2.6)$$

The Booth function is a continuous, uni-model test function for minimization with a single local minima of 0 located at (1, 3), which makes it the global optima point. The model of the test function is as shown in Equation (2.6). The Booth function is a two-dimensional test function. Figure 2.6 shows the plot of the function. This test function is usually evaluated on a square from the range of -10 to 10 (Yua et. al., 2015).

### 2.5.4 De Jong's First (Sphere) Test Function

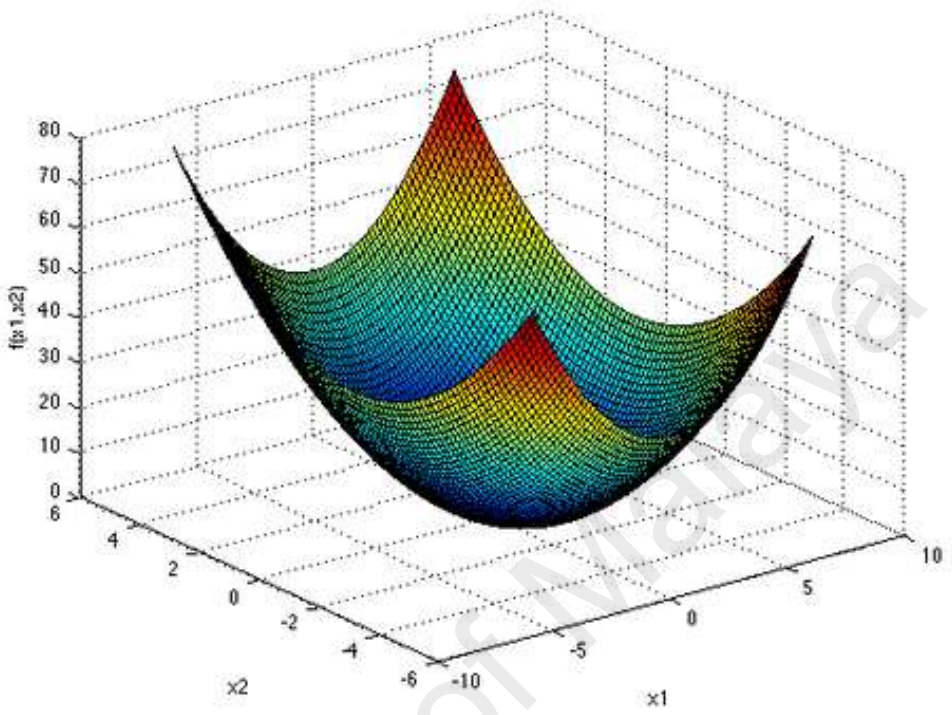


Figure 2.7: 2-dimensional Sphere test function

$$f_1(x) = \sum_{i=1}^{d} x_i^2 \qquad (2.7)$$

The De Jong's Sphere function is a uni-model test function for minimization with a single local optima of 0 located at (0, … 0), which is also the global minima point. The model of the test function is as shown in equation (2.7). The dimension can be set to any value, depending on the need of the test. Figure 2.7 shows the plot of the function in 2 dimensions. This test function is usually evaluated on a hypercube in the range of -5.12 to 5.12 (Yua et. al., 2015).

### 2.5.5 Himmelblau Test Function

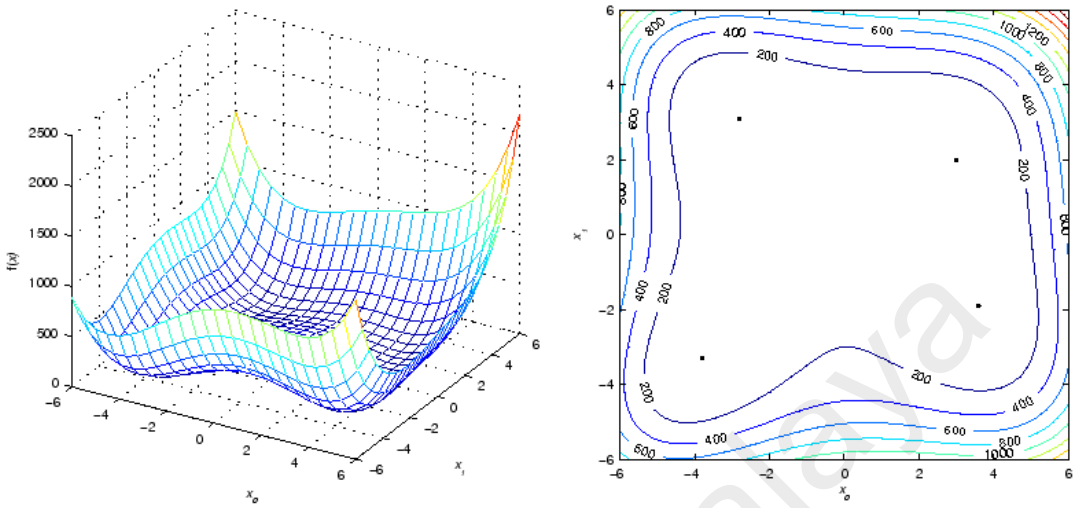

Figure 2.8: Himmelblau test function

$$f(x) = (x_1^2 + x_2 - 11)^2 + (x_1 + x_2^2 - 7)^2 \quad (2.8)$$

The Himmelblau function is a multi-model test function with four global optima points. These global minima points share the same value of 0 and are located at (3, 2), (-2.805118, 3.131312), (-3.779310, -3.283185), and (3.584428, -1.848126). The 4 global minima points can be observed from Figure 2.8. Search mechanisms that manage to find any of the 4 points are considered successful. This test function is suitable to test the diversification of the results returned by the algorithm. The model of the test function is as shown in equation (2.8). It has a fixed dimension of 2. This test function is usually evaluated on a square from the range of -6 to 6 (Yua et. al., 2015).

### 2.5.6 Rastrigin Test Function

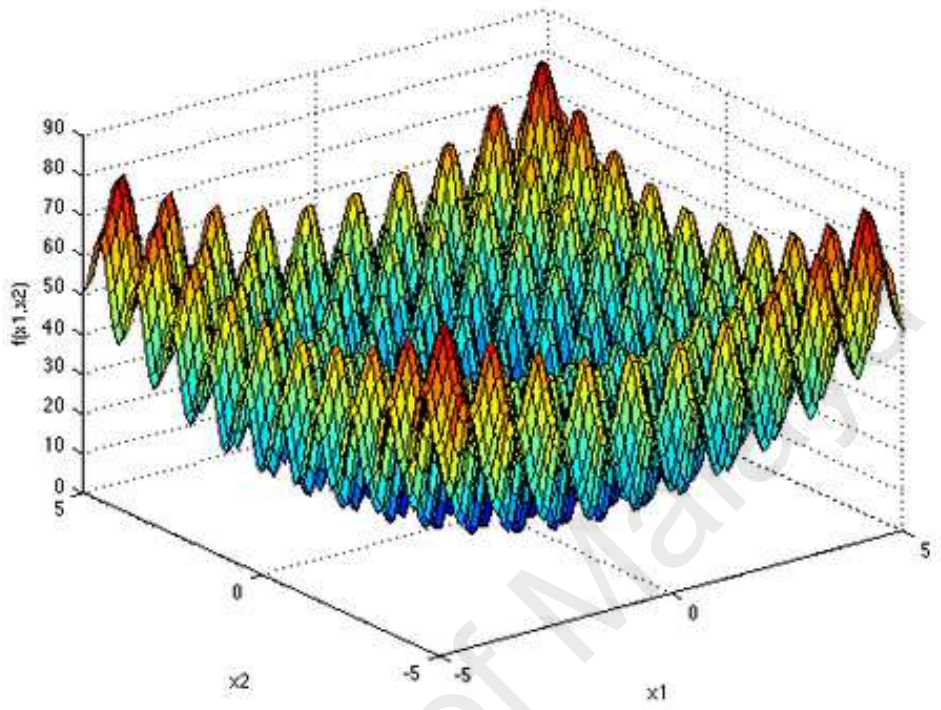


Figure 2.9: 2-dimensional Rastrigin test function

$$f(x) = 10d + \sum_{i=1}^{d}[x_i^2 - 10cos(2\pi)x_i] \quad (2.9)$$

The Restrigin function is a continuous, highly multi-model test function for minimization with multiple local optima. It has one global minima of 0 located at (0, … 0). Equation (2.9) shows the model of the test function. The dimension of this test function can be set to any value, depending on the need of the test. Figure 2.9 shows the plot of a 2-dimensional Rastrigin test function. It can be observed from Figure 2.9 that this function displays vary jagged and regularly distributed local optima points. The search algorithm can easily be trapped in any of the local minima points, especially the ones located in the immediate surroundings of the global minima. This test function is usually evaluated on a hypercube from the range of -5.1 to 5.1 (Zhu & Kwong, 2010).

### 2.5.7 Rosenbrock Test Function

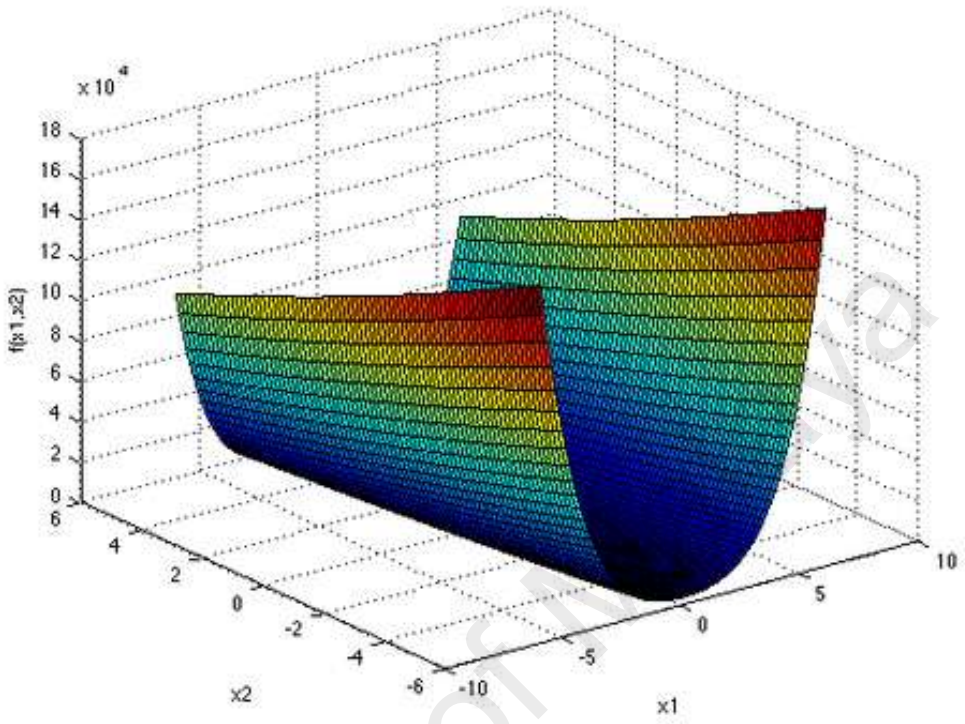


Figure 2.10: Rosenbrock test function

$$f(x) = \sum_{i=1}^{d-1}[100(x_{i+1} - x_i^2)^2 + (x_i - 1)^2] \quad (2.10)$$

The Rosenbrock function is a continuous uni-model test function for minimization with one local optima of 0 that is located at (1, … 1) in a narrow, parabolic valley. The dimension of this test function can be set to any value, depending on the need of the test. Figure 2.10 shows the plot of a 2-dimensional Rosenbrock test function. The Rosenbrock test function is also known as the Rosenbrock Valley or Rosenbrock Banana function, due to the shape of the plot-form as shown in Figure 2.10. This test is very popular for gradient based search algorithms. It is easy for the search algorithm to locate the valley, but it is difficult to converge to the minima point (Picheny et. al., 2013). Equation (2.10) shows the model of the test function. This test function is usually evaluated on a hypercube from the range of -5 to 10 (Zhu & Kwong, 2010).

### 2.5.8 Schaffer Test Function

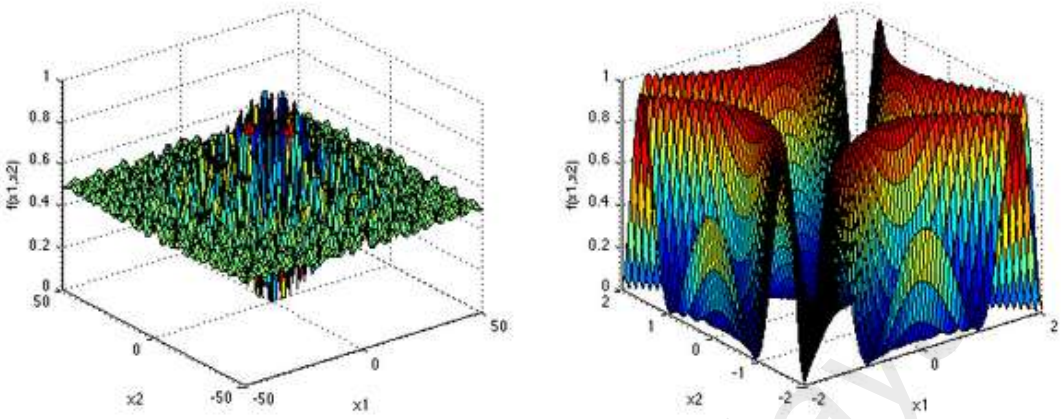


(a) (b)

Figure 2.11: Schaffer N2 test function

$$f(x) = 0.5 + \frac{sin^2(x_1^2 - x_2^2) - 0.5}{[1 + 0.001(x_1^2 + x_2^2)]^2} \quad (2.11)$$

There are multiple types of Schaffer test functions. Here, the Schaffer N2 test function is shown. The Schaffer N2 function is a minimization test function with many local optima and a single global minima point of 0 located at (0, 0). The model of the test function is as shown in equation (2.11). The Schaffer N2 is a 2 dimensional test function. Figure 2.11 (a) shows the plot of the function. To expose the details of it, the plot of the test function is shown in smaller input domain in Figure 2.11 (b). This test function is usually evaluated on a square from the range of -100 to 100 (Zhu & Kwong, 2010).

### 2.5.9 Shubert Test Function

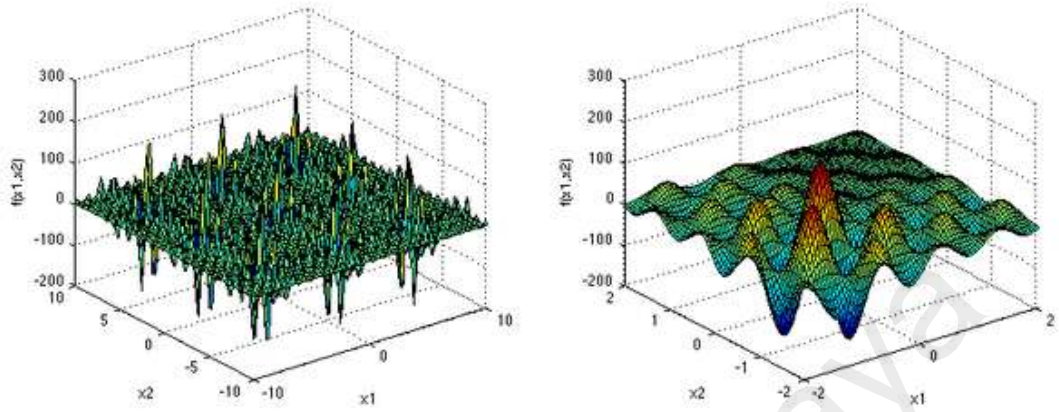


(a) (b)

Figure 2.12: Shubert test function

$$f(x) = \left[\sum_{i=1}^{5} i\cos\big((i+1)x_1 + i\big)\right]\left[\sum_{i=1}^{5} i\cos\big((i+1)x_2 + i\big)\right] \quad (2.12)$$

The Shubert test function is a continuous, multi model test function for minimization with many global minima points at the value of -186.7309, each accompanied with many local optima points in the surroundings. Any search algorithm that return value of -186.7309 is considered successful. The model of the test function is as shown in equation (2.12). The Shubert function is a 2-dimensional test function. Figure 2.12 (a) shows the plot of the function. To provide a better viewing on one of the global optima points, the plot is shown in smaller input domain in Figure 2.12 (b). This test function is usually evaluated on a square from the range of -10 to 10 (Liang et. al., 2014).

### 2.5.10 Six-Hump Camel Test Function

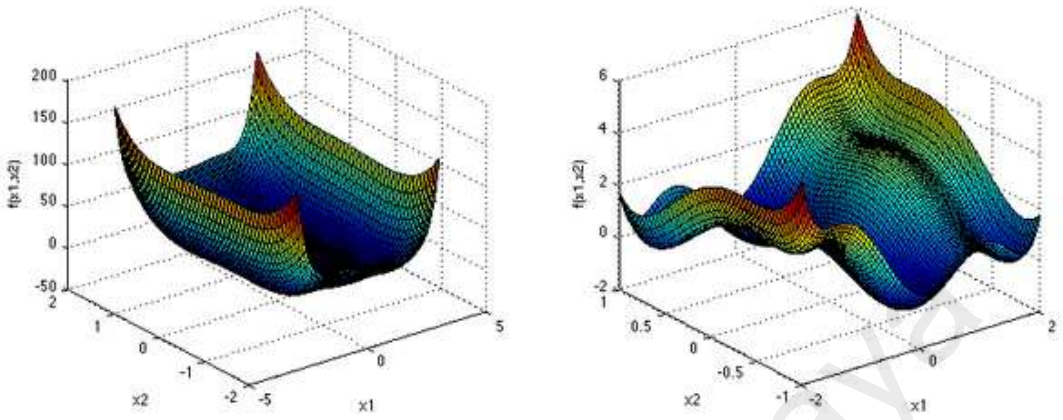


(a) (b)

Figure 2.13: Six-Hump Camel test function

$$f(x) = (4 - 2.1x_1^2 + x_1^4/3)x_1^2 + x_1x_2 + (4x_2^2 - 4)x_2^2 \quad (2.13)$$

The Six-Hump Camel test function is a continuous, multi model test function for minimization. As the name suggests, this test function comes with 6 local minima points, with 2 of them being the global minima at the value of -1.0316, located at (0.0898, -0.7126) and (-0.0898, 0.7126). Search algorithms that found any of the global optima points are considered successful. The model of the test function is as shown in equation (2.13). The Six-Hump Camel function is a 2-dimensional test function. This test function is usually evaluated on a rectangle of $X_1 \epsilon$ (-3, 3) and $X_2 \epsilon$ (-2, 2). Figure 2.13 (a) shows the plot of the function on its recommended input domain. Figure 2.13 (b) shows only a portion of this domain in order to allow easier viewing of the function's key characteristics.

## 2.6 Artificial Intelligence in Solar Energy

With the rapid growth in industries and the ever increasing sophistication of modern lifestyles, the world energy supply has been subjected to a tremendous strain. These phenomena have raised concerns over the energy security and environmental sustainability. With the fossil fuel diminishing, researchers around the globe are turning their attention into more renewable energy sources. Among others is the solar energy (Hoffert et al. 2002). Due to the abundance of the source itself, solar PV is envisaged to an important renewable energy source of the future.

A PV system is easy to install, almost maintenance free and shows minimal environmental damage (Cacciato et. al., 2010 & Esram et. al., 2006). Over the years, the development of PV energy harvesting systems has been very rapid. AI has been integrated into the harvesting systems research in order to maximize the energy they harvest. Research and development in the area of optimization of solar systems using various deterministic and stochastic techniques have been carried out to achieve an optimum performance on the design and operating parameters. In the literature, many optimization methods have been attempted onto PV systems in several different aspects. Many of the techniques proposed proved to be effective to further enhance the efficiency of the solar energy harvesting system.

### 2.6.1 PV Sizing

Sizing is an important part of PV systems design. It includes the optimal selection of the number of solar cell panels, the size of the storage battery, the regulator and the inverter to be used for certain applications at a particular site is an important economical task for electrification of villages in rural areas, telecommunications, refrigeration, water pumping and water heating. Besides being an economic waste, an oversized system can also adversely affect further utilization of solar cells and the pollution-free PV energy. At the present stage of development of PV technology, one of the impediments to a wider market penetration, as noted by Haas (1995), is the high investment costs of the PV systems.

The conventional methodology such as empirical, analytical, numerical, and hybrid for sizing PV systems have been used generally for a location where the required weather data and the information concerning the site where the PV system will be implemented are available. In such cases, these methods present a good solution for sizing PV systems, particularly the hybrid method. However, these techniques could not be used for sizing PV systems in remote areas, where the required data are not available. Moreover, the majority of the above methods need long-term meteorological data such as total solar irradiation, air temperature, clearness index, and wind speed for its operation. When the relevant meteorological data are not available, these methods cannot be used, especially in isolated areas. In order to overcome this issue, AI-based methods have been developed for sizing the parameters for PV systems (Mellit, 2006). Table 2.4 summarizes several representative examples of the use of AI in sizing PV systems.

Table 2.4: AI techniques in PV sizing.

| AI Technique | Area | Number of Applications |
|---|---|---|
| Neural networks | Sizing of stand-alone PV systems<br>Identification of the optimal parameter of PV system | 5 |
| Neuro-fuzzy | Sizing of stand-alone PV system | 1 |
| Wavelet and neural network | Sizing of stand-alone PV systems | 1 |
| Genetic algorithm | Sizing of hybrid system<br>Stand-alone wind-generator system<br>Optimization of control strategies for stand-alone<br>Optimal allocation and sizing for profitability and voltage enhancement of PV systems. | 6 |
| Neural network, neuro-fuzzy and genetic algorithm | Sizing of stand-alone PV system in isolated area. | 2 |

Mellit et al. (2003) developed an ANN model for the estimation of the sizing parameters of SAPVs. In this model, the inputs are the latitude and longitude of the site, while the outputs are two hybridizing parameters. These parameters allow the designers of PV systems to determine the number of solar PV modules and the storage capacity of the batteries necessary to satisfy a given consumption. Senjyua et al. (2007) developed an optimal configuration of renewable energy generating systems in isolated islands using GAs. This methodology can be used to determine the optimum number of solar-array panels, wind turbine generators and batteries configurations. Using the proposed method, the operation cost can be reduced by about 10% in comparison with diesel generators. A methodology for optimal sizing of standalone PV/wind-generator systems was also developed by Koutroulis et al. (2006), in which the proposed methodology is based on the GA and compared with linear programming.

Herna´ deza et. al. (2007) presented a systematic algorithm to determine the optimal allocation and sizing of photovoltaic grid-connected systems (PVGCSs) in

feeders that provide the best overall impact onto the feeder. The optimal solution is reached by a multi objective optimization approach. According to the authors, the results obtained with the proposed methodology for feeders found in the literature demonstrate its applicability. The method has been used to test alternative PVGCSs allocation solutions. Simulations in actual feeders prove that the allocation based on the stability voltage distribution achieves the best results. This outcome allows a significant reduction of computation involved in future analysis.

GAs and neural networks have been implemented to determine the optimal sizing parameters in isolated areas in Algeria (Mellit & Kalogirou, 2006). The GA optimized the sizing parameters relative to 40-sites in Algeria while the ANN predicted the optimal parameters in remotes area. Mellit (2006) developed a hybrid model to determine the optimal sizing parameters of PV system. This model combined neural network and fuzzy logic (FL) and is known as neuro-fuzzy. This neuro-fuzzy was implemented to predict the optimal sizing coefficient of PV systems based only on the geographical coordinates. Mellit et. al. (2004) also developed a suitable approach, which combines the ANN with wavelet analysis for the sizing of stand-alone PV. The proposed approach presents more accurate results compared with other methods in the benchmarking.



### 2.6.2 Tilt Angle Optimization

The design and development of solar energy systems require the knowledge of variation and maximum utilization of solar radiation falling on it. The measured solar

radiation data are not available for large number of sites, so it has to be estimated. A number of techniques are used for the estimation of solar radiation on horizontal surface (Bakirci, 2009, Chandel et. al., 2005). The amount of solar radiation received by a PV panel or a solar thermal collector is mainly affected by its orientation and tilt angle (El-Sebaii et. al., 2010. Demain et. al., 2013).

The solar panels are generally oriented toward the equator, in the northern hemisphere oriented toward south and in the southern hemisphere toward north. However, the solar radiation is site specific with diurnal, monthly, seasonal and yearly variations; as such the optimum tilt angle for capturing maximum solar radiation will also vary for every location. Armstrong and Hurley (2010) developed a methodology to determine optimum tilt angle for locations with frequently overcast skies using monthly sunshine duration data and hourly cloud observations. Under cloudy skies, it is important to differentiate between direct and diffuse radiation for a particular site to calculate optimum tilt angle so the Perez model is useful to calculate diffuse radiation falling on the solar panel. The tilt angle is changed from 0° to 90° in steps of 1°. The angle that maximizes the incident solar radiation on solar panel is selected by taking into account the frequencies of cloudy skies. The optimum tilt angle of grid connected and standalone PV system that matches the available solar radiation with the load demand is chosen.

In tilt angle optimization, solar radiation on the tilted surface is taken as the objective function. Several attempts have been carried out in the literature to solve this function using different optimization techniques like GA, SA and PSO. GA is suitable for optimization problems with complex nonlinear variables (Goldberg, 1989, Yadav et. al., 2011). A population of points is used for starting the GA instead of a single design point

(Sivanandam & Deepa, 2008). As discussed in previous sections, a GA involves principles of natural genetics and natural selection. The natural genetics are reproduction, crossover and mutation which are used in the genetic search procedure (Beasley et. al., 1993). Talebizadeha et. al. (2011) used GA to calculate hourly, daily, monthly, seasonally and yearly optimum tilt angle in Iran. The report showed that the optimum hourly surface azimuth angle is not zero and optimum tilt angles of photovoltaic panels and solar collector are found to be the same. The solar energy gain at daily, monthly optimum tilt angle is found to be the same but energy gain is found to show significant increment with hourly tilt angle adjustment. Therefore, it was concluded that hourly variation of tilt angle increased the harvested energy. Čongradac et. al. (2012) used GA and FL process to track the optimum blind tilt angle with angle rotated in anticlockwise and clockwise direction to maintain an accurate brightness in a room. This process is useful in maintaining user's comfort and saving energy.

SA derives its name from the simulation of thermal annealing of critically heated solids and is used to find the global optimum with a high probability of objective functions which contain numerous local minima. Chen et al. (2005) implemented SA in a fixed solar cell panel system. The SA was implemented as a one-off calculation for the optimum installation angle of the PV panels. The PSO, on the other hand, is a stochastic technique for exploring the search space for optimization with swarms of particles (Kennedy & Eberhart, 1995). Optimum angles can be tracked using PSO, in which the convergence is achieved by particles in multi-dimensional space, carrying a solution and a velocity value (Beasley et. al., 1993). Chang (2010) used the varying inertia weight methods (Shi & Eberhart1998a, 1999b) and proposed a particle-swarm optimization method with nonlinear time-varying evolution (PSO-NTVE) to determine the optimum tilt angles of PV modules for the maximization of output energy of the modules in Taiwan. The yearly

optimal angles were found to be 18.16° and 17.30°, 16.15°, 15.79°, 15.17°, 17.16°, 15.94° for Taipei, Taichung, Tainan, Kaosiung, Hengchung, Hualian, and Taitung respectively. The PSO-NTVE proved to converge quicker than the other variants of PSO and the GA in achieving an optimum solution.

### 2.6.3 PV Control, Modelling, and Simulation

A PV system can be combined with another energy source, such as wind, hydrogen and diesel, in order to develop a hybrid PV system. Modelling and simulation of a PV system is a very important step before implementation. Literature shows several AI in the modelling and control of PV systems and its components, which are based on analytical or numerical simulation.

Tawanda (2000) presented a method for predicting the long-term average conventional energy displaced by a PV system comprising a PV array, a storage battery, some power conditioning equipment with maximum-power tracking capability and an auxiliary power facility. System simulation is done over the average day of the month. A PV stand-alone system model is developed by Joyce et al. (2001). This model is based on current–voltage characteristic of the modules and on a linear relation between the battery voltage and the state of charge (SOC). The model was validated against experimental data of a 150Wp stand-alone system in Portugal and the performance of the measured system and model results were compared. A variable structure controller used to regulate the output power of SAPV hybrid generation system was proposed by Valenciaga et. al.

(2001). The proposed system comprises PV and wind generation, a storage battery bank and a variable monophasic load.

Karatepe et al. (2006) used a neural network-based approach to improve the accuracy of the electrical equivalent circuit of a PV module. The equivalent circuit parameters of a PV module mainly depend on solar irradiation and temperature. The dependence on environmental factors on the circuit parameters was investigated by using a set of current–voltage curves. It was shown that the relationship between them is nonlinear and cannot be easily expressed by any analytical equation. Ohsawa et al. (1993) applied an ANN for the operation and control of PV-diesel systems. El-Tamaly and Elbaset (2006) presented a complete study, from the reliability point of view to determine the impact of interconnecting PV/Wind Energy System (WES) Hybrid Electric Power System into utility grid (UG). Four different configurations of PV/WES/UG were investigated and a comparative study between these four different configurations was carried out. The overall system was divided into three subsystems, containing the UG, PV and WES. A generation capacity outage table was built for each configuration of these subsystems. The capacity outage tables of UG, PV/UG, WES/UG and PV/WES/UG were calculated and updated to incorporate their fluctuating energy production. A FL technique was used to calculate and assess the reliability of the system.

A simple PV simulation model capable of predicting the average PV output as a function of array geometry (slope and azimuth) and location was described and validated by Perez et al. (2004). This simulation tool is used in the Clean Power Estimator–a web-based PV economic evaluation program available in the US and several other countries. Results showed that the simplified model accurately captures array geometry, seasonal

and daily PV output variations when benchmarked against a standard PV simulation program. A methodology to estimate PV electrical production from outdoor testing data was presented in by Rosell & Ibanez (2006). The method was based on the adjustment of the well-known I–V model curve and a new maximum-power output expression. The method was developed to provide PV module performance parameters for all operating conditions encountered by typical PV systems.

## 2.7 Maximum Power Point Tracking

Photovoltaic cells are semiconductor devices that convert light energy into electricity at the atomic level through the photovoltaic effect (Wang et al., 2011). However, the low energy conversion efficiency of PV cells remains a barrier to the prolific growth of the PV energy source (Boukenoui et. al., 2016). For this reason, it is necessary to design a power converter that is not only high in efficiency, but also optimizes the energy production of the PV generator and ensures the harvest of maximum energy under any weather conditions. Although enormous amount of work has been carried out to improve the solar cell fabrication technologies (Parida et. al., 2011, Han et. al., 2011, Krebs, 2009), literature shows that the most economical way to boost the power yield of a PV system is by improving its maximum power point tracking (MPPT) capability (Seyedmahmoudian, 2016).

### 2.7.1 The Basic Idea

The aim of employing an MPPT mechanism is to ensure that at any environmental condition, particularly solar irradiance and temperature, maximum power is extracted from the PV modules. This is achieved by matching the MPP with its corresponding converter's operating voltage and current. A typical MPPT mechanism works as follows. First, the current and voltage of the PV array are sensed by a current and voltage sensors, respectively. These values are fed into an MPPT block that computes the MPP at that particular sampling cycle. Once found, the MPPT block delivers the reference values for the current (*I*) and voltage (*V*). These are the values that need to be matched by converter; in most cases, only one variable is selected and it is usually the voltage (Liu et. al., 2015). Then, the measured power value is compared with the present value of MPP. If there is a difference between the two, the duty cycle of the converter is adjusted in an effort to reduce the difference. The control is usually carried out by a PI or hysteresis controller. In certain cases, the duty cycle is determined directly without PI controller. Once the measured equals the reference values, the maximum power from the array is extracted. The basic block diagram of a typical PV system with MPPT is shown in Figure 2.14.

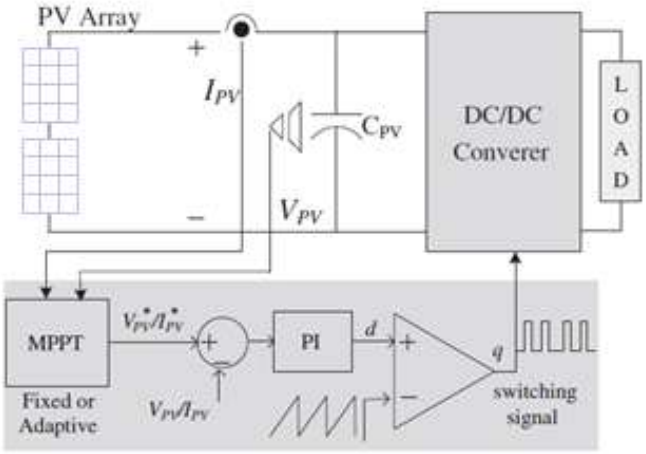


Figure 2.14: Basic MPPT with converter.

An accurate modelling is crucial for the simulation of the solar harvesting system. Single diode model is found to be the most common mathematical representation of the solar cell in the literature, even though there are other models available which uses additional diodes to represent the recombination effects of charge carriers (Liu et. al., 2015). In this work a single diode model is considered for the simulation of PV system as it is effective and provides a good compromise between simplicity and accuracy (Bounechba et. al., 2016). The equivalent circuit of this model is given in Figure 2.15.

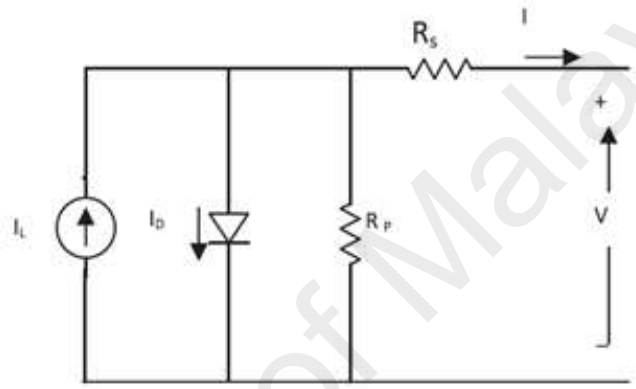


Figure 2.15: The single diode model.

The output current of photovoltaic cell is given below:

$$I = I_L - I_D - \frac{V+R_S I}{R_P} = I_L - I_S\left[\exp\left(\frac{V+R_S I}{V_t a}\right) - 1\right] - \frac{V+R_S I}{R_P} \quad (2.14)$$

Where, $V_t = \frac{kT}{q}$.

The photocurrent of PV cell is proportional to solar irradiation and is also influenced by the temperature according to the following equation:

$$I_L = (I_{Ln} + K_i \Delta T)\frac{G}{G_n} \quad (2.15)$$

The diode saturation current $I_s$ is given by

$$I_s = I_{sn}\left(\frac{T_n}{T}\right)^3 \exp\left[\frac{qE_g}{ak}\left(\frac{1}{T_n} - \frac{1}{T}\right)\right] \quad (2.16)$$

$$I_{sn} = \frac{I_{scn}}{\exp\left(\frac{Vocn}{aV_{tn}}\right)-1} \quad (2.17)$$

The remaining two unknown parameters $R_s$ and $R_p$ in (2.14) can be obtained iteratively by making the maximum power calculated from model to coincide with peak power from the datasheet at MPP. By varying *V* the corresponding values of *I* are obtained by solving (2.14) using numerical methods. Then, the P-V curve of the PV module can be obtained directly by multiplying $N_s$ series connected PV cells with voltage, *V* and $N_p$ parallel connected cells with current, *I*.

### 2.7.2 The P-V and I-V Curve

A PV module can be modelled as a current source that is dependent on the solar irradiance and temperature. The complex relationship between the temperature and irradiation results in a non-linear current–voltage characteristics. An example of I–V and P–V curve for the variations of irradiance and temperature is shown in Figure 2.16(a) and (b), respectively. It can be observed that the MPP is not a fixed point; it fluctuates continuously as the temperature or the irradiance does. Due to this dynamics, the controller needs to track the MPP by updating the duty cycle of the converter at every control sample. A quicker response from the controller to match the MPP will result in better extraction of the PV energy and vice versa.

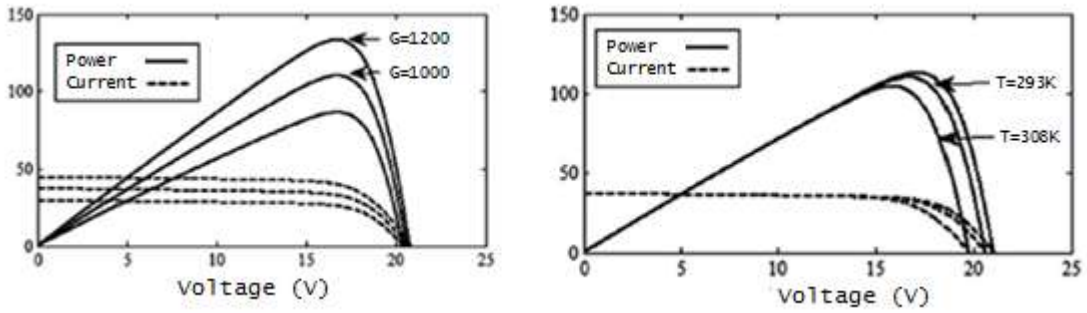


(a) (b)

Figure 2.16: Example of I-V and P-V cures under different temperature and solar irradiance.

### 2.7.3 Partial Shading Condition (PSC)

The MPP tracking becomes more complicated when the entire PV array does not receive uniform irradiance. This condition is known as partial shading. Typically, it is caused by the clouds that strike on certain spots of the solar array, while other parts are left uniformly irradiated (Di Piazza & Vitale, 2012). Another source of partial shading-like characteristics is exhibited by module irregularities; a common example would be the presence of cracks on one or more modules of the PV array. Figure 2.17(a) shows a PV array in a typical series–parallel configuration. Commonly, a bypass diode is fitted across the module to ensure that hot spot will not occur if that module is shaded. In this example, three modules are connected in a single string. In a normal condition, when the solar irradiance on the entire PV array is uniform, the P–V curve exhibits a unique maximum power point as shown in curve 1 of Figure 2.17(c). However, during partial shading in Figure 2.17(b), the difference in irradiance between two modules activates the

bypass diode. As a result, two stairs current waveform is created on the I–V curve, while the P–V curve is characterized by multiple maxima points, as depicted by curve 2 of Figure 2.17(c). The MPPT needs to ensure that the tracked maximum point is the true global peak, not one of the local maxima. If the algorithm is trapped at the local peak, significant loss in power incurs.

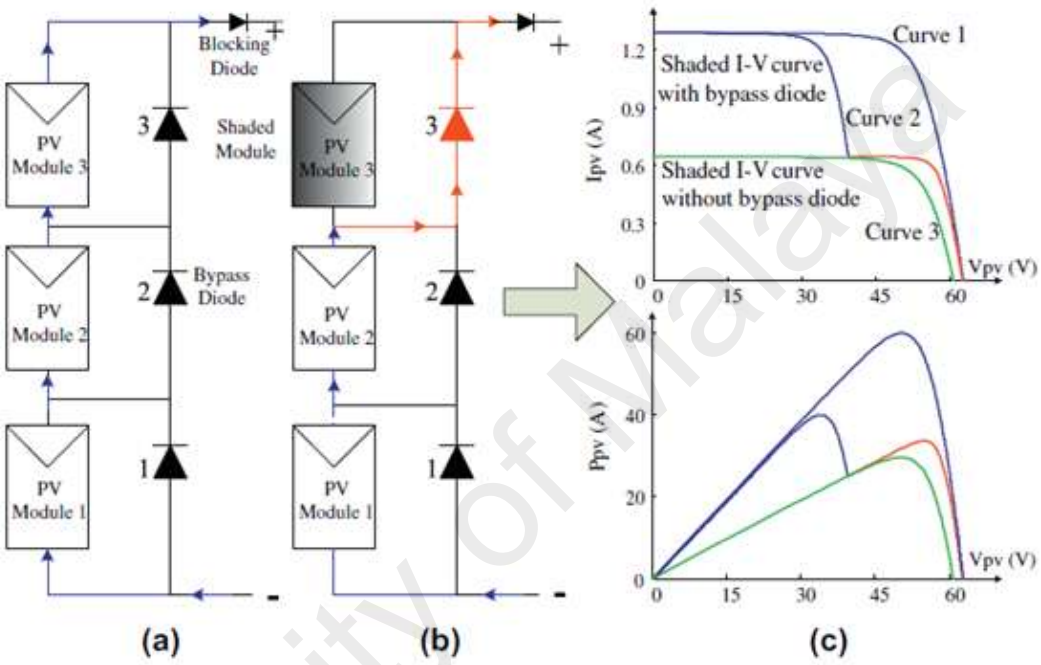


Figure 2.17: Example of the condition of a PV array under (a) uniform irradiance and (b) partial shading condition. The resulting I-V and P-V curves is shown in (c).

### 2.7.4 AI in MPPT

Conventional MPPT operates by sensing the current and voltage of the PV array; the power is calculated and accordingly the duty cycle of the converter is adjusted to match the MPP. With the recent availability of vast and low cost computing power, MPPT

based on soft computing (SC) techniques are attracting considerable interests. The guiding principle of SC is exploiting the tolerance for imprecision, uncertainty, partial truth and approximation to achieve tractability, robustness and low cost solution. The most important feature of SC is the flexibility of the algorithms, which allows for the development of robust MPPT schemes. This is made possible as SC techniques are fully digital. Furthermore, SC is known to be very effective in handling non-linear complexities.

Since MPPT problem primarily centres on its non-linear PV curve (Ioulia & Purvins, 2012, Amrouche et. al., 2012), it is natural to solve it using SC techniques. In addition, due to the adaptive nature of their algorithms, SC is envisaged to be easily adaptable to cater for the adverse environmental conditions such as partial shading (Ishaque et. al., 2011) and rapid changes in irradiance (Kobayashi et. al., 2004). Many SC based MPPT schemes have been developed over the years. Examples include Perturb and Observe (P&O) (Jainand & Agarwal, 2004, Femia et. al., 2005), GA (Mohajeri et. al., 2012, Shaiek et.al., 2013), Hill Climbing (HC) (Koutroulis et. al., 2001, Xiao & Dunford, 2004), Artificial Neural Network (Hiyama et. al., 1995, Al-Amoudi & Zhang, 2000), and Incremental Conductance (IC) (Kuo et. al., 2001, Kobayashi et. al., 2003, Lin et. al., 2011). They are widely employed in many commercial dc–ac inverters (for grid-tied) and dc–dc converters (for battery chargers). Despite having the same objectives, the various MPPT techniques differ markedly in terms of convergence speed, accuracies and cost effectiveness.

### 2.7.4.1 Perturbation and Observation (P&O)

The perturb and observe (P&O) algorithm is one of the most commonly used MPPT mechanisms in practice because of its ease of implementation (Verma et. al., 2016). The method is an iterative approach, in which operating point of solar PV oscillates around the maximum power point. This method has a structure of a simple regulation, and few parameters of measurement. The PV voltage and current are measured initially and the corresponding power, $P$ is calculated. Then, as the name suggests the conventional P&O algorithm operate periodically by perturbing the duty cycle of the DC–DC converter and comparing the PV output power with that of the previous perturbation cycle. If the power is increasing the perturbation will continue in the same direction in the next cycle, otherwise the perturbation direction will be reversed (Jubaer & Zainal, 2015, Saravanan & Ramesh, 2015). The slope is obtained using Equation (2.18).

$$\frac{dP}{dV_{PV}}(n) = \frac{P(n) - P(n-1)}{V_{PV}(n) - V_{PV}(n-1)} \tag{2.18}$$

where $\frac{dP}{dV_{PV}}(n)$ is actual derivative of power and voltage of PV, $P(n)$ is actual power, $P(n-1)$is previous power, $V_{PV}(n)$ is actual voltage and $V_{PV}(n-1)$ is previous voltage. If $V > V_{mpp}$ the operating point slides towards left and when $V < V_{mpp}$ the operating point slides towards right of the curve, where $V_{mpp}$ is voltage at maximum power point. The P&O algorithm is shown in Figure 2.18.

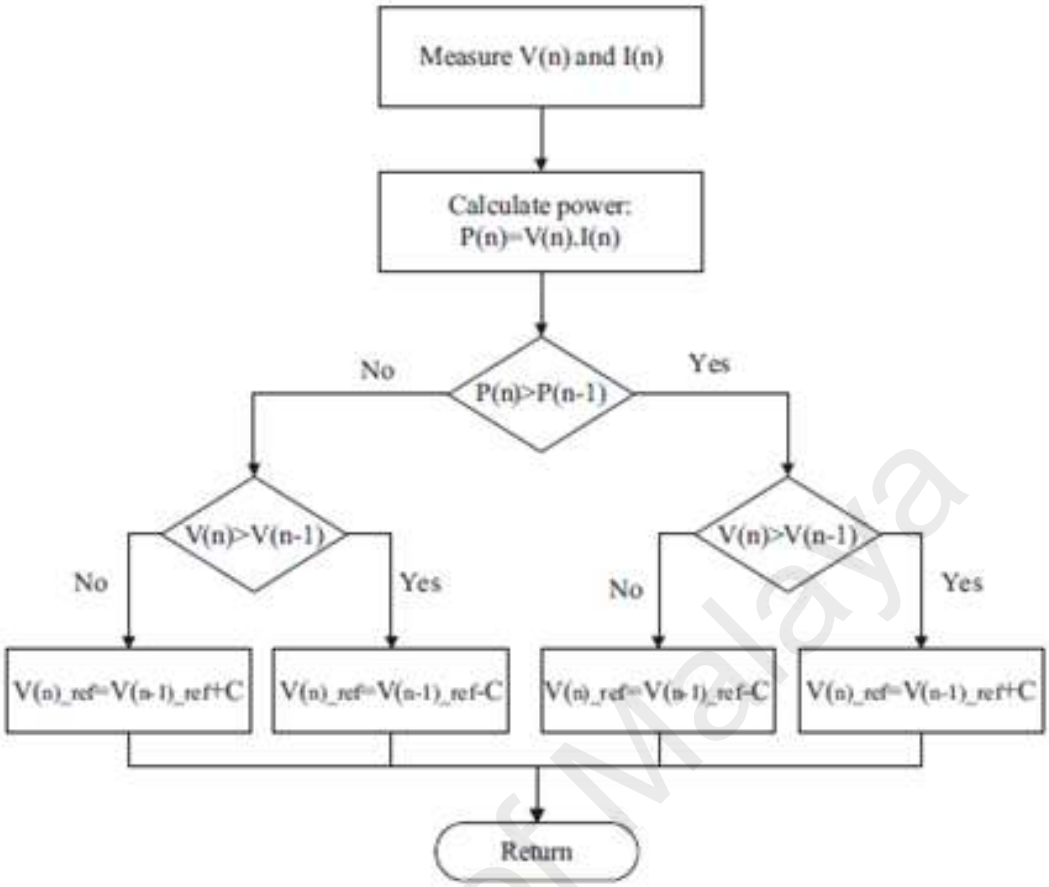


Figure 2.18: The flow of P&O algorithm.

The benefit of the P&O method is that it is easy to implement. The simple structure of the process and few required parameters make these algorithms widely used in commercial systems (Zhang, 2008). The limitations of this method include relatively slower response speed, oscillation around the MPP in steady state condition and tracking deviation from the maximum operating point under fast changing environmental condition. In the P&O method, treatments have to be in opposite direction when the additive contribution is negative. Under these conditions, the tracker seeks the maximum of power permanently. Nevertheless, the change in power is only considered as a perturbation of the output voltage and the algorithm does not compare this voltage with the present MPP voltage. As a consequence, when the MPP is reached, the tracker will oscillate around it, resulting in a loss of PV available power, especially in shaded atmospheric conditions with constant or slowly varying changes. Thus, the setting of the

perturbation size is important to provide good performance in both steady state and dynamic response (Liu, 2008, Xiao & William, 2004). In addition, in presence of rapidly changing atmospheric conditions e.g. occurrence of clouds, the P&O algorithm can be confused. It is noted that due to the change of the solar radiation, the P&O algorithm deviates from the MPP until a slow solar radiation change occurs or settles down (Sera et. al., 2007).

Over the years, many variations of the P&O method were proposed by various authors. In (Abdelsalam et. al., 2011, Al-Amoudi & Zhang, 1998, Zhang et. al., 2000), adaptive P&O methods were presented. The systems operated according to the previous data. It used the previous duty ratio as the perturb step rather than PV array current or voltage. The main disadvantage in this method is the computational problem for heavy loading conditions. A multivariable P&O is proposed by Petrone et. al. (2011). This method uses many perturb variables instead of one variable. It is used to extract more power from the PV. The system will manage the variables and perturbations which lead to the best operating point in steady state conditions. The drawback of the system is the complexity when compared to conventional method. In the research conducted by Khaehintung et. al. (2006), a variable perturbation size adaptive P&O was proposed. This method was mainly used to track the maximum power under rapidly changing condition. An estimated perturb–perturb (EPP) method was proposed by Ansari et. al. (2009). The EPP method used two operating modes, mode 1 for estimate process and mode 2 for perturbation. The name "estimated-perturb–perturb" gives all information about the principle of this method. After two perturbations (mode 2 in which determination of next PV voltage is done) there is one estimation mode in which controller stops tracking MPP by keeping PV voltage constant and measures only the power variation or voltage variation due to environmental changes for the next control period.

### 2.7.4.2 Hill Climbing

Similar to P&O, the hill climbing (HC) method involves a perturbation in the duty ratio of the power converter. P&O, on the other hand, involves perturbation in terminal voltage to perform MPPT (Teulings et. al., 1993, Koutroulis et. al., 2001). There are several authors who focused their work on hill climbing MPPT (Teulings et. al., 1993, Hashimoto et. al., 2000, Koutroulis et. al., 2001, Veerachary et. al., 2001, Xiao & Dunford, 2004). The methodology is explained in the Table 2.5.

Table 2.5: Methodology of hill climbing method.

| Perturbation in terminal voltage | Change in power | Next perturbation |
|---|---|---|
| Positive | Positive | Positive (increment in duty ratio '$\delta$' ) |
| Positive | Negative | Negative ( decrease in duty ratio '$\delta$' ) |
| Negative | Positive | Negative ( decrease in duty ratio '$\delta$' ) |
| Negative | Negative | Positive (increment in duty ratio '$\delta$' ) |

HC tunes the duty ratio of the power converter periodically, and then it compares the PV output power with that of the previous cycle of perturbation (Xiao & Dunford, 2004). When PV power and PV voltage increase at the same time and vice versa, a movement step size, $\Delta D$ will be added to the duty cycle, $D$ to generate the next cycle of movement in order to force the operating point to move towards the MPP. When PV power increases and PV voltage decreases and vice versa, the movement step will be subtracted for the next cycle of tuning (Ngan & Tan, 2011). This process will be carried on continuously until MPP is reached. It should be noted that, the system will also oscillate around the MPP throughout this process, and this will result in loss of energy. Therefore, reducing the movement step size will minimize these oscillations but it slows down the MPP tracking system (Fangrui et. al., 2008, Marcelo & Ernesto, 2009).

The advantages of this algorithm are simplicity and ease of implementation. However, HC has limitations that reduce its MPPT efficiency. One such limitation is that as the amount of sunlight decreases, the P–V curve flattens out. This makes it difficult for the algorithm to discern the location of the MPP, owing to the small change in power with respect to the movement of the voltage. Another fundamental drawback of HC is that it cannot determine when it has actually reached the MPP. Instead, it oscillates around the MPP, changing the direction of the movement after each $\Delta P$ measurement. Also, it has been shown that HC can exhibit erratic behaviour under rapidly changing irradiance levels (Chee Wei et. al., 2007). Femia et. al. (2005) optimized the sampling process while D'Souza & Lopes (2005) simply applied a high sampling rate. Xiao and Dunford (2004) introduced a toggling between the traditional hill climbing algorithm and a modified adaptive hill climbing mechanism to prevent deviation from the MPP. Kasa et. al. (2005) estimated the PV array current from the PV array voltage, eliminating the need for a current sensor. Kim et. al. (1996) found out that digital signal processor or microcomputer control is more suitable for hill climbing and P&O even though discrete analogue and digital circuitry can be used.



#### 2.7.4.3 Genetic Algorithm and MPPT

GA is categorized under the evolutionary algorithm. As mentioned in the previous sections, it is a problem-solving techniques based on principles of biological evolution. In the process, some inputs are assigned as chromosomes, which are recombined or mutated and then tested to fulfil a predefined fitness function. Since the objective of the

evolution is to create a better species than its predecessor, GA finds the best solution by a random combination of different genes.

The initial set of chromosome is defined as the searching parameters of the optimization problem. In case of MPPT, such parameters can be either voltage or duty cycle. The initial parent population is shown in equation (2.19).

$$X^i = [Parent^1 \cdot Parent^2 \cdots Parent^N] \quad (2.19)$$

where *n* is the population size, and each parent represents initial voltage values in which the algorithm starts the evaluation process. Chromosome can be defined in a real or binary coded numbers. The objective function $f(x^i)$ is the generated power at the output of the PV system, which is the PV curve equation (Kumar et. al., 2015).

For the case of MPPT, it is important to decide the length of the chromosome because a larger population requires less time to converge but such generation increases processing time. Next, the algorithm utilizes the crossover and mutation operation to change the DNA of the chromosomes, creating new generations of chromosomes. This new generation is evaluated through fitness function and is assigned a new fitness value. After consecutive iteration chromosome with the highest fitness value is chosen as the optimized parameter for MPP.

In the research conducted by Mohajeri et. al. (2012), an MPPT controller was developed based on the GA approach, and the proposed method was verified through two different case studies, each presenting different PS patterns. The verification part of both studies is limited to simulation validations. In another study by Shaiek et. al. (2013), the

performance of the GA-based MPPT method was compared with conventional P&O and the incremental conductance method under two predefined partial shading conditions (PSCs). As in previous work, the verification part is limited to simulations. In addition, the mutation steps are eliminated in the report. Therefore, the stochastic characteristic of the designed GA is diminished. Daraban et. al. (2014) integrated the P&O method with GA, reduced the population size, and decreased the number of iterations. The proposed method shows a faster convergence, as well as a more accurate output, for a PV system under various PSCs.

The GA has also been used in hybrid methods to improve the performance of other MPPT techniques. For instance, in the research conducted by Messai et. al. (2011), the GA was used to tune the parameters of a fuzzy logic controller (FLC) used in MPPT under PSCs where GA chooses optimally and simultaneously both membership functions and control rules for the FLC. GA-FLC-based MPPT is better than the ones obtained with classical P&O controller, since the response time in the transitional state is shortened and the fluctuations in the steady state are considerably reduced. The performance of the fuzzy logic controller improved as parameters, such as rule base and membership functions, are tuned to their optimized values by using GA techniques. In another study, the GA method was used as a tool to train the ANN system (Kulaksız & Akkaya, 2012). In this approach, the GA trained ANN provided the reference voltage corresponding to the maximum power for any environmental changes.

### 2.7.4.4 Artificial Neural Network (ANN)

An ANN is a computational model that uses interconnected artificial neurons to mimic the ability of biological brains. Primarily, it comprises of an input, hidden and output layers. A possible structure of ANN, tailored for MPPT is shown in Figure 2.19. The input variables can be PV array parameters such as irradiance, temperature, wind speed or any combination of these. The neurons in the input layer are responsible only for transmitting the input information to the hidden layer. By using large amounts of training data, the ANN continually adjusts the weighting and bias values, allowing the network-calculated output to approximate the target output. One of the most common ANN learning methods is the back-propagation method. The output can be designated as either the voltage, current or duty cycle, depending on the control variables used for the converter. In each layer the numbers of nodes varies and is user defined.

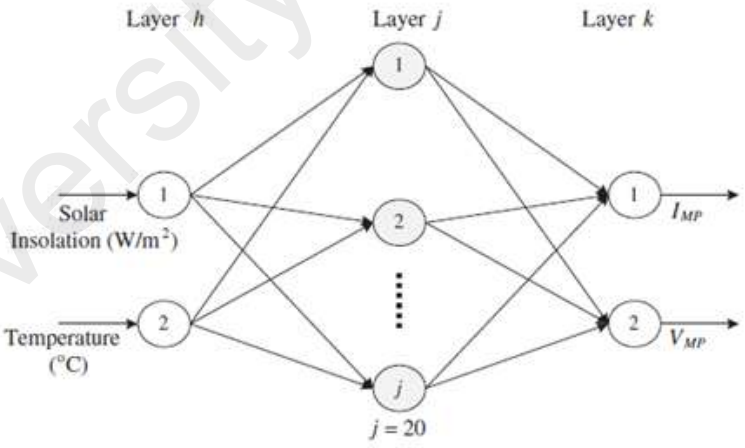


Figure 2.19: A typical ANN structure for MPPT.

The advantage of ANNs is their parallel computing capability. Other SC methods may require multiple iterations to obtain the optimal solution, whereas ANNs can use simple multiplication and addition to rapidly calculate output. Therefore, ANNs enable

rapid calculation. However, the accuracy of an ANN is determined based on its training data. If the training data are insufficient, or the data do not cover the entire problem space, then the accuracy of the ANN will be reduced accordingly. The ability of the ANN to track the MPP depends on hidden layer's algorithm and how careful and extensively the networks are trained. Typically, the ANN needs to be trained and tested for months or even years to ensure that the MPPT responds correctly to various meteorological conditions (Hiyama et. al., 1995). During the training, the neurons are weighted appropriately to match the input–output pattern correlation.

Currently, the ANN-based MPPT method are mostly used in uniform insolation conditions (Al-Amoudi & Zhang, 2000) primarily because at a single irradiance level, the location of the MPP is only related to the irradiance and the temperature. It is important to note that once a particular ANN is trained and designed for a specific PV module or climate, it may not respond accurately if employed in a different condition. Thus, when a PSC occur, the irradiance of the module, module temperature and shading pattern all affect the MPP location. Consequently, the training data required by the ANN substantially increase, and these data are not easily collected. This is the primary limitation of applying ANNs to MPPT. Therefore, only a few works in current literature proposed using ANNs as the primary method for addressing PSC. The input variables used in (Veerachary & Yadaiah, 2000) and (Yadaiah et. al., 2005) were the averaged irradiance of selected modules, and the design was affected by the arrangement method of PV modules. Therefore, if the architecture of the PV array changes, such as adding new PV panels, the ANN must be re-trained. In addition, irradiance and temperature sensors are more expensive compared with the voltage and current sensors used in other MPPT methods.

Table 2.6: Summary of ANN related work for MPPT.

| Authors | Control variable | Converter type/ Application | Remarks |
|---|---|---|---|
| Veerachary and Yadaiah | Voltage | Buck-boost converter for standalone applications | ANN is used as the MPPT controller. The MPP is identified using gradient descent algorithm training. Work is extended for permanent magnet series motor. |
| Alabedin et al. | Duty cycle | Buck converter for standalone applications | ANN is used as an optimizer for P&O MPPT controller. Improved performance in dealing with the fluctuations in the array power. |
| Jinbang et al. | Duty cycle | Boost converter for standalone applications | ANN is used as an optimizer for IC/P&O MPPT controller. Faster than the IC and exhibits smaller steady- state error than the P&O algorithm. |
| Islam and Kabir | Voltage and Current | Buck converter for standalone applications | ANN is used as the MPPT controller. Utilizes only 20 nodes in the hidden layer, which reduces its complexity and increases the execution time. |
| Jie and Ziran | Voltage | Buck-boost converter for standalone applications | ANN is used as the MPPT controller. The method uses a 2 level ANN, which has higher speed and accuracy compared to single level ANN. |
| Veerachary et al. | Voltage | Boost converter for standalone applications | ANN is used as an optimizer for the feed forward FLC MPPT. The ANN is trained using the BP algorithm to estimate the reference voltage on-line. Tracking performance is improved. It also avoids the tuning of PI controller parameters. |

In certain cases, ANN is not used as the MPP tracker itself; rather it is utilized to identify the optimized parameters of another MPPT controller. For example, ANN is used as optimizers for traditional MPPT such as P&O or IC methods (Alabedin et.al, 2011, Jinbang et. al., 2011). In general, these combinations result in improved performances (Jie & Ziran, 2011, Veerachary et. al., 2003, Ramaprabha et. al., 2011). A summary of the ANN related researches for MPPT is shown in Table 2.6.

### 2.7.4.5 Fuzzy Logic Controller

Traditional control system design requires understanding the system being controlled; that is, using precise mathematical models to describe the system. However, when the controlled system becomes overly complex, it is often difficult to use system identification method to establish a system model. In early studies, the FLC is introduced for MPPT, where $dP_{pv}/dI_{pv}$ and its change $\Delta(dP_{pv}/dI_{pv})$ are considered fuzzy controller inputs (Simoes et. al., 1998). A general FLC structure is shown in Figure 2.20. It consists of three processing stages, namely fuzzification, rules inferences and defuzzification. In addition, it has a rule table in which the designed rules are stored. The process in which the FLC performs the calculation is called rules inference.

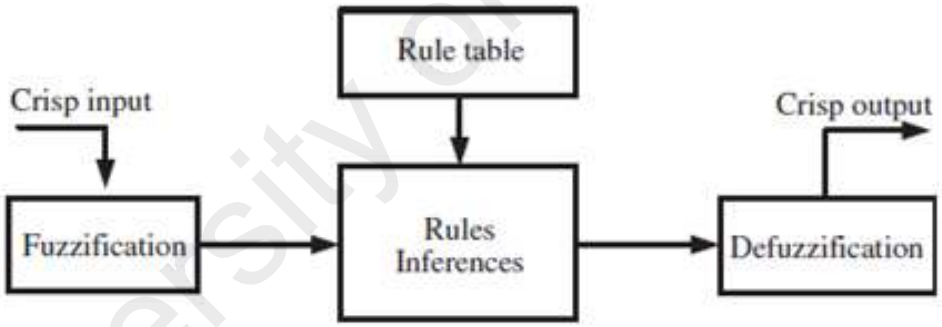


Figure 2.20: Basic fuzzy logic structure.

In a FLC-based MPPT, the inputs are usually an error $E$ and a change in error $\Delta E$. Since $dP/dV$ vanishes at the MPP, both inputs can be calculated as follows:

$$E(K) = \frac{P(k)-P(k-1)}{V(k)-V(k-1)} \quad or \quad E(K) = \frac{P(k)-P(k-1)}{I(k)-I(k-1)} \tag{2.20}$$

$$\Delta E = E(k) - E(k-1) \tag{2.21}$$

where $P$ and $V$ represent the power and voltage in P–V curve, respectively. Once $E$ and $\Delta E$ are computed, they are converted to the linguistic variables based on a membership function. The variable assignment is user dependent and are typically designed based on the user's experience for a specific control problem. The membership function is sometimes made less symmetric to give more importance to specific fuzzy levels (Chian-Song, 2010).

In the defuzzification process, the FLC output is defined linguistically in terms of voltage, current or duty ratio of the power converter. It can be looked up in a rule table. The linguistic variables assigned to the output for the different combinations of $E$ and $\Delta E$ are based on the power converter as well as the knowledge of the user. Next, the linguistic output signal is converted to numerical values by a process known as defuzzification. This can be achieved using several methods; one example is the "centre of gravity", which utilize the following formula:

$$D = \frac{\sum_{j=1}^{n} \mu(D_j) - (D_j)}{\sum_{j=1}^{n} \mu(D_j)} \tag{2.22}$$

where $j$ is the number of sampled duty cycle.

FLC provides a systematic approach to create automatic control algorithm by exploiting linguistic variables, based on experts' knowledge. In contrast to the binary logic, fuzzy variables may assume a value between 0 and 1. Such controllers are advantageous when working with imprecise inputs as it does not require an accurate mathematical model. The latter is a significant advantage because the uncertainties such as un-modelled physical quantities, non-linearity and unpredictable changes in operating

point can be excellently dealt with (Wu et. al., 1999). Furthermore, FLC is known to be very efficient in handling non-linearity problems.

One of the major disadvantages of pure FLC is its inability to handle partial shading. In order for it to do so, the rule table needs to change dynamically. However, this is not possible because once the rule table is set, it would be very difficult to change it as the controller is in tracking mode. Hence, there is no reported work on partial shading using standalone FLC. Karatepe et al. (2008) used distributed architecture and utilized FLC to replace traditional MPPT methods. Because each power converter contained a designated MPPT controller, the system guaranteed that the global MPP can be tracked. The advantage of the method used by Karatepe et. al. (2008) is its rapid tracking speed and high tracking accuracy; its disadvantage is that it exhibited a higher hardware cost compared with that of centralized architectures.

In Larbe et. al. (2009) and Letting et. al. (2010) optimized the performance of fuzzy logic controller through GA and PSO approaches, respectively. Alajmi et. al. (2013) used a method similar to the two-stage searching method to conduct MPPT. This method first swept the P–V characteristic curve and recorded various local MPPs, then replaced P&O by using FLC to conduct global MPPT. This method yielded a rapid tracking speed, but demonstrated disadvantages similar to those of other two-stage searching methods. In most work, FLC is used to design MPPT by manipulating different types of PV inputs. Combination of FLC with other SC algorithms is also attempted to increase the MPPT efficiency and tracking ability. Some of the important research on FLC based MPPT are summarized in Table 2.7.

Table 2.7: Summary of FLC related work for MPPT.

| Authors | Control variable | Converter type/ Application | Remarks |
|---|---|---|---|
| Mahmoud et al. | Voltage | Buck converter for stand-alone application | Does not need modification in membership functions and rules while testing with different resistive loads. |
| Veerachary et al. | Voltage | Interleaved dual boost converter for stand-alone application | A feed-forward MPPT for dual boost converter. The reference voltage for the feed-forward loop, is obtained by an off-line trained ANN. |
| Khaehintung et al. | Voltage | Boost converter for stand-alone application | FLC membership functions are made less symmetric to give more significance to the specific linguistic variables. |
| Chung-Yuen | Duty cycle | Boost converter for stand-alone application | FLC is operated into two modes: coarse and fine. Has higher efficiency than traditional hill climbing method. |
| Simoes et al. | Duty cycle | Boost converter for stand-alone application | PV array power variation and duty ratio are used as inputs for the FLC. It does not need any parameter information. |
| Masoum et al. | Duty cycle | Buck converter for stand-alone application | Three inputs FLC MPPT: array current, power and duty-cycle of converter. |
| Chian-song and Fuzzy | Duty cycle | Buck converter for stand-alone application | FLC-MPPT based on A Takagi-Sugeno (T-S) observer for state feedback to achieve asymptotic control. Directly drives the system to MPP without searching the maximum power point and measuring irradiance. |
| Kottas et al. | Duty cycle | Boost converter for stand-alone application | A Fuzzy Cognitive Networks (FCN) with voltage, current, temperature and solar irradiance used as the nodes. Exhibits excellent tracking speed but at the expense of an additional switch and a sensor. |
| Alajmi et al. | Duty cycle | Boost converter for micro-grid application | Application of FLC to improve the performance of the conventional HC method. The FLC is developed by translating the HC algorithm into 16 fuzzy rules to ensure better tracking speed and efficient convergence. |

Table 2.7, continued: Summary of FLC related work for MPPT.

| Authors | Control variable | Converter type/ Application | Remarks |
|---|---|---|---|
| Patcharapraand | Duty cycle | Boost converter for grid-connected application | An adaptive FLC is proposed to facilitate the constant tuning of the membership functions and the rule based table in order to achieve optimum performance. |
| Wu et al. | Duty cycle | Inverter for grid-connected application | The scaling factor of both fuzzy inputs and output are automatically tuned to achieve the better dynamic performance of MPPT. |
| Pumama et al. | Duty cycle | Boost converter for DC-DC application | FLC is optimized by Hopfield Neural Network which is proven applicable in partial shading. Convergence time is less than P&O and typical FLC controller. |
| Subiyanto et al. | Voltage | Boost converter for DC-DC application | Fuzzy P&O MPPT (FMPPT) is developed which is supported by offline tracking function to avoid local maxima. |
| Syafaruddin et al. | Duty cycle | Buck-Boost converter for DC-DC application | A novel method is proposed which is a combination of ANN and polar coordinated FLC. ANN is offline trained under several conditions including partial shading. |



### 2.7.4.6 Other Immerging Techniques

Aside from these techniques discussed above, there are other emerging approaches for MPPT which have only recently been proposed and discussed in a limited number of publications. These emerging approaches do present good approaches to global MPP tracking, and are likely to be the focus of future research attention. Among the others is the DE algorithm, which is used for global optimization applications. The DE has a

similar concept to GA and was first introduced by Stornand Price (1997, 1995). In this algorithm, existing particles with the best fitness records remain in the population, while the others are replaced by new particles. The DE method was recently applied in different extents to solve the control issues of renewable energy systems, including the problem of global MPP tracing in PSCs. In the DE-based MPPT method, the target vector is normally considered the duty cycle of the designed DC-DC converter. The DE approach in the MPPT problem was first presented in (Taheri et. al., 2010, Tajuddin et. al., 2012) where a standard DE algorithm was used. However, the method is based on static objective function in which the P-V curve must be predetermined, which makes the method impractical for real-time MPPT application (Mohammad et. al., 2013).

The ACO has also been attempted in the MPPT. It is an optimization method based on swarm intelligence; its primary advantage is immediately adapting command values according to environmental changes. Thus, ACOs are suitable for conducting MPPT in changing environments. As mentioned in previous sections, each agent in an ACO selects its path randomly at first. If the path the agent chooses is short with has high fitness value, the agent leaves concentrated pheromone on the path. In the next iteration, the agent chooses its path based on the concentration of pheromone on that path. The more concentrated the pheromone is, the higher probability it will be for the agent to choose that path. Based on the principle represented by the mentioned equations, Jianga et al. (2013) used ACO to solve MPPT problems. Simulated results were given in the report.

PSO is also an optimization method based on swarm intelligence. In the PSO method, each particle is defined by its own position and velocity. The behaviour of particles within the swarm is influenced by the experiences of neighbouring particles.

Each particle follows the current best-performing particle to search within the solution space. Since PSO is an optimization method based on swarming, it can conduct MPPT in distributed architecture (Chowdhury & Saha, 2010, Chen et. al., 2010, Miyatake et. al., 2011) or centralized architecture (Ishaque et. al., 2012a, 2012b, Liu et. al., 2012, Ishaque & Salam, 2013). Regarding algorithms, Chowdhury and Saha (2010) used adaptive perceptive PSO, whereas the remaining references used basic PSO algorithms. In (Ishaque & Salam, 2013), random number in the accelerations coefficient is removed, developing a deterministic PSO mechanism that improved the tracking speed. A few conference papers also show similar PSO methods (Kamejima et. al., 2011, Phimmasone et. al., 2011, Keyrouz & Georges, 2011, Keyrouz et. al., 2012).

In the Incremental Conductance (IC) technique, the PV array voltage gets modified based on the instantaneous and adjusted value of PV module. As the tracking of control variable is done rapidly it helps to overcome the disadvantage of some other methods which fail to track the peak control variable under fast varying conditions. The slope of the PV array power curve is zero at the MPP, positive when the operating point is on the left of MPP, and negative when the operating point is on the right of MPP (Saravanan & Ramesh, 2015). The control algorithm increase or decrease the voltage reference at which the PV array is forced to operate ($V_{ref}$) to track the new MPP. The main disadvantage of this system is its adjustment size and complex control circuits (Esram & Chapman, 2007, Kuo et. al., 2001, Irisawa et. al., 2000, Wu et. al., 2003). To overcome the disadvantage of the adjustment size, some modified IC methods can also be found in the literature (Soon & Mekhilef, 2014, Hiren & Vivek, 2008, Xiao & Dunford, 2007).

Beside the mentioned techniques, there are other simpler methods such as the Fractional Short Circuit Current (Masoum et. al., 2002, Noguchi et. al., 2000), Fractional Open Circuit Voltage (Hart et. al., 1984, Noh et. al., 2002) and Ripple Correlation Control (Midya et. al., 1996, Arcidiacono et. al., 1982) that are used for low cost applications, such as street lightings. These MPPTs exhibit limited accuracy but they require fewer sensors; thus offering a reliable, low cost solution. Other methods include Current Sweep (Bodur & Ermis, 1994), DC-link Capacitor Drop Control (Kitano et. al., 2001), Load Current and Load Voltage Minimization (Shmilovitz, 2005), *dP/dV* or *dP/dI* Feedback Control (Sugimoto & Dong, 1997), Linear Current control (Pan et. al., 1999), State-based MPPT (Solodovnik et. al.,2004), Best Fixed Voltage algorithm (De Carvalho et. al., 2004), Linear Reoriented Coordinate (Rtiz-Rivera & Peng, 2004) and Slide Control method (Zhang et. al., 2004, Kim, 2006). These techniques are reported in various in academic journals but it is unclear if they are practically implemented in commercial PV systems.

#### 2.7.4.7 Handling Partial Shading Condition

Shading has always been a major challenge in the MPPT research field. Salam et. al. (2013), in their report, mentioned that some traditional MPPTs like the P&O, IC and HC methods face difficulties in identifying the global MPP from the local MPPs when the PV curve consists of more than one peak. The aforementioned methods tend to converge to the first peak in the P–V curve, which can be a local peak. Hence, the power produced by the PV system is significantly reduced, resulting in low MPPT efficiency (Mellit and Kalogirou, 2014; Rezk and Eltamaly, 2015). For the case of ANN, handling

partial shading is also impractical, unless the shading is predictable; for example fixed spots shadows from building structures or trees. In such cases, the ANN can be trained to adapt for such conditions. However, with regard to environmental uncertainties, such as shading due to clouds, training the ANN is not possible due to the random nature of their occurrences. For the standalone FLC, tracking the varying global peak is not a straightforward task. This is because its membership function and control variables are static, while partial shading incidences can be highly dynamic (Patcharaprakiti & Premrudeepreechacharn, 2004). Thus, it is found that the search based SC techniques are naturally suitable to handle partial shading. This is primarily due to their ability to scan the entire P–V curve and subsequently discriminate between the global and local peaks. The challenge, however, is to optimize the search time so that the MPPT dynamic response can be improved.

From the study, it can be concluded that the output power of a PV system can be significantly boosted by optimizing the operating voltage value of the system to the maximum power point. Pattern recognition techniques are not suitable for the MPPT applications as the weather and climate can change rapidly and even unpredictably. As for optimization algorithms, there is still room for improvement with the techniques available today as some of the methods can cause the search to be trapped in local optima points due to the lack of exploration ability. Thus, in this research, an enhanced EM is proposed to be implemented as the MPPT scheme of the PV systems.

# CHAPTER 3: METHODOLOGY

The methodologies adopted in this research are discussed in details in this chapter. This chapter is divided into several major sections. Section 3.1 gives a general picture of the flow and setup of the research. In section 3.2, the search mechanism of a conventional EM is discussed. The methods and modifications to investigate the effect of search step size are also included in this section. A Split, Probe and Compare mechanism is introduced into the EM in section 3.3. The mechanisms and modifications of the new feature are discussed in details. In section 3.4, and experience-based EM is proposed. The experience learning and analysis mechanisms are presented and discussed. And finally, the implementation of the enhanced EM in the MPPT of a PV system is presented in section 3.5. The simulation and experiment designs are discussed in details.

## 3.1 Research Flow

A general methodological framework was developed for this research. It involved literature study, algorithms development, algorithm test run, optimization problem simulations, performance benchmarking, and documentations. The general flow of the research is shown in Figure 3.1.

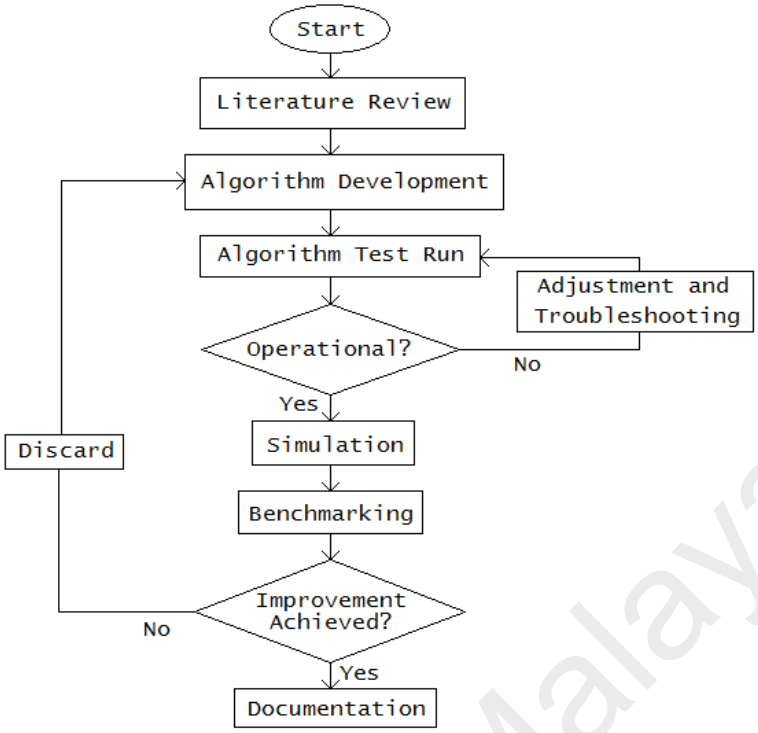


Figure 3.1: General flow of the research.

All the algorithms were developed using Microsoft Visual Basic.Net of Microsoft Visual Basic Studio 2008. The simulations were conducted with a 1.6Ghz Intel Core i5 CPU with 4GB-RAM, in WIN-7OS.

### 3.1.1 The Test Suite.

In order to validate and demonstrate the performance of the developed algorithms and the proposed modifications, a test suite of 10 numerical optimization test problems with different features was employed. The test problems included Ackley, Beale, Booth, De Jong's Sphere, Himelblau, Rastrigin, Rosenbrock, Schaffer, Shubert, and Six-hump

Camel test. All the benchmark functions used in this research are minimization problems. These classical optimization problems are commonly used by researchers around the world to test the performance of optimization algorithms. The details of the test functions are shown in Table 3.1. *F1*, *F4*, *F6*, and *F7* were set to be conducted in a 10-dimensional hypercube.

Table 3.1: The test suite setup.

| Function | Formulations | Range |
|---|---|---|
| *F1 Ackley* | $\min f(x) = -20\exp\left(-0.2\sqrt{\frac{1}{d}\sum_{i=1}^{d} x_i^2}\right) - \exp\left(\frac{1}{d}\sum_{i=1}^{d}\cos(2\pi x_i)\right) + 20 + e$ | [-32.768, 32.768] |
| *F2 Beale* | $\min f(x) = (1.5 - x_1 + x_1x_2)^2 + (2.25 - x_1 + x_1x_2^2)^2 + (2.625 - x_1 + x_1x_2^3)^2$ | [-4.5,4.5] |
| *F3 Booth* | $\min f(x) = (x_1 + 2x_2 - 7)^2 + (2x_1 + x_2 - 5)^2$ | [-10,10] |
| *F4 Sphere* | $\min f(x) = \sum_{i=1}^{d} x_i^2$ | [-5.12, 5.12] |
| *F5 Himmelblau* | $\min f(x) = (x_1^2 + x_2 - 11)^2 + (x_1 + x_2^2 - 7)^2$ | [-5.12, 5.12] |
| *F6 Rastrigin* | $\min f(x) = 10d + \sum_{i=1}^{d}[x_i^2 - 10cos(2\pi)x_i]$ | [-5.12, 5.12] |
| *F7 Rosenbrock* | $\min f(x) = \sum_{i=1}^{d-1}[100(x_{i+1} - x_i^2)^2 + (x_i - 1)^2]$ | [-5, 10] |
| *F8 Schaffer N2* | $\min f(x) = 0.5 + \frac{sin^2(x_1^2 - x_2^2) - 0.5}{[1 + 0.001(x_1^2 + x_2^2)]^2}$ | [-100, 100] |
| *F9 Shubert* | $\min f(x) = \left[\sum_{i=1}^{5} i\cos\big((i+1)x_1 + i\big)\right]\left[\sum_{i=1}^{5} i\cos\big((i+1)x_2 + i\big)\right]$ | [-10, 10] |
| *F10 Six-Hump Camel* | $\min f(x) = (4 - 2.1x_1^2 + x_1^4/3)x_1^2 + x_1x_2 + (4x_2^2 - 4)x_2^2$ | $x_1$,[-3, 3] $x_2$,[-2, 2] |



### 3.2 EM and the Impact of Search Step Size

The setting of the search step size, especially on the local search segment of population-based optimization methods, shows significant impact on the outcome and convergence efficiency (Ratnaweera et. al., 2004, Yu et. al., 2015). One of the objectives of this study is to investigate the impact of search step size setting onto the convergence

performance of EM. In order to do that, some modifications and adjustments were carried out onto the conventional EM in order to expose the advantages and disadvantages of different search step size employed in the algorithm.

### 3.2.1 The Original EM Scheme

The EM is a population-based meta-heuristic search algorithm. Mimicking the attraction-repulsion mechanism of the electromagnetism theorem, the particles move within the search space in search for the best global optima value. The pseudocode in Table 3.2 summarizes the procedure of the original EM proposed by Birbil and Fang (2003). Figure 3.2 shows a better picture of the algorithm flow in the form of a flowchart.

Table 3.2: Original EM proposed by Birbil and Fang (2003).

| EM (*m, MAXITER, LSITER, δ*) |
|---|
| *m*= number of initial particles<br>*MAXITER*: maximum number of iterations<br>*LSITER*: maximum number of local search iterations<br>*δ*: local search parameter, $\delta \in (0,1)$ |
| 1: Initialize ( )<br>2: iteration 1<br>3: **while** iteration < *MAXITER* **do**<br>4: Local (*LSITER*, *δ*)<br>5: *F* ← *CalcF* ( )<br>6: Move (*F*)<br>7: iteration ← iteration + 1<br>8: **end while** |

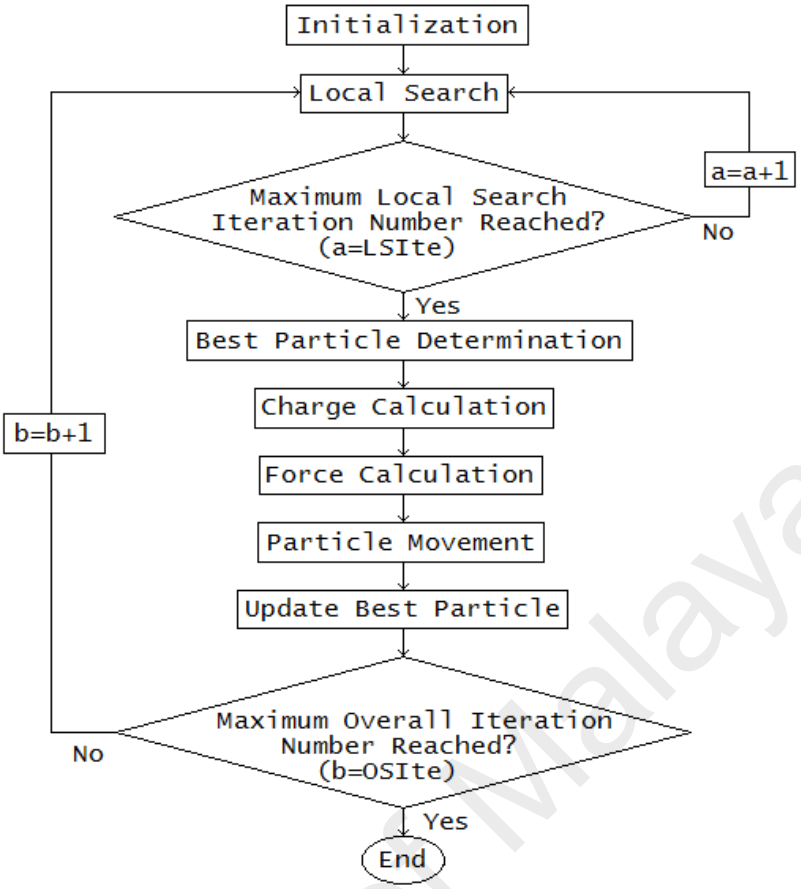


Figure 3.2: The flow of a conventional EM algorithm, where *a* and *b* denote the iteration number of local and global search respectively, while *LSIte* and *OSIte* refer to the pre-determined maximum iteration number in local and overall search.

For the ease of convergence analysis, 10 particles were used for all the variants of EM in this research. As discussed in Section 2.3, a conventional EM consist of 5 major stages. Similar to most population-based optimization algorithms, it begins with initialization.

In the initialization stage, all 10 particles are randomly assigned with solution values within the feasible range. Each solution value of a particle is assumed to be uniformly distributed between the corresponding upper and lower bounds of the

dimension. Then, the algorithm moves on to the local search stage. The original local search proposed by Birbil and Fang (2003) is a simple line search which tune the particle along the line of a dimension based on a random step size between (0,1) in a random direction. The local search terminates immediately upon achieving any better solution or when the pre-determined iteration number is reached. The pseudocode of the original local search procedure is as shown in Table 3.3.

Table 3.3: Original local search proposed by Birbil and Fang (2003).

**Local Search ( $LSITER$,$\delta$ )**

counter ← 1
Length ← $\delta(max_k\{u_k - l_k\})$
**for** $i = 1$ *to* $m$ **do**
  **for** $k = 1$ *to* $n$ **do**
    $\lambda_1 \leftarrow U(0,1)$
    **while** $counter < LSITER$ **do**
      $y \leftarrow x^i$
      $\lambda_2 \leftarrow U(0,1)$
      **if** $\lambda_1 > 0.5$ **then**
        $y_k \leftarrow y_k + \lambda_2(Length)$
      **else**
        $y_k \leftarrow y_k - \lambda_2(Length)$
      **end if**
      **if** $f(y) < f(x^i)$ **then**
        $x^i \leftarrow y$
        $counter \leftarrow LSITER -$
      **end if**
      $counter \leftarrow counter + 1$
    **end while**
  **end for**
**end for**
$x^{best} \leftarrow argmin\{f(x^i), \forall_i\}$

Upon completion of the local search, the particle with the best objective value is determined and marked as the best particle. The following step of the procedure is to determine the charge values. The charge for each of the particle is calculated based on the

objective function of the particle in relative to the best objective function in among the particles, as shown in equation (3.1) below.

$$q^i = exp\left(-n\frac{f(x^i)-f(x^{best})}{\sum_{k=1}^{m}\left(f(x^k)-f(x^{best})\right)}\right), \forall i \quad (3.1)$$

With the charge of each particle obtained, the algorithm can now move on to the force calculation. Each particle will consider all the forces generated by every other particle. The sum of all the forces generated onto a particle is calculated using equation (3.2) below.

$$F^i = \sum_{j\neq i}^{m}\begin{Bmatrix}(x^j-x^i)\frac{q^iq^j}{||x^j-x^i||^2} & if \quad f(x^j)<f(x^i) \\ (x^i-x^j)\frac{q^iq^j}{||x^j-x^i||^2} & if \quad f(x^j)\geq f(x^i)\end{Bmatrix}, \forall i \quad (3.2)$$

where $f(x^j) < f(x^i)$ denotes attraction and $f(x^j) \geq f(x^i)$ refers to repulsion. The psuedocode of the force calculation procedure is as shown in Table 3.4.

Table 3.4: Total force calculation procedure for a particle.

**Force Calculation (*CalcF ( )*)**

1: **for** $i = 1\ to\ L$ **do**
2: $q_i = \exp\left(-n\ \frac{f(x_i)-f(x_{best})}{\sum_{k=1}^{L}(f(x_i)-f(x_{best}))}\right)$
3: $F_i = 0$
4: **end for**
5: **for** $i = 1\ to\ L$ **do**
6: **for** $j = 1\ to\ L$ **do**
7: **If** $i \neq j$ **then**
8: $F_i^j = \left(x_j - x_i\right)\frac{q_iq_j}{\|x_jx_i\|_2}$
9: **If** $f(x_j) < f(x_i)$ **then**
10: $F_i = F_i + F_j^i$ (Attraction)
11: **else**
12: $F_i = F_i - F_j^i$ (Repulsion)
13: **end if**
14: **end if**
15: **end for**
16: **end for**

Next, the particles are relocated to a new location in the search space. Equation (3.3) shows the calculation of the particles movement in accordance to the total force generated. The pseudocode of the particle movement stage is as shown in Table 3.5.

$$x_k^i \leftarrow x_k^i + \lambda F_k^i \left( u_k - x_k^i \right) \qquad ; F_k^i \geq 0$$

$$x_k^i \leftarrow x_k^i + \lambda F_k^i \left( x_k^i - l_k \right) \qquad ; F_k^i < 0 \tag{3.3}$$

Table 3.5: Particle movement procedure.

| **Particle Movement (*Move ()*)** |
|---|
| 1: **for** $i = 1$ *to* $L$ **do** |
| 2: **If** $i \neq best$ **then** |
| 3: $\lambda = random\ (0,1)$ |
| 4: $F_i = \frac{F_i}{\|F_i\|}$ |
| 5: **for** $k = 1$ *to* $n$ **do** |
| 6: **If** $F_k^i > 0$ **then** |
| 7: $x_k^i = x_k^i + \lambda F_k^i (u_k - x_k^i)$ |
| 8: **else** |
| 9: $x_k^i = x_k^i + \lambda F_k^i (u_k - l_k)$ |
| 10: **end if** |
| 11: **end for** |
| 12: **end if** |
| 13: **end for** |

Holding the absolute power of attraction towards all other particles, the best particle of the iteration does not move (Cuevas et. al., 2012).

### 3.2.2 EM with Large and Small Search Step Sizes

In order to examine the gravity of different step size setting to the convergence performance of EM, a conventional EM was set to search in two different extremes of search step length settings in the local search procedure. EM with Larger Search Steps

(EMLSS) was modified and set to search in a fixed search step of 0.99. EM with Smaller Search Steps (EMSSS), on the other hand, was set to conduct search with a fixed search step of 0.01. Since the local search procedure of a conventional EM terminates immediately upon achieving any better objective value, this experiment setting can expose the difference in the performances if the search ended in comparatively bigger or smaller search steps. Table 3.6 and Table 3.7 show the local search procedures of EMLSS and EMSSS respectively. Samples of the simulation results were analysed to investigate the performance of each.

Table 3.6: Local procedure for EMLSS.

**EMLSS Local Search ( LSITER,$\delta$ )**

counter ← 1
Length ← $\delta(max_k\{u_k - l_k\})$
**for** $i = 1$ *to* $m$ **do**
  **for** $k = 1$ *to* $n$ **do**
    $\lambda_1 \leftarrow U(0,1)$
    **while** $counter < LSITER$ **do**
      $y \leftarrow x^i$
      $\lambda_2 \leftarrow U(0, 0.99)$
      **if** $\lambda_1 > 0.5$ **then**
        $y_k \leftarrow y_k + \lambda_2(Length)$
      **else**
        $y_k \leftarrow y_k - \lambda_2(Length)$
      **end if**
      **if** $f(y) < f(x^i)$ **then**
        $x^i \leftarrow y$
        $counter \leftarrow LSITER -$
      **end if**
      $counter \leftarrow counter + 1$
    **end while**
  **end for**
**end for**
$x^{best} \leftarrow argmin\{f(x^i), \forall_i\}$

Table 3.7: Local procedure for EMSSS.

**EMSSS Local Search ( LSITER,$\delta$ )**

1: counter ← 1
2: Length ← $\delta(max_k\{u_k - l_k\})$
3: **for** $i = 1$ *to* $m$ **do**
4: **for** $k = 1$ *to* $n$ **do**
5: $\lambda_1 \leftarrow U(0,1)$
6: **while** $counter < LSITER$ **do**
7: $y \leftarrow x^i$
8: $\lambda_2 \leftarrow U(0.01,1)$
9: **if** $\lambda_1 > 0.5$ **then**
10: $y_k \leftarrow y_k + \lambda_2(Length)$
11: **else**
12: $y_k \leftarrow y_k - \lambda_2(Length)$
13: **end if**
14: **if** $f(y) < f(x^i)$ **then**
15: $x^i \leftarrow y$
16: $counter \leftarrow LSITER -$
17: **end if**
18: $counter \leftarrow counter + 1$
19: **end while**
20: **end for**
21: **end for**
22: $x^{best} \leftarrow argmin\{f(x^i), \forall_i\}$

### 3.3 Split, Probe and Compare

The local search segment is a crucial part in EM. The efficiency of an optimization algorithm to exploit further around a particular solution depends heavily on this part of the algorithm (Ratnaweera et. al., 2004). The local search procedure ensures a more refined search for a particular solution to hit a better optimum locally. As shown in the previous sections, the local search in a standard EM employs a random step length value between 0 and 1. The search direction of each iteration is randomly picked, and the search step size for all the iterations is randomly set between the value of 0 and 1, be it early or near-end of the search. The local search iteration is terminated immediately when a

relatively better objective outcome is achieved, or when the iteration number meets the terminating criteria. Randomized search direction and step length are obviously inappropriate as they may jeopardize the efficiency of the convergence and the accuracy of the final outcome. In order to solve these issues, a new Split, Probe, and Compare (SPC) feature is proposed into the EM (SPC-EM) in this study.

The SPC-EM is an enhanced version of EM that can grant the algorithm the ability to hit a more accurate solution without heavily slowing down the entire convergence process. The general idea is to replace the local search mechanism of a conventional EM with the SPC search procedure. Analogically speaking, SPC-EM probes around the neighbourhood of a solution with two separate probes. The results returned by the probes will give the algorithm an idea of the direction to a better solution. The lengths of the probes are dynamically and systematically regulated based on the feedback results. As the name suggests, the SPC consists of three segments, namely Split, Probe, and Compare.

**Split**: Randomly selecting the search direction can result in unnecessary objective function evaluations and thus significantly lower the efficiency of the convergence process. The SPC feature provides a more systematic way of exploration in the search direction. In this Split segment, the search mechanism is split into two probes (Probe A and Probe B) in all respective dimensions. The probes then reach out to test the surroundings for any better solution in two different directions. The purpose of splitting the search is to gain a sense of direction to any better solution in the neighbourhood of the particle. Probe A explores towards the lower bound while Probe B searches towards the upper bound of the feasible solution range for any better solution.

**Probe**: In a conventional EM, the sizes of the local search steps are randomly selected. The search procedure ends immediately upon achieving any better objective value. Since there is no telling on what search step size the iterations will end with, this conventional method does not guarantee the accuracy or the efficiency of the search. This can cause problems due to several reasons. Big search steps can speed up the overall convergence. However, they may skip the best optimal solution when it is in the vicinity of the particle, thereby reducing search performance of the best optimal solution. Small search steps, on the other hand, can ensure a better accuracy of the convergence. The trade off, however, is that it will significantly slow down the whole convergence process. Taking these problems into account, the SPC mechanism is designed in such a way that the Compare segment will decide if the length of the probes need to be adjusted for each iteration. Depending on that decision, the lengths of the probes are dynamically regulated by a carefully designed nonlinear equation. The calculation of the probe length, $L$ is as shown in equation (3.4).

$$L = \frac{2}{1+\exp(\frac{10i}{Max\_LSIte})} \tag{3.4}$$

In equation 5, $i$ represents the current number of local search iteration while $Max\_LSIte$ refers to the pre-set maximum number of iteration. Figure 3.3 shows an example of the $L$ variation over the iterations with $Max\_LSIte$ set to 1000. The decreasing nature of the resultant $L$ causes the search steps to be relatively larger at early stage, and then decreases as the iterations go on. This can ensure the algorithm hits a more accurate solution at the end of the iterations, in the meanwhile not slowing down the whole convergence process by probing around too finely at the beginning of the search.

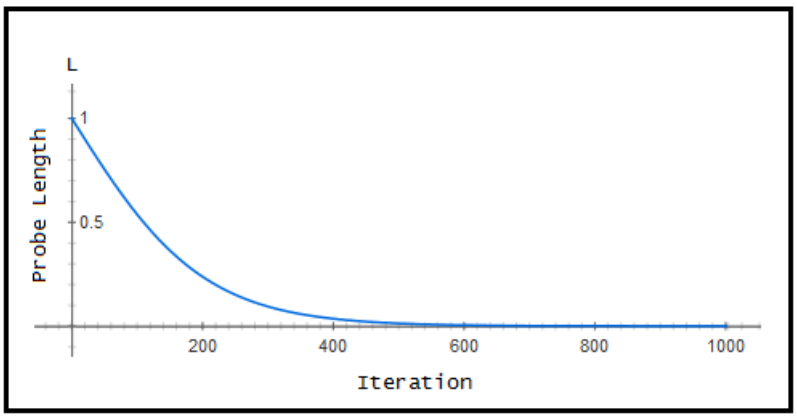


Figure 3.3: Variation of probe length, *L* over 1000 iterations.

**Compare**: The purpose of this segment is to check for objective value improvement of the particle and to update the current particle with the best solutions found in every iteration. A common issue with the local search of most population-based algorithm is that the particle might move out of the feasible range in search for a better solution. In order to overcome this issue, each time the probes returned with new found solutions, the feasibility of them are first checked. The new found solution is immediately disqualified and replaced with the previous value if it falls outside the feasible range. After making sure of the feasibility, a 3-way comparison of solutions is carried out. Comparison between the two new solutions provides the algorithm an idea on the direction to a better solution, if any. The particle moves towards the lower bound of the dimension if Probe A obtains a better solution. In contrast, if Probe B proves to provide a relatively better solution, the particle will move towards the upper bound of the dimension. The rate of the movement is dependent on the length of the probe at that particular iteration. If the best result among the probes is better than the current solution, the particle will adapt to the new found best solution and the position of the particle will then be updated. This solution improvement process continues until no better solution can be returned by the

probes. Then, the length of the sticks is adjusted according to equation (3.4), and the iterations continue until the predetermined terminating criteria is met.

The proposed SPC local search procedure is shown in Table 3.8. Figure 3.4 shows a better explanation of the decision making process in the form of a flowchart. The proposed SPC-EM was tested in the designed test suite. The results and analysis are shown in Chapter 4.

Table 3.8: Local search procedures for SPC-EM**.**

| SPC-EM Local Search Procedures | |
|---|---|
| Step 1 | Set maximum number of iteration as terminating criteria. |
| Step 2 | Calculate the length of the probes using equation 5. |
| Step 3 | Split the search into Probe A and Probe B. |
| Step 4 | Extend the probes towards lower and upper bounds respectively to search for better solutions. |
| Step 5 | Check if the solutions returned by the probes are within feasible range. |
| Step 6 | Compare the new found solutions and move particle towards the better yield. |
| Step 7 | Adapt the new found solution if it is better than the current solution. |
| Step 8 | From the new location of the particle, repeat Steps 3 to 8 until no further solution improvement is possible. |
| Step 9 | Exit if the iteration number reaches termination criteria. Otherwise adjust the probe length, move on to the next iteration $i = (i + 1)$ and repeat from Step 2. |

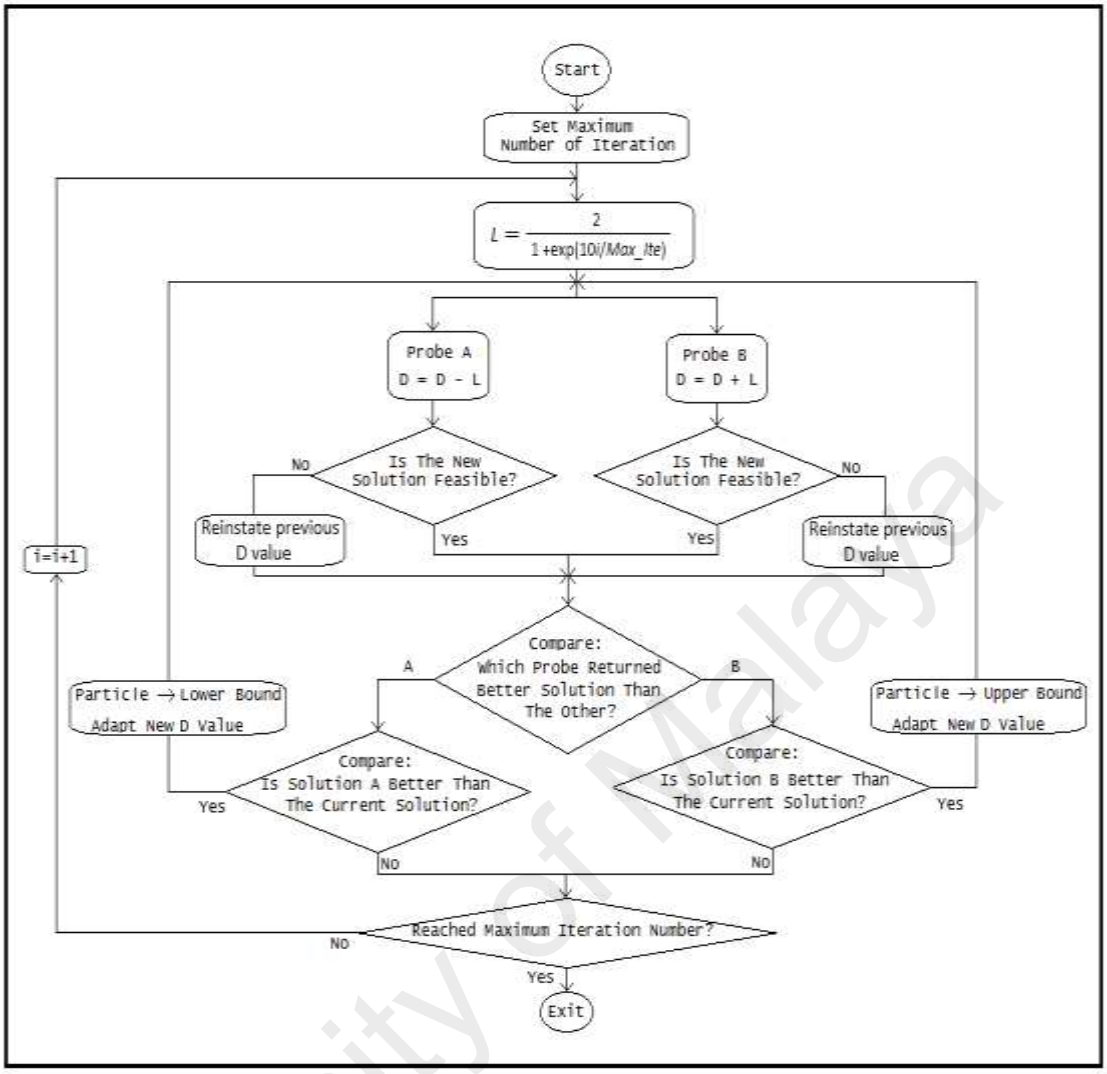


Figure 3.4: The flow of the proposed modification on SPC-EM, where *D* denotes the parameter of a particular dimension in a particular solution and $\lambda$ refers to the search step size.

### 3.4 An Experience-Based EM

Besides SPC-EM, another successful attempt in improving the EM is recorded by enhancing the EM with the ability to learn from previous search experience. In order to impart a stronger and more solid exploitation capability to the EM, a new Experiential Learning EM (ELEM) is proposed in this research.

Kolb (1984), in his book defined experiential learning as the process of creating knowledge from experience. As the name suggests, the Experiential Learning EM is an algorithm designed with the ability to learn from previous experience, from which a better projection can be generated for the iterations to come. ELEM adapts a guided search mechanism with previous search information analysis and backtracking memory into the EM algorithm. This enhanced local search mechanism operates on guided displacements in every dimension by analysing the rate of improvements and comparison with the experience from the past iterations. With the ability to backtrack the search to previous solutions and improvement gradients, this local search mechanism can ensure a better exploitation on the solutions by adjusting the scale and direction of the search as iterations go. Combining with the powerful exploration procedures of the EM, ELEM yields accurately exploited and well diversified solutions. The details of the modified local search mechanism is described in the following subsections.

### 3.4.1 Particle Memory Setup

To backtrack the evolution of the solution in the neighbourhood search and gain experience from it, a memory block, $MB_i$ is set up to store particle values from previous search results. This memory leaves a trail of information on previous search efforts, such as the rates of improvement (*M*), best achieved base values (*B*), and the search direction matrices (*SD*). Every successful search will update the memory on the achievements, while unsuccessful search will backtrack to previous base values, recalculate settings based on the experience, and reattempt the search with the new settings. At the end of every iteration, the $MB_i$ is updated with new information. That way, every success or failure reduces unnecessary searches in the region and drive the results to higher accuracies.

### 3.4.2 Guided Search Mechanism

Instead of a simple line search with random search steps, the local search procedure of the modified ELEM is carried out by a proposed local search with a stronger exploitation ability named Guided Search (GS). Inspired by the naive directed search mechanism (Sharifi et. al., 2012), the GS mechanism is further enhanced by Improvement Gradient Analysis and Memory Backtracking feature, which are discussed in details in the following subsections.

In general, the movement of GS is based on guided displacements in every dimension. An initial search step $\lambda_{init}$ is set in the first iteration. A search direction vector, $SD_i=(SD_i^1, SD_i^2, \ldots, SD_i^d)$ is employed to set the direction of the next local search movement in all dimensions, where $sd_i^d \in \{-1,1\}$. For the initial stage, the direction of the search is randomly selected. The current position of the particle is set to be the base solution, $B_i(t)$. The value of this $B_i(t)$ is then stored as the old base value, $B_{iOld}$ in the memory of the particle.

At each iteration, the $B_i(t)$, is moved in the search direction vector in attempt to find a better solution. Upon completion of the displacement, the feasibility of the new found solution, $B_{inew} = B_i(t) + sd_i \times \lambda_i^T$ is then checked. If $B_{inew}$ falls outside the feasible range of the solution, it will be discarded and the search direction is flipped to the opposite direction of the dimension with $B_i(t)$ restored to $B_{iOld}$ value. If $B_{inew}$ is found to be feasible, the objective value of the new found solution is then compared to $B_{iOld}$. The result of this comparison determines the action to be taken by the algorithm the the next steps. The corresponding actions are as shown in Table 3.9. The gradient of the new particle base and $B_{iOld}$ is also calculated and stored in the $MB_i$ as $M_{old}$ before moving on to the next iteration.

### 3.4.3 Search Experience Analysis

The search experience analysis stage is activated when a feasible new solution is found. The first step of this analysis is to compare the rate of improvement with that of the previous iterations. This can provide a better estimation on the position of the current solution to the optima point, and thus the search step size can be adjusted accordingly. The mechanism begins with the calculation of the gradient formed by the solutions of previous and current iterations. The calculation of the improvement gradient, $M$ is as shown in equation (3.5) below:

$$M_{Current} = \left(B_{inew}(t) - B_{iOld}(t)\right)/\lambda_{Current} \quad (3.5)$$

where $\lambda$ refers to the search step size. With the current gradient of improvement obtained, the algorithm then recalls the memory of the previous gradient, $M_{Old}$ to understand how the improvement rate of the search has evolved up to the current iteration. This information, pairing with the result from the fitness functions comparison, enable the algorithm to decide better on the best corresponding action. If the fitness of $B_{inew}$ is better than $B_{iold}$, the new found solution is adapted, and the search direction maintains for the next iteration. Meanwhile, based on the improvement gradient comparison, the size of the search step for the next iteration is determined by the rate of the gradient change, as shown in equation (3.6) and (3.7).

$$\lambda_{Next} = \lambda_{Current} * \alpha\ (M_{Current} / M_{Old}) \quad ; |M_{Current}| \geq |M_{Old}| \quad (3.6)$$

$$\lambda_{Next} = \lambda_{Current} * \beta\ (M_{Current} / M_{Old}) \quad ; |M_{Current}| < |M_{Old}| \quad (3.7)$$

where parameters $\alpha$ and $\beta$ denote the gain and penalty factors respectively. On the other hand, if the fitness of $B_{inew}$ is found to be worse than $B_{iold}$, the new found solution is then discarded, and the particle is backtracked to the previous base $B_{iold}$. The direction of the

search in the dimension is reversed with the adjusted search step as shown in equation (3.8) and (3.9).

$$\lambda_{Next} = \lambda_{Current} * \beta\ (M_{Old} / M_{Current}) \quad ; |M_{Current}| \geq |M_{Old}| \tag{3.8}$$

$$\lambda_{Next} = \lambda_{Current} * \alpha\ (M_{Old} / M_{Current}) \quad ; |M_{Current}| < |M_{Old}| \tag{3.9}$$

where parameters $\alpha$ and $\beta$ denote the gain and penalty factors respectively. Note that equation (3.8) and (3.9) share the same gain and penalty parameters as equation (3.6) and (3.7). The settings of parameters $\alpha$ and $\beta$ show certain impact on the performance of the algorithm. A parameter sensitivity test was conducted. The effects are further discussed in Chapter 4.

The fitness and improvement gradient memory of the particle are then updated with the latest values before moving on to the next iteration. The search procedure is terminated when the search direction is flipped up to a pre-determined number of times in a row, *j* without any further improvement in the fitness value. Table 3.9 summarizes the corresponding actions of the comparison results.

Table 3.9: Memory comparison and the corresponding actions.

| $B_{iNew}$ vs $B_{iOld}$ | $M_{Current}$ vs $M_{Old}$ | Action | Search Step Tuning |
|---|---|---|---|
| Better | Bigger | Adapt new solution | $\lambda_{Next} = \lambda_{Current} * \alpha\ (M_{Current} / M_{Old})$ |
| | Smaller | Remain *SD* | $\lambda_{Next} = \lambda_{Current} * \beta\ (M_{Current} / M_{Old})$ |
| Worse | Bigger | Backtrack to $B_{iOld}$ | $\lambda_{Next} = \lambda_{Current} * \beta\ (M_{Old} / M_{Current})$ |
| | Smaller | Reverse *SD* | $\lambda_{Next} = \lambda_{Current} * \alpha\ (M_{Old} / M_{Current})$ |

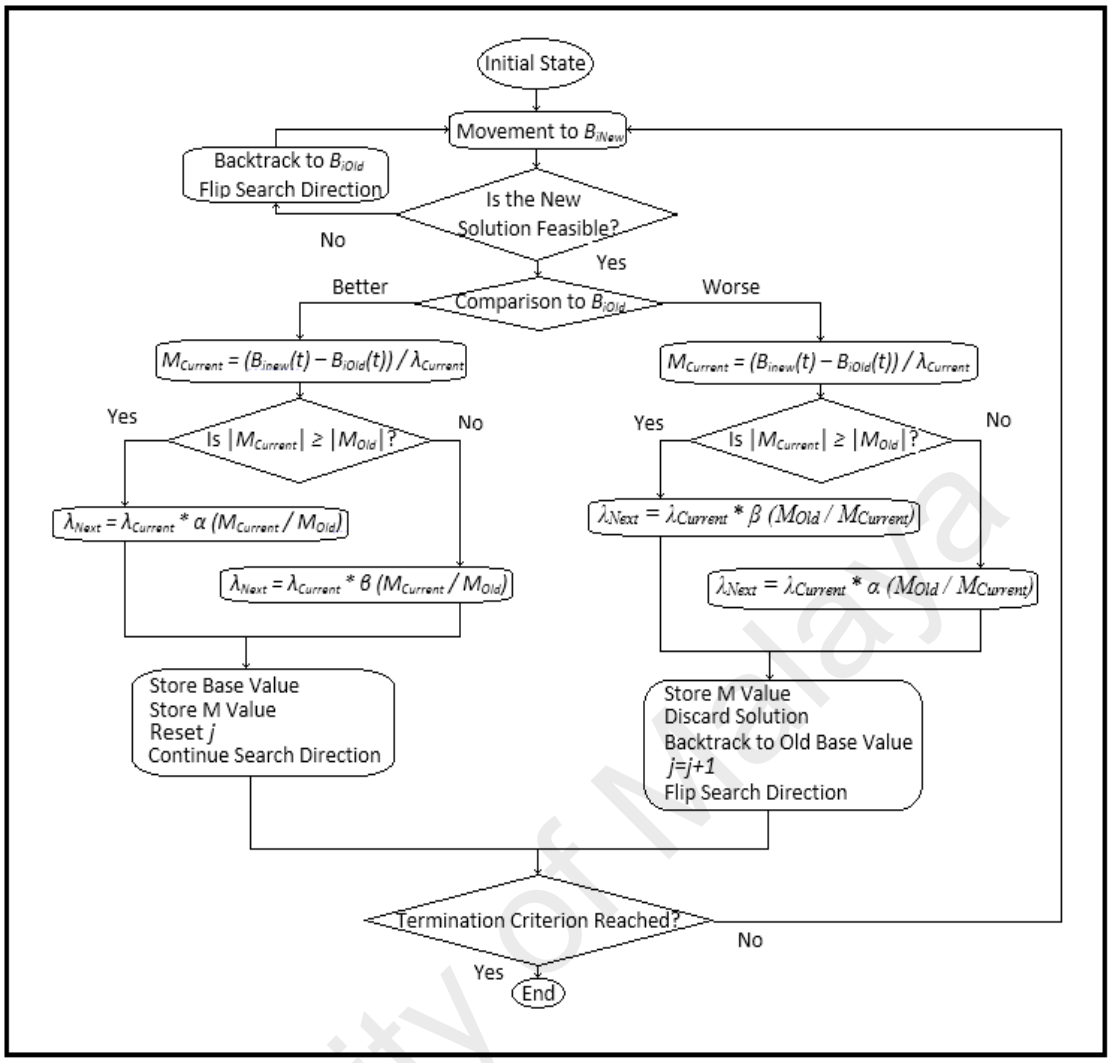


Figure 3.5: Decision making flow on corresponding actions.

Figure 3.5 gives a clearer picture of the decision making process in the form of a flowchart. Leveraged by the memory and experience from previous search efforts, the changing nature of the resultant $\lambda$ causes the search steps to be more fine-tuned as the search approaches the optima point. This can ensure the algorithm achieves solutions with higher accuracies at the end of the iterations, in the meanwhile not slowing down the overall convergence process by searching around too finely at the beginning of the search. Unlike SPC-EM, the tuning mechanism of the ELEM is based on the improvement rate and immediate search experience, instead of search iteration number. This unique strategy provides the local search mechanism with a powerful exploitation capability. Combining

with the strong exploration technique of the EM, the ELEM gains advantages from both and strikes a good balance between the accuracy and diversity of the solutions returned. The enhanced ELEM is tested in the designed test suite. The results and analysis are shown in Chapter 4.

### 3.5 MPPT via EM

The enhanced ELEM was implemented in the MPPT simulation of a PV solar energy harvesting system in this research. For the application in MPPT, the tuning parameter of the EM was set to be the voltage of the PV harvesting system output. The objective of the algorithm was to maximize the generated power. In the initialization stage, all the particles in the algorithm were assigned with a voltage value randomly selected within ($V_{min}$, $V_{max}$) where $V_{min}$ and $V_{max}$ represents the minimum and maximum values of the operating voltage of the PV array. Then, the particles went through the enhanced local search procedure. For the objective function evaluation, the dc-dc converter was activated using digital controller corresponding to the position of each particle. The fitness value (power) of a particle was calculated after the allowable converter settling time of 0.1s. The power value obtained by the particles were compared. The position with the highest power value was marked as the best particle. The charge and force of the particles were then calculated. In the particle movement stage, the voltage value obtained by the best particle with the highest output power achieved was kept, while all other particles were moved based on superposition theorem within the feasible range.

### 3.5.1 Simulation Environment

Simulations were designed to evaluate the performance of EM in tracking the MPP of the PV system. The PV arrays in the simulation mode consisted of 3 commercial PV modules BP Solar MSX-120W connected in series, as shown in Figure 3.6. The key specifications of the BP Solar MSX-120W is given in Table 3.10. The details of the BP Solar MSX-120W characteristics can be found in (Boukenoui, 2016). The specification sheet of BP Solar MSX-120W is attached in Appendix A.

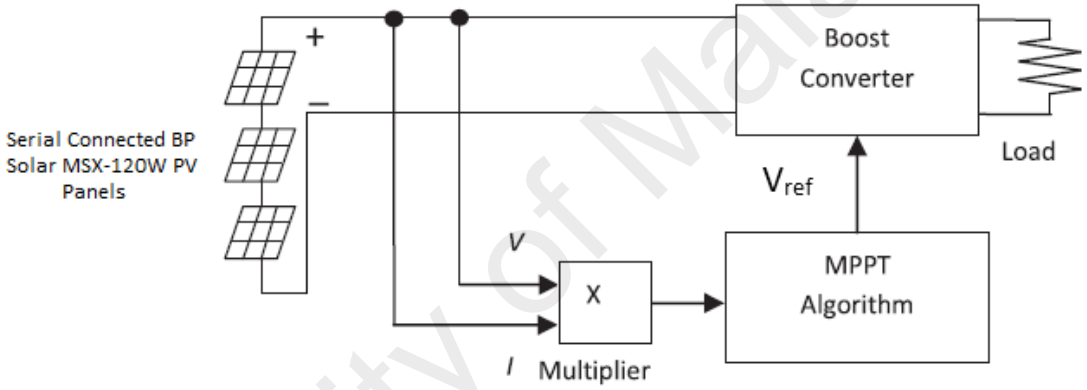


Figure 3.6: Simulation model of the PV system.

Table 3.10: Electrical characteristic of BP Solar MSX-120W.

| Parameters | Value |
|---|---|
| Maximum Power ($P_{max}$) | 120W |
| Voltage at $P_{max}$ ($V_{PPM}$) | 33.7V |
| Current at $P_{max}$ ($I_{PPM}$) | 3.56A |
| Open Circuit Voltage ($V_{OC}$) | 42.1V |
| Short Circuit Current ($I_{SC}$) | 3.87A |

Under ideal and uniform irradiance, the P-V curve of the serial connected BP Solar MSX-120W shows a single peak, as shown in Figure 3.7. In practical applications, the actual atmospheric condition can change very rapidly due to clouds, trees, electric poles,

and the shadow of neighbouring buildings. Thus, 3 different shading patterns were designed with different irradiance on each of the PV panels to simulate the challenging and dynamic shading conditions in practical applications. The P-V curves of the designed shading patterns and the corresponding MPPs are as shown in Figure 3.8 (a), (b), and (c). The peaks and the shaped of the curves are randomly designed within the feasible range to simulate the random shading patterns in actual applications. The EM was tested in the simulations to track for the MPPs as the shading condition changed from pattern1 to pattern 2 and then to pattern 3. The results are analysed in Chapter 4.

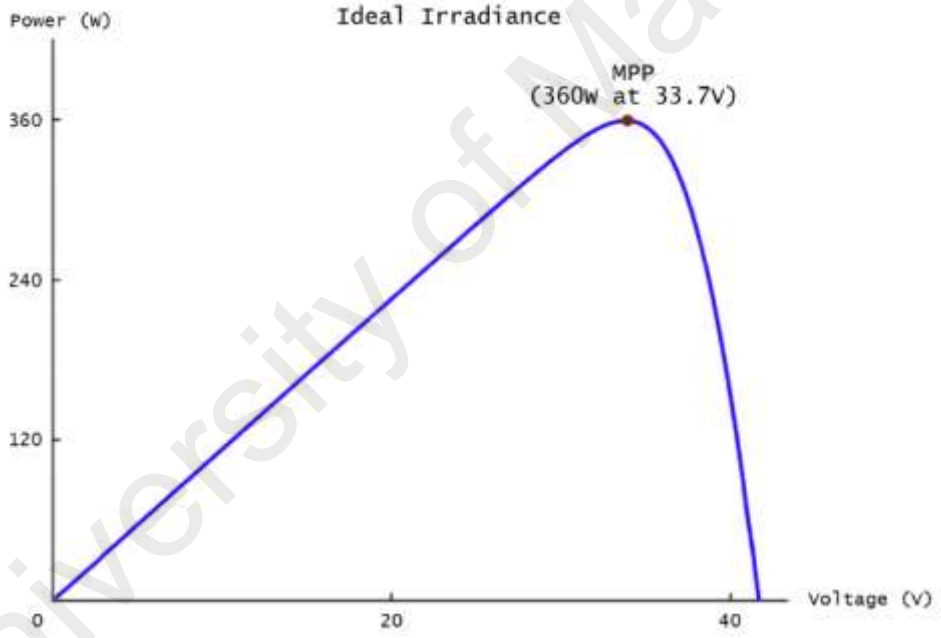


Figure 3.7: The P-V curve of the serial connected PV panels under ideal and uniform irradiance.

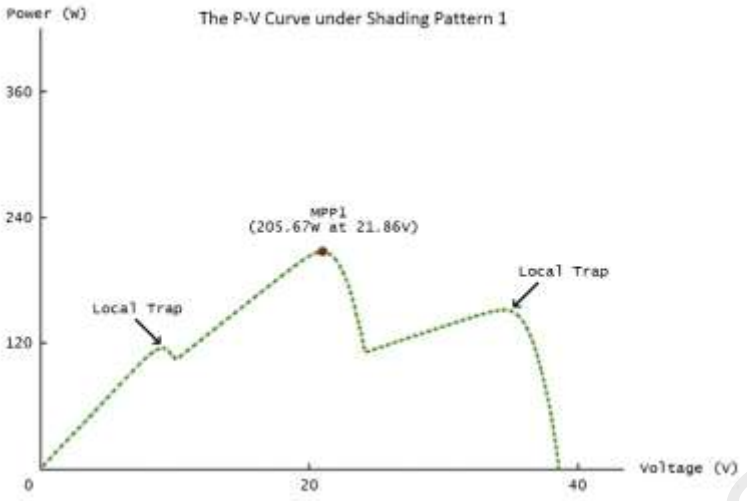


(a)

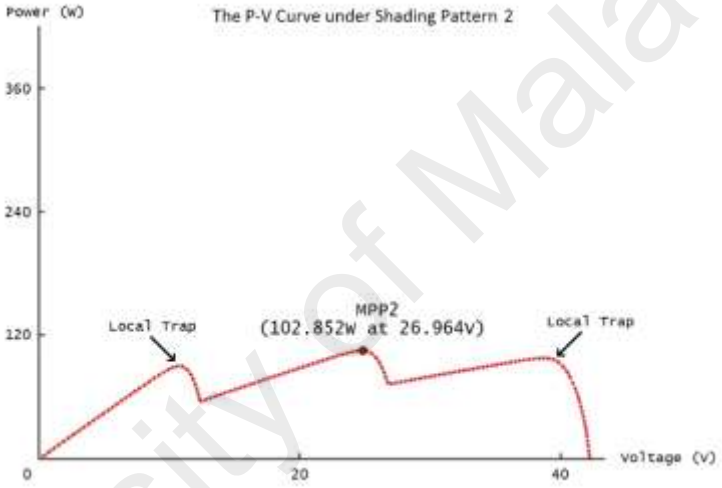


(b)

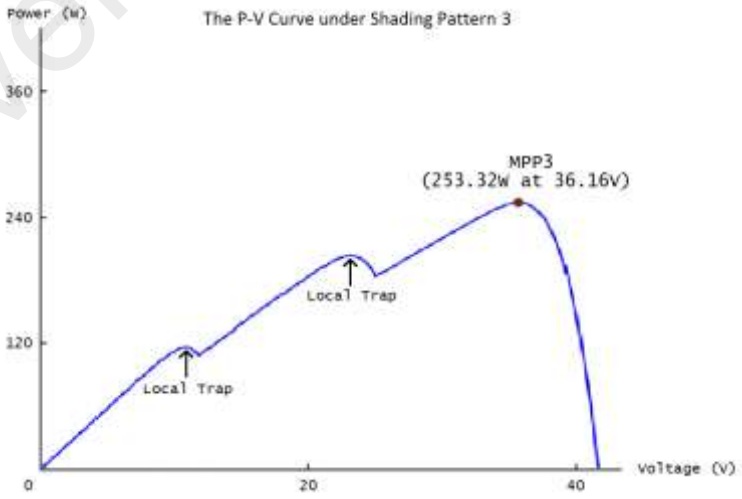


(c)

Figure 3.8: The P-V curves of the simulated shading patterns. PSC varied from pattern 1 to pattern 2, and then to pattern 3 in the simulation.

# CHAPTER 4: RESULTS AND DISCUSSION

This chapter presents the results and analysis of the simulations, experiments and verifications. The chapter can generally be divided into 4 major sections. Section 4.1 focuses on the impact of search step size settings onto the performance of the EM. Experiments and simulations were carried out to analyse the performance of the proposed SPC-EM and ELEM in solving numerical optimization problems. The results are analysed in details in section 4.2 and 4.3 respectively. The enhanced EM was then implemented in the MPPT simulation of a PV system. The results and discussions are presented in the final section.

## 4.1 Algorithm Development Environment

The algorithms were developed and simulated in Microsoft Visual Basic.Net of Microsoft Visual Basic Studio 2008. Figure 4.1 shows the integrated development environment of the software while Figure 4.2 gives an example of the GUI developed for one of the algorithms. The tuning dimensions and the results were set to be in the data type of 'Double' with the decimal accuracy up to 1E-16. Any number smaller than that was considered as '0' in the algorithms. The data and results of the experiments were recorded and exported in the format of notepad text document files. Examples of the exported data are shown in Figure 4.3. For the ease of convergence analysis, 10 particles were employed in all variants of EM, and the algorithms were set to iterate up to 100

times. As for ELEM, the value of $j$ was set to 8 while parameters $\alpha$ and $\beta$ were set to 1.2 and 0.8 respectively. The reason behind this parameter setting of ELEM and related parameter sensitivity analyses are given in Section 4.4.

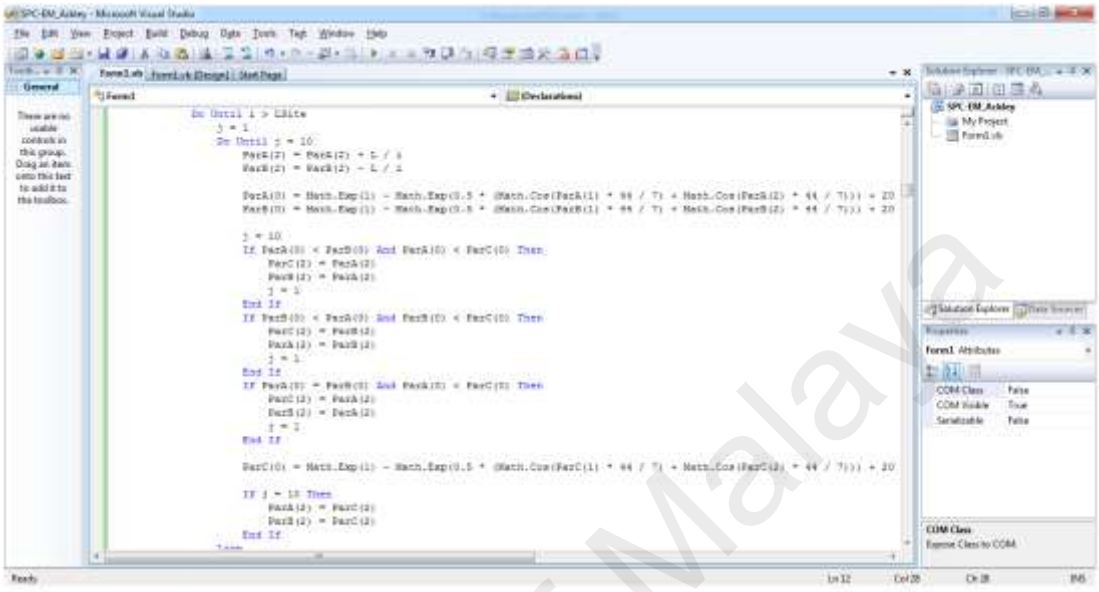

Figure 4.1: The integrated development environment of the software.

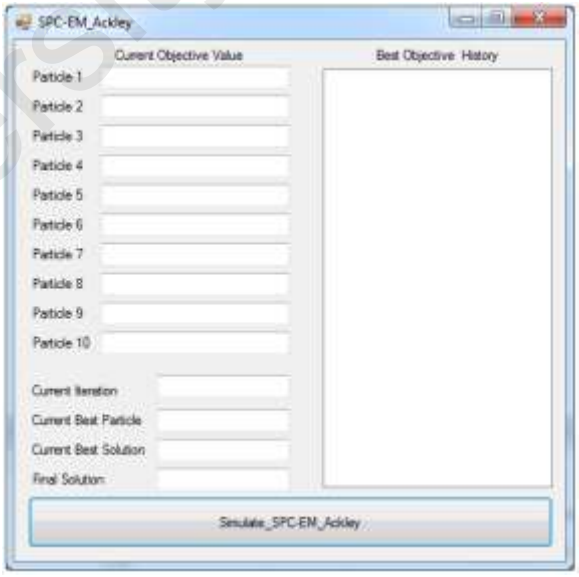


Figure 4.2: An example of the developed GUI.

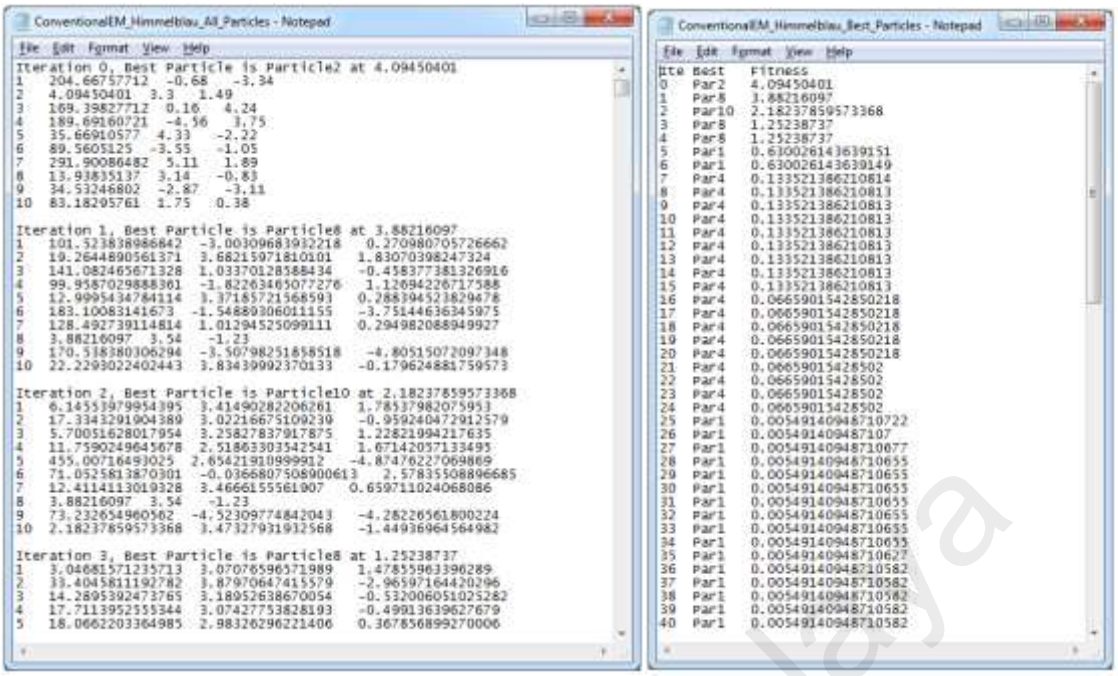


(a) (b)

Figure 4.3: Data export text document files examples: (a) all particles search history details and (b) best particle trails.

### 4.1.1 Impact of Search Step Size Setting in EM

Experiments were conducted to analyse the impact of search step size setting onto the performance of EM. The modified EMLSS and EMSSS were experimented to solve the designed test suite consisted of 10 commonly used numerical test functions as shown in Chapter 3. The performance and results are benchmarked with that of a conventional EM. All the benchmark functions used in this research were minimization problems. Thus, in this context, solutions with lower objective values are considered to be relatively more accurate. Due to the fact that experiments from the literature such as (Filipovic et. al., 2013, Arab & Alfi, 2015, Kratica, 2013) were repeated 20 times, the same scheme was

adopted in this research. 20 independent runs were conducted for each of the algorithms to avoid stochastic discrepancy.

### 4.1.2 Performance Benchmarking

Table 4.1 and Table 4.2 compare the best solutions, the worst solutions, the standard deviations and the average values of 20 runs on all 10 of the optimization functions. The original conventional EM is marked as EM. It can be observed that EMSSS found highest accuracy solutions in most of the test functions in terms of best value, worst value, and average value. The performance of the conventional EM is very unstable as there is no telling on the size of the search steps it ends with. However, it can be observed that some of the solutions obtained by the conventional EM are very competitive with that of EMSSS. It even beats EMSSS in terms of the best values obtained in some of the test functions such as *f1*, *f3* and *f8*.

Table 4.1: Best and worst solutions obtained in 20 runs.

| | Best Value | | | Worst Value | | |
|---|---|---|---|---|---|---|
| | EM | EMLSS | EMSSS | EM | EMLSS | EMSSS |
| *f1* | **3.5488E-03** | 4.5921E-02 | 3.8573E-03 | 2.7525E-01 | 4.1649E-01 | **1.2121E-02** |
| *f2* | 3.9145E-05 | 2.5787E-04 | **9.5861E-07** | 4.9154E-03 | 3.7381E-03 | **4.6775E-04** |
| *f3* | **1.4551E-05** | 5.4168E-04 | 5.3497E-05 | 9.7606E-03 | 9.3487E-03 | **5.2585E-04** |
| *f4* | 7.9371E-06 | 1.2766E-04 | **2.8497E-06** | 1.2945E-03 | 3.3039E-03 | **2.1470E-05** |
| *f5* | 1.5761E-05 | 1.7194E-04 | **1.1683E-05** | 9.1845E-03 | 9.5083E-03 | **4.6511E-04** |
| *f6* | 1.4493E-04 | 1.8655E-03 | **6.0471E-05** | 3.0677E-02 | 4.9664E-02 | **9.7521E-04** |
| *f7* | 4.8441E-05 | 9.8546E-04 | **4.1846E-05** | 2.8021E-02 | 3.9921E-02 | **1.2764E-03** |
| *f8* | **4.4633E-12** | 1.5314E-07 | 6.4951E-11 | 3.0381E-05 | 2.3740E-05 | **7.1495E-06** |
| *f9* | -186.7259 | -186.7010 | **-186.7300** | -186.5277 | -186.3577 | **-186.6749** |
| *f10* | -1.03162337 | -1.03159788 | **-1.03162720** | -1.03011631 | -1.03007554 | **-1.03152877** |

Table 4.2: Average and standard deviation values of all 20 runs.

| | Average | | | Standard Deviation | | |
|---|---|---|---|---|---|---|
| | EM | EMLSS | EMSSS | EM | EMLSS | EMSSS |
| *f1* | 1.0603E-01 | 2.0480E-01 | **7.6152E-03** | 5.6446E-03 | 1.5163E-02 | 5.4233E-06 |
| *f2* | 1.7701E-03 | 1.3424E-03 | **1.6460E-04** | 2.5603E-06 | 7.9994E-07 | 2.5631E-08 |
| *f3* | 3.5775E-03 | 5.1289E-03 | **1.5220E-04** | 1.0620E-05 | 6.8173E-06 | 1.2121E-08 |
| *f4* | 3.7616E-04 | 9.0476E-04 | **1.0529E-05** | 1.3192E-07 | 6.0240E-07 | 3.5227E-11 |
| *f5* | 3.3685E-03 | 4.3701E-03 | **1.9505E-04** | 8.8754E-06 | 9.1427E-06 | 1.8427E-08 |
| *f6* | 1.1116E-02 | 1.9877E-02 | **5.1123E-04** | 9.6784E-05 | 2.2039E-04 | 7.4025E-08 |
| *f7* | 8.4205E-03 | 1.4243E-02 | **4.7670E-04** | 5.4449E-05 | 1.3299E-04 | 1.6155E-07 |
| *f8* | 3.3250E-06 | 4.5667E-06 | **1.8545E-06** | 4.6258E-11 | 4.5498E-11 | 6.1744E-12 |
| *f9* | -186.6603 | -186.5090 | **-186.7030** | 3.4926E-03 | 9.7112E-03 | 2.7069E-04 |
| *f10* | -1.03101462 | -1.03104713 | **-1.03157383** | 2.2573E-07 | 1.2621E-07 | 6.3617E-10 |

Table 4.3 shows the difference of the average values obtained in EMLSS and EMSSS to that of the original conventional EM. The comparison gives an indication on how much closer the values obtained by EMLSS and EMSSS are to the global optimal point in relative to the original EM. Positive values suggest that the result of the algorithm is farther away from the global optimal point and less accurate compared to the original EM. Negative values, on the other hand, indicate that the algorithm returns results with better accuracy. It can be observed from the comparison that EMSSS shows better accuracies compared to EMLSS and original EM.

Table 4.3: Average values difference of EMLSS vs EM and EMSSS vs EM.

| | **EMLSS - EM** | **EMSSS - EM** |
|---|---|---|
| *f1* | 3.0322E-01 | -9.8414E-02 |
| *f2* | -4.2770E-04 | -1.6055E-03 |
| *f3* | 1.5514E-03 | -3.4253E-03 |
| *f4* | 5.2860E-04 | -3.6563E-04 |
| *f5* | 1.0017E-03 | -3.1734E-03 |
| *f6* | 8.7604E-03 | -1.0605E-02 |
| *f7* | 5.8226E-03 | -7.9438E-03 |
| *f8* | 1.2416E-06 | -1.4705E-06 |
| *f9* | 1.5126E-01 | -4.2732E-02 |
| *f10* | -3.2516E-05 | -5.5922E-04 |

### 4.1.3 Convergence History Comparisons

Convergence histories were sampled from the 20 runs and the convergence process of the algorithms were compared. The series of figures in Figure 4.4 show the convergence curves of EMLSS and EMSSS on all 10 of the test functions in comparison with the conventional EM. The negative values of the best fitness functions in F9 and F10 prohibit the presentation of the graphs in logarithmic axis.

From the graphs, it can be observed that all the variants of EM performed well in different complex optimization problems. It can be noticed in the convergence curves that EMLSS progress in bigger steps and reach near-optimal values in comparatively earlier iterations in most of the cases. EMSSS, on the other hand, has slower convergences, which in turn lead to comparatively smoother curves. This slow search processes, however, enabled EMSSS to obtain results with higher accuracy compared to both the standard EM and EMLSS. This phenomenon can be observed as the curves of the EMSSS show the ability to achieve comparatively lower values in most of the minimization test functions.

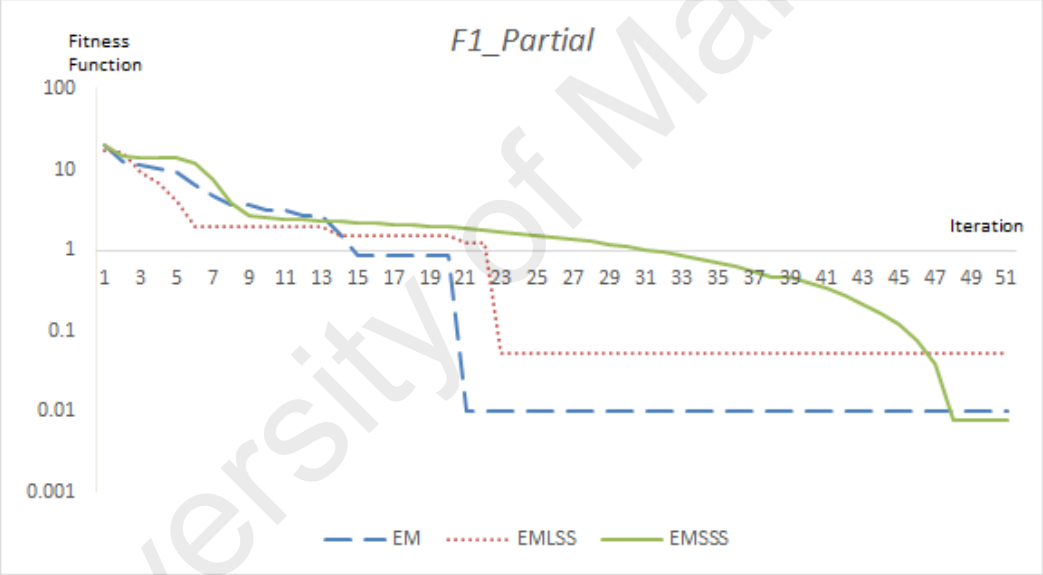


(a)

Figure 4.4: Convergence histories of conventional EM, EMLSS and EMSSS.

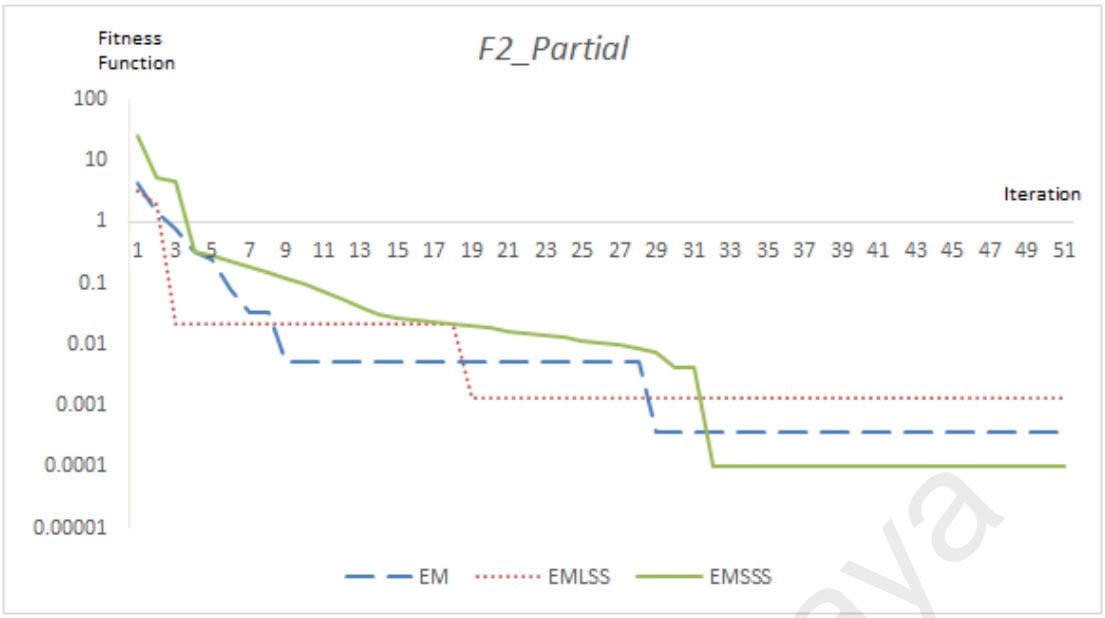


(b)

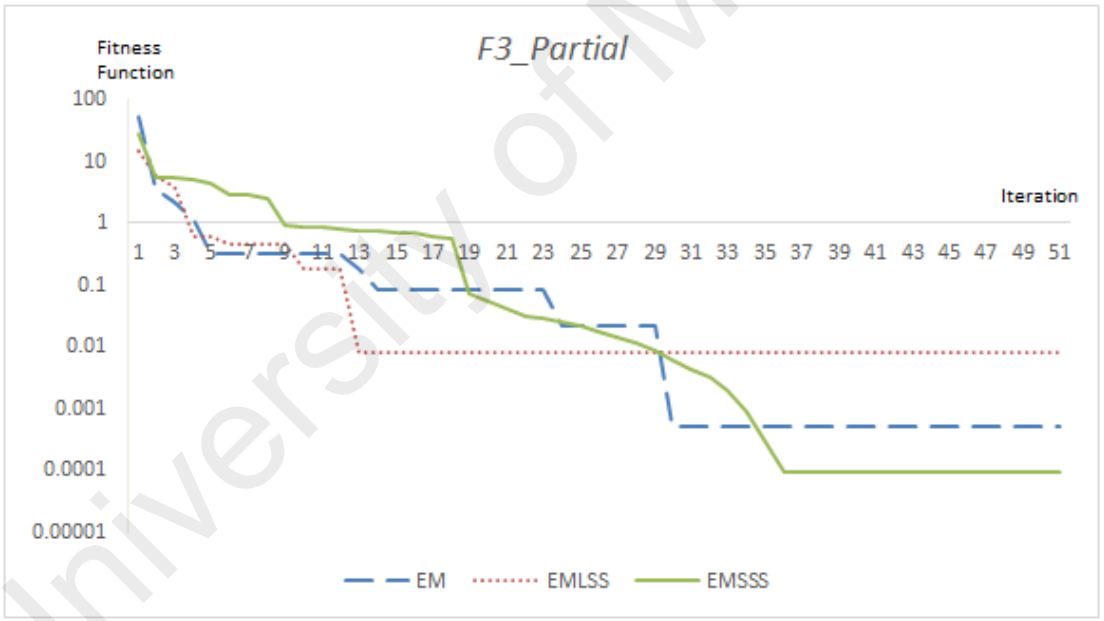


(c)

Figure 4.4, continued: Convergence histories of conventional EM, EMLSS and EMSSS.

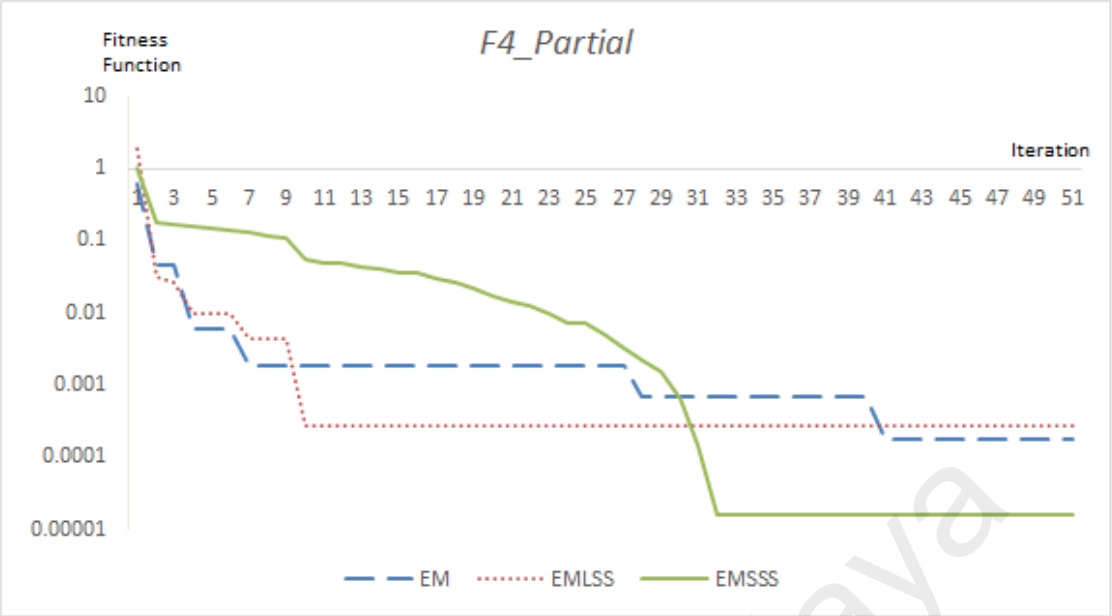


(d)

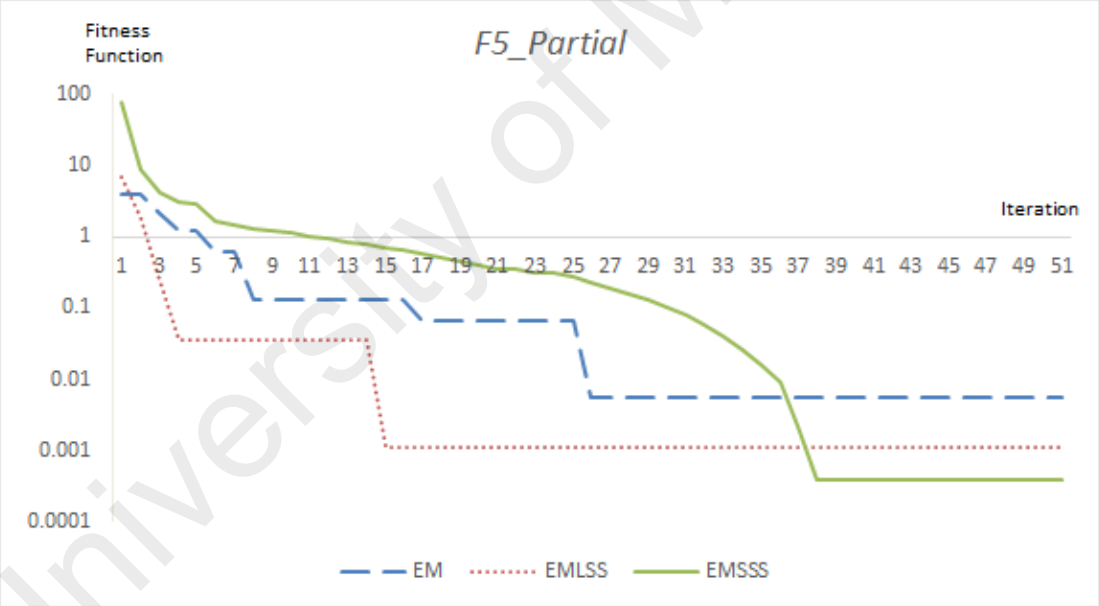


(e)

Figure 4.4, continued: Convergence histories of conventional EM, EMLSS and EMSSS.

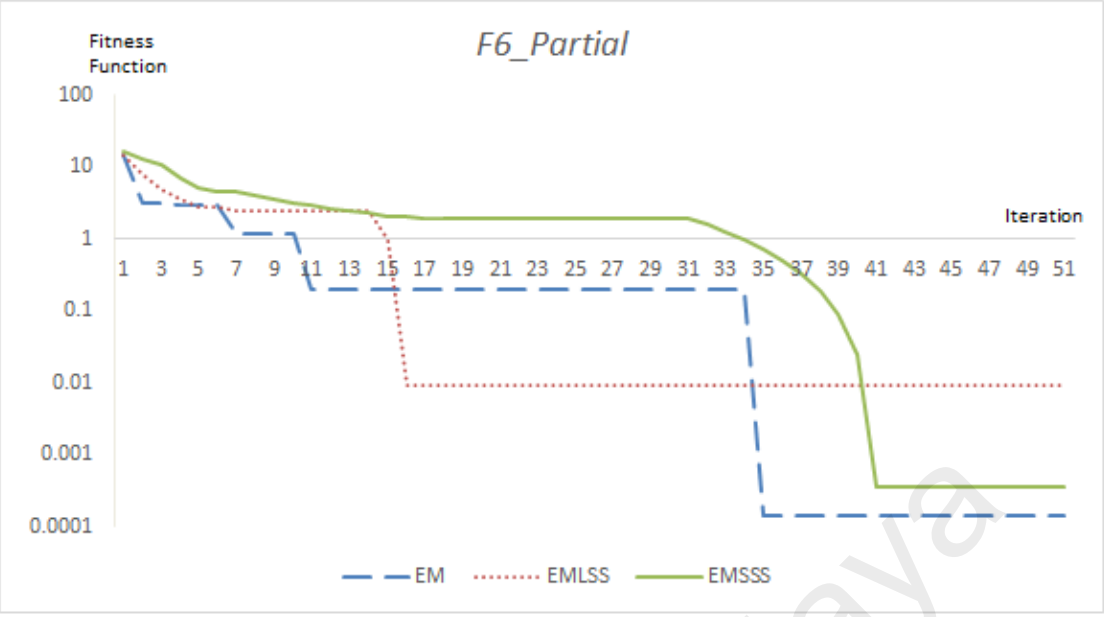


(f)

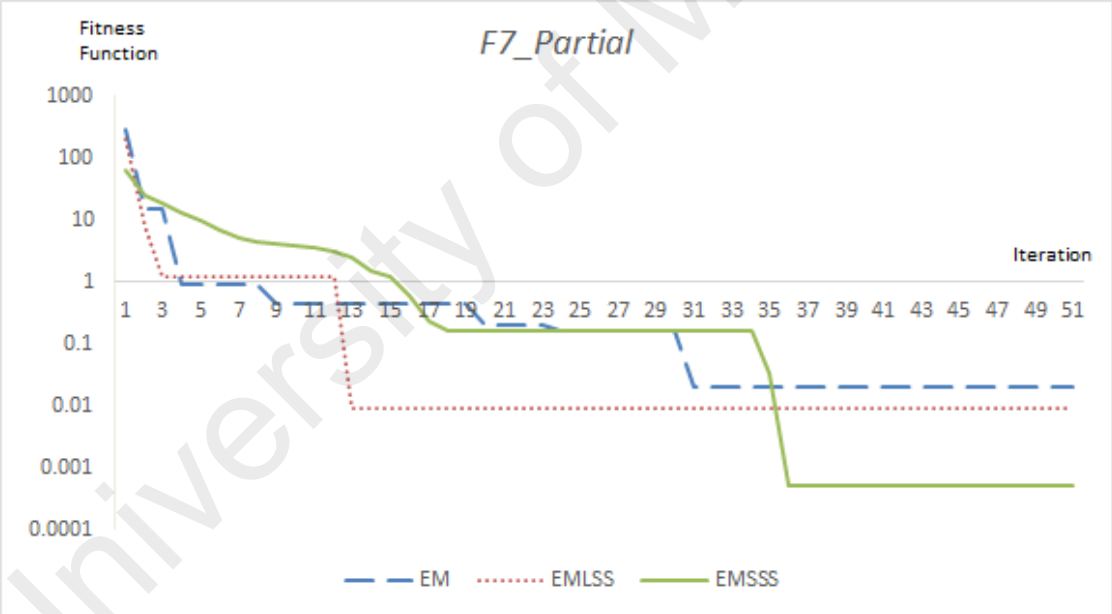


(g)

Figure 4.4, continued: Convergence histories of conventional EM, EMLSS and EMSSS.

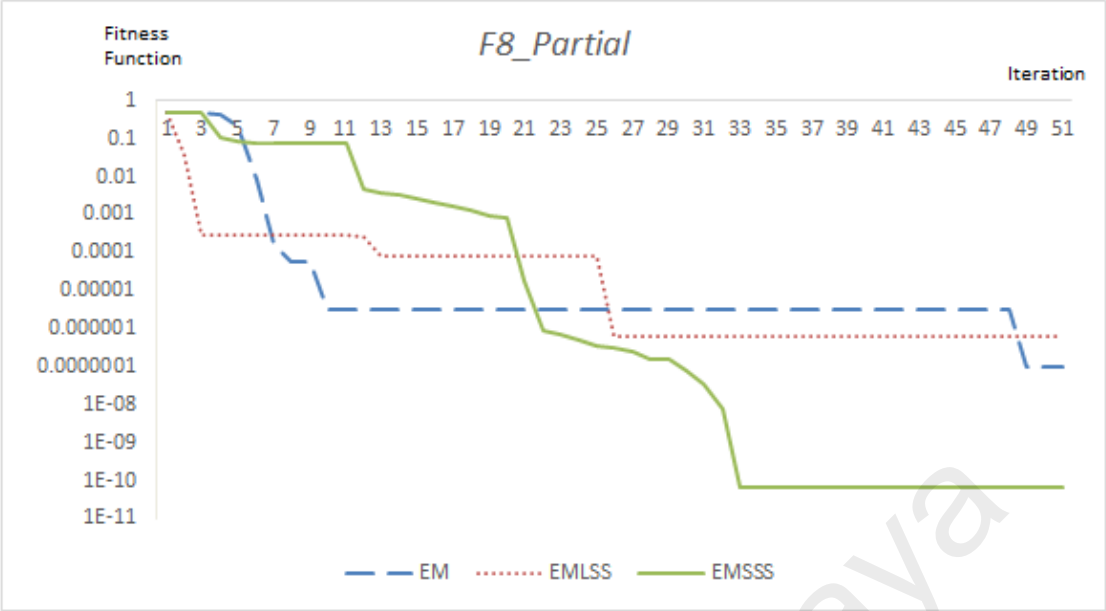


(h)

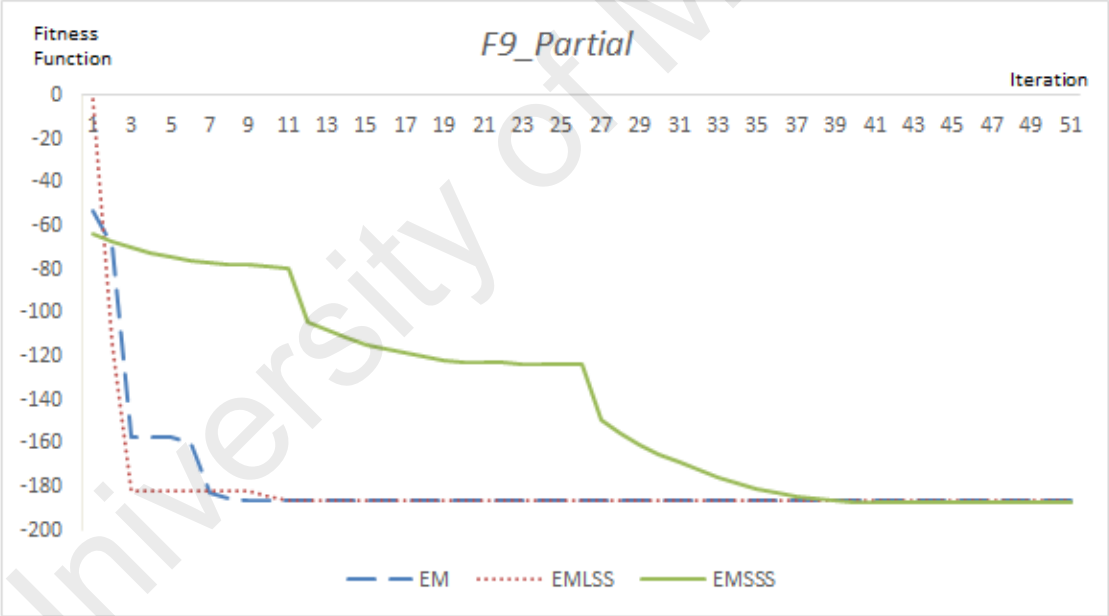


(i)

Figure 4.4, continued: Convergence histories of conventional EM, EMLSS and EMSSS.

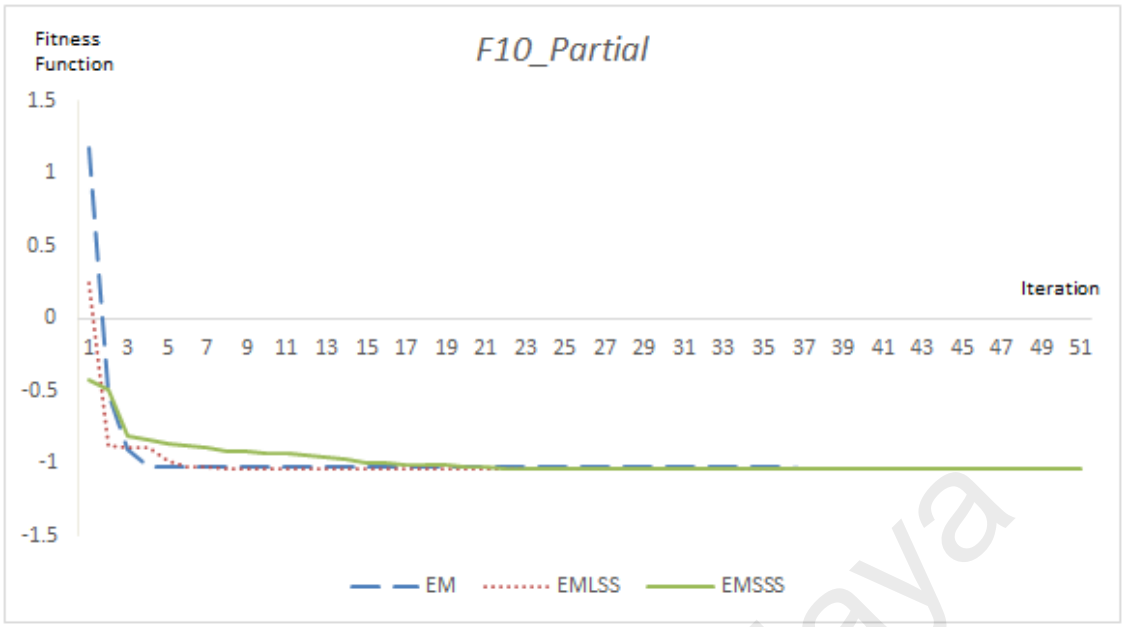


(j)

Figure 4.4, continued: Convergence histories of conventional EM, EMLSS and EMSSS.

### 4.1.4 Particles Movement Analysis

In order to better expose the movement of the particles during the convergence process, the EMLSS and EMSSS were tested to solve the bowl-shaped Sphere test function. For the ease of movement analysis, the dimension number of the test function was set to 2. Table 4.4 shows the results of the best particles in a search for the minima point performed by EMLSS.

Table 4.4: Performance of EMLSS.

| Ite | Best Particle | $X_{\text{Best Particle}}$ | $Y_{\text{Best Particle}}$ | $f_{Best\ Particle}$ |
|---|---|---|---|---|
| 0 | Particle 7 | 0.26 | -1.66 | 2.8232 |
| 1 | Particle 7 | 0.26 | -0.67 | 0.5165 |
| 2 | Particle 7 | 0.26 | 0.32 | 0.17 |
| 3 | Particle 2 | 0.094943093 | 0.078857467 | 0.015232691 |
| 4 | Particle 5 | 0.054285117 | 0.101797292 | 0.013309563 |
| . | . | . | . | . |
| . | . | . | . | . |
| . | . | . | . | . |
| 17 | Particle 5 | 0.054285117 | 0.101797292 | 0.013309563 |
| 18 | Particle 3 | -0.024974939 | 0.049636075 | 0.003087488 |
| . | . | . | . | . |
| . | . | . | . | . |
| . | . | . | . | . |
| 100 | Particle 3 | -0.024974939 | 0.049636075 | 0.003087488 |

As shown in Table 4.4, particle number 7 had the initialized random values of 0.26 and -1.66 for *X* and *Y* respectively. This yielded an objective value of 2.8232, which was the best among all other particles in the initialization. Particle 7 then searched locally and achieved better result of 0.5165 in the first iteration and further improved it to 0.17 in the second iteration. Upon completing the third iteration, particle number 2 found a better result, thus replaced particle number 7 to be the best particle in the iteration. In iteration 4, particle 5 found an even better objective value at $X$= 0.054285117 and $Y$ = 0.101797292. It maintained its position as the best particle until iteration 17. The search reached its best minima point at the end of iteration 18, when particle number 3 found a new best minima of 0.003087488 at $X$= -0.024974939 and $Y$ = 0.049636075. The result for the best particle remained the same from iteration 18 onwards to iteration 80.

Figure 4.5 shows the movement of the best particles from initialization (*i0*) to iteration 18 (*i18*). All the different positions of the particles yielded different objective values, as shown on the right side of the graph. The best particles moved from iteration to iteration towards the origin point (*0,0*), where the best minima is located.

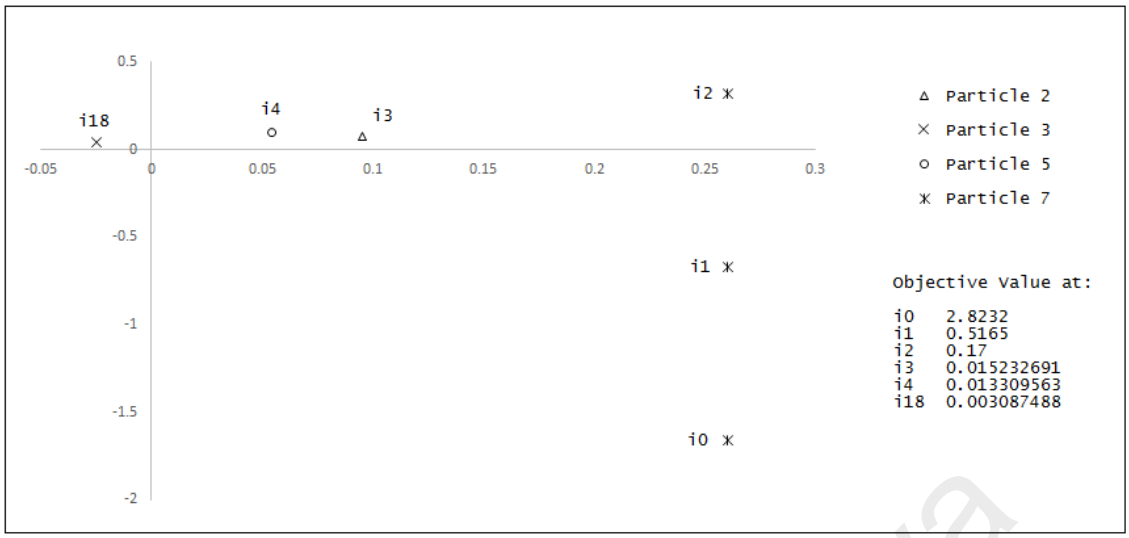


Figure 4.5: Movement of best particles in EMLSS from iteration to iteration.

EMSSS, on the other hand, performed a much detailed search. Table 4.5 shows the search history of the experiment. Since the search steps in EMSSS were comparatively smaller, it caused the improvement in objective values to be relatively smaller as well. A plot of graph in Figure 4.6 gives a better image on how the search mechanism was carried out with a sample movement from iteration 8 to iteration 37 by particle 6, which was the best particle in those iterations as it found the lowermost value in the minimization test function. Particle 4 took over when it found a better objective value in iteration 38. The movement scale of the plot shows smaller search steps compared to the movements in BSL.

Table 4.5. Performance of EMSSS.

| Ite | Best Particle | $X_{\text{Best Particle}}$ | $Y_{\text{Best Particle}}$ | $f_{\textit{Best Particle}}$ |
|---|---|---|---|---|
| 0 | Particle 7 | 0.97 | -0.75 | 1.5034 |
| 1 | Particle 7 | 0.96 | -0.74 | 1.4692 |
| 2 | Particle 7 | 0.95 | -0.73 | 1.4354 |
| 3 | Particle 6 | -0.521062359 | -0.667410792 | 0.716943148 |
| 4 | Particle 6 | -0.511062359 | -0.657410792 | 0.693373685 |
| 5 | Particle 9 | -0.225239608 | -0.629136921 | 0.446546146 |
| 6 | Particle 9 | -0.215239608 | -0.619136921 | 0.429658615 |
| 7 | Particle 9 | -0.205239608 | -0.609136921 | 0.413171085 |
| 8 | Particle 6 | -0.249784768 | 0.096136126 | 0.071634585 |
| 9 | Particle 6 | -0.239784768 | 0.086136126 | 0.064916167 |
| 10 | Particle 6 | -0.229784768 | 0.076136126 | 0.058597749 |
| 11 | Particle 6 | -0.229784768 | 0.066136126 | 0.057175027 |
| 12 | Particle 6 | -0.219784768 | 0.056136126 | 0.051456609 |
| 13 | Particle 6 | -0.209784768 | 0.046136126 | 0.046138191 |
| 14 | Particle 6 | -0.199784768 | 0.036136126 | 0.041219773 |
| 15 | Particle 6 | -0.189784768 | 0.026136126 | 0.036701355 |
| 16 | Particle 6 | -0.179784768 | 0.016136126 | 0.032582937 |
| 17 | Particle 6 | -0.169784768 | 0.006136126 | 0.028864519 |
| 18 | Particle 6 | -0.159784768 | -0.003863874 | 0.025546101 |
| 19 | Particle 6 | -0.149784768 | -0.003863874 | 0.022450406 |
| 20 | Particle 6 | -0.139784768 | -0.003863874 | 0.019554711 |
| 21 | Particle 6 | -0.129784768 | -0.003863874 | 0.016859015 |
| 22 | Particle 6 | -0.119784768 | -0.003863874 | 0.01436332 |
| 23 | Particle 6 | -0.119784768 | -0.003863874 | 0.01436332 |
| 24 | Particle 6 | -0.109784768 | -0.003863874 | 0.012067625 |
| 25 | Particle 6 | -0.099784768 | -0.003863874 | 0.009971929 |
| 26 | Particle 6 | -0.089784768 | -0.003863874 | 0.008076234 |
| 27 | Particle 6 | -0.079784768 | -0.003863874 | 0.006380539 |
| 28 | Particle 6 | -0.069784768 | -0.003863874 | 0.004884843 |
| 29 | Particle 6 | -0.059784768 | -0.003863874 | 0.003589148 |
| 30 | Particle 6 | -0.049784768 | -0.003863874 | 0.002493453 |
| 31 | Particle 6 | -0.039784768 | -0.003863874 | 0.001597757 |
| 32 | Particle 6 | -0.029784768 | -0.003863874 | 0.000902062 |
| 33 | Particle 6 | -0.019784768 | -0.003863874 | 0.000406367 |
| 34 | Particle 6 | -0.009784768 | -0.003863874 | 0.000110671 |
| 35 | Particle 6 | 0.000215232 | -0.003863874 | 1.50E-05 |
| 36 | Particle 6 | 0.000215232 | -0.003863874 | 1.50E-05 |
| 37 | Particle 6 | 0.000215232 | -0.003863874 | 1.50E-05 |
| 38 | Particle 4 | 0.001504167 | -0.001954916 | 6.08E-06 |
| . | . | . | . | . |
| . | . | . | . | . |
| . | . | . | . | . |
| 100 | Particle 4 | 0.001504167 | -0.001954916 | 6.08E-06 |

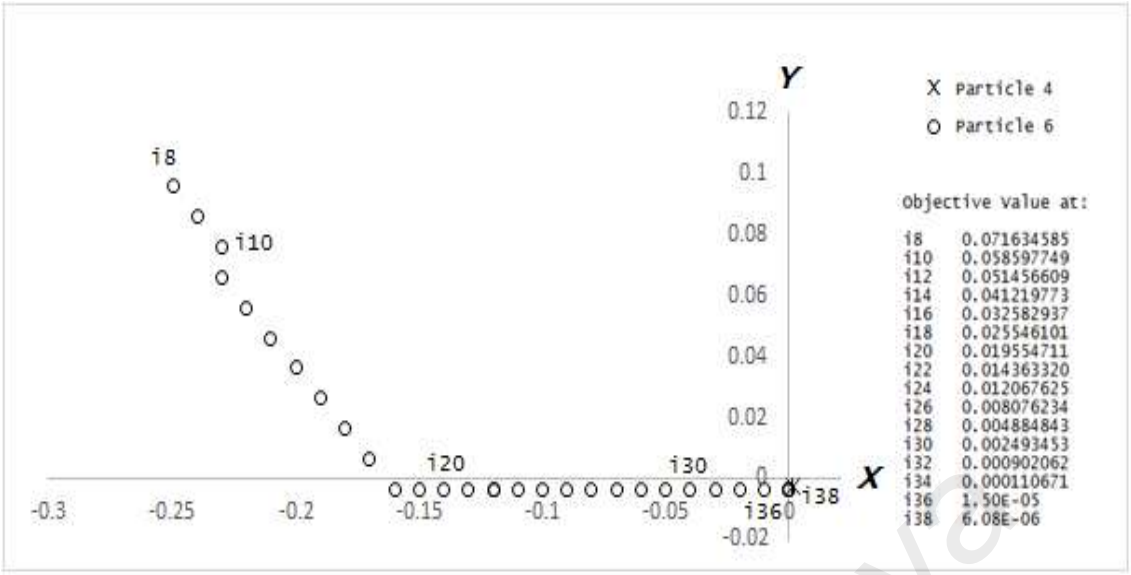


Figure 4.6: EMSSS local search movement by particle 6.

The solutions with highest accuracies are highlighted in boldface. The results show EM with larger search steps reached near-optimal values faster with less iteration number needed. The trade-off, however, is that the solutions returned by EMLSS are generally less accurate compared to all the other EM algorithms. The large steps may skip some of the better solutions between the steps, resulting in outcomes with lower accuracies. EM with smaller search steps, on the other hand, returned outcomes which are more accurate compared to EMLSS. Its small search steps enabled it to better exploit the solutions, granting the algorithm to achieve final results with consistently higher accuracies. However, the small steps employed requires more iterations to complete the convergence, which in turn slow down the overall convergence process.

## 4.2 SPC-EM

The proposed SPC-EM was tested in the designed test suite to analyse its performance in solving numerical optimization problems. The results are compared with that of the conventional EM, EMLSS and EMSSS. From the literature, Genetic Algorithm (GA) is found to be one of the most established and well-known meta-heuristic algorithms. Therefore, it is also included in the results benchmarking in order to effectively justify the performance of the proposed algorithm. 20 independent runs were adopted in SPC-EM to avoid stochastic discrepancy.

### 4.2.1 Performance Benchmarking

The comparisons of the computational results are shown in Tables 4.6. In each table, "*Best*" indicates the best value ever obtained by the algorithm in the corresponding test function throughout the 20 independent runs. "*Mean*" refers to the mean value of the 20 results obtained from the independent runs in solving the corresponding benchmark function. "*SD*" denotes the respective standard deviation value of the results. "*Rank*" stands for the performance comparison ranking of the search algorithm based on the mean results ("*Mean*").

Table 4.6: Best values, worst values, mean values and standard deviations comparison

| | | SPC-EM | EM | EMLSS | EMSSS | GA |
|---|---|---|---|---|---|---|
| F1 | Best | 1.4193E-03 | 3.5488E-03 | 4.5921E-02 | 3.8573E-03 | 3.0947E-02 |
| | Worst | 1.4353E-03 | 2.7525E-01 | 4.1649E-01 | 1.2121E-02 | 2.6375E+00 |
| | Mean | **1.4247E-03** | 1.0603E-01 | 2.0480E-01 | 7.6152E-03 | 5.9336E-01 |
| | SD | 2.3926E-11 | 5.6446E-03 | 1.5163E-02 | 5.4233E-06 | 5.6891E-01 |
| | Rank | 1 | 3 | 4 | 2 | 5 |
| F2 | Best | 3.9364E-07 | 3.9145E-05 | 2.5787E-04 | 9.5861E-07 | 1.5779E-06 |
| | Worst | 3.2743E-05 | 4.9154E-03 | 3.7381E-03 | 4.6775E-04 | 8.5408E-02 |
| | Mean | **4.6110E-06** | 1.7701E-03 | 1.3424E-03 | 1.6460E-04 | 1.3026E-02 |
| | SD | 6.1325E-11 | 2.5603E-06 | 7.9994E-07 | 2.5631E-08 | 5.5266E-04 |
| | Rank | 1 | 4 | 3 | 2 | 5 |
| F3 | Best | 1.2472E-06 | 1.4551E-05 | 5.4168E-04 | 5.3497E-05 | 1.7997E-05 |
| | Worst | 2.0052E-06 | 9.7606E-03 | 9.3487E-03 | 5.2585E-04 | 2.2922E-02 |
| | Mean | **1.3958E-06** | 3.5775E-03 | 5.1289E-03 | 1.5220E-04 | 1.2109E-02 |
| | SD | 5.9082E-14 | 1.0620E-05 | 6.8173E-06 | 1.2121E-08 | 9.4126E-05 |
| | Rank | 1 | 3 | 4 | 2 | 5 |
| F4 | Best | 2.4944E-07 | 7.9371E-06 | 1.2766E-04 | 2.8497E-06 | 4.0000E-06 |
| | Worst | 2.4997E-07 | 1.2945E-03 | 3.3039E-03 | 2.1470E-05 | 9.0000E-04 |
| | Mean | **2.4962E-07** | 3.7616E-04 | 9.0476E-04 | 1.0529E-05 | 2.6330E-04 |
| | SD | 2.8795E-20 | 1.3192E-07 | 6.0240E-07 | 3.5227E-11 | 5.4418E-08 |
| | Rank | 1 | 4 | 5 | 2 | 3 |
| F5 | Best | 3.6616E-06 | 1.5761E-05 | 1.7194E-04 | 1.1683E-05 | 3.2809E-05 |
| | Worst | 5.8058E-06 | 9.1845E-03 | 9.5083E-03 | 4.6511E-04 | 4.5956E-02 |
| | Mean | **3.8741E-06** | 3.3685E-03 | 4.3701E-03 | 1.9505E-04 | 7.9481E-03 |
| | SD | 2.1121E-13 | 8.8754E-06 | 9.1427E-06 | 1.8427E-08 | 1.4531E-04 |
| | Rank | 1 | 3 | 4 | 2 | 5 |
| F6 | Best | 4.9526E-05 | 1.4493E-04 | 1.8655E-03 | 6.0471E-05 | 1.9855E-04 |
| | Worst | 5.7421E-05 | 3.0677E-02 | 4.9664E-02 | 9.7521E-04 | 1.9884E+00 |
| | Mean | **5.1338E-05** | 1.1116E-02 | 1.9877E-02 | 5.1123E-04 | 2.6310E-01 |
| | SD | 5.6796E-12 | 9.6784E-05 | 2.2039E-04 | 7.4025E-08 | 2.7924E-01 |
| | Rank | 1 | 3 | 4 | 2 | 5 |
| F7 | Best | 2.4945E-05 | 4.8441E-05 | 9.8546E-04 | 4.1846E-05 | 1.4607E-04 |
| | Worst | 2.8149E-05 | 2.8021E-02 | 3.9921E-02 | 1.2764E-03 | 9.0797E-02 |
| | Mean | **2.5914E-05** | 8.4205E-03 | 1.4243E-02 | 4.7670E-04 | 3.3102E-02 |
| | SD | 8.6973E-13 | 5.4449E-05 | 1.3299E-04 | 1.6155E-07 | 9.1038E-04 |
| | Rank | 1 | 3 | 4 | 2 | 5 |
| F8 | Best | 1.1102E-16 | 4.4633E-12 | 1.5314E-07 | 6.4951E-11 | 1.1000E-07 |
| | Worst | 2.0630E-05 | 3.0381E-05 | 2.3740E-05 | 7.1495E-06 | 7.1922E-04 |
| | Mean | **1.4542E-06** | 3.3250E-06 | 4.5667E-06 | 1.8545E-06 | 1.8244E-04 |
| | SD | 2.0079E-11 | 4.6258E-11 | 4.5498E-11 | 6.1744E-12 | 4.7147E-08 |
| | Rank | 1 | 3 | 4 | 2 | 5 |
| F9 | Best | -186.7304 | -186.7259 | -186.7010 | -186.7300 | -186.7299 |
| | Worst | -186.7303 | -186.5277 | -186.3577 | -186.6749 | -169.5802 |
| | Mean | **-186.7303** | -186.6603 | -186.5090 | -186.7030 | -185.3659 |
| | SD | 5.4656E-10 | 3.4926E-03 | 9.7112E-03 | 2.7069E-04 | 1.3925E+01 |
| | Rank | 1 | 3 | 4 | 2 | 5 |
| F10 | Best | -1.03162780 | -1.03162337 | -1.03159788 | -1.03162720 | -1.03162500 |
| | Worst | -1.03162745 | -1.03011631 | -1.03007554 | -1.03152877 | -1.02697000 |
| | Mean | **-1.03162749** | -1.03101462 | -1.03104713 | -1.03157383 | -1.03044870 |
| | SD | 5.2578E-15 | 2.2573E-07 | 1.2621E-07 | 6.3617E-10 | 1.1913E-06 |
| | Rank | 1 | 4 | 3 | 2 | 5 |

The benchmarking reveals the striking capability of SPC-EM in obtaining optimal solutions with higher accuracy and precision. The solutions found by SPC-EM are relatively much better than the solutions found by the conventional EM, EMLSS, EMSSS, and GA. The systematically-self-regulating probe length feature of the SPC-EM enabled it to effectively exploit the solutions. The fine-tuned search steps towards the end of the local search every time also ensured the precision of the algorithm, which in turn resulted in lower standard deviation values as shown in the table. From the overall analysis on the results benchmarking, SPC-EM outperformed all the other algorithms involved.

### 4.2.2 Convergence Process Analysis

Figures 4.7 show the convergence curves of the benchmarked algorithms in all the test functions. The graphs are focused on the first 50 iterations of the convergences where most of the movements took place. Logarithmic axis is not applicable in test functions *F9* and *F10* due to the negative values of the objective functions. It can be noted from the graphs that the SPC-EM performed well in solving variable types of complex optimization problems in terms of the accuracy of the solutions and overall convergence performance. The SPC-EM progressed very rapidly in early stages and found near-optimal values in relatively earlier iterations in most of the cases. The ability for the SPC-EM to reach near optimum values in earlier stage of convergence was due to its long probe lengths at the beginning of the search. The regulated and fine-tuned probe lengths towards the end of the local search of SPC-EM enabled it to achieve solutions with relatively higher accuracy. The tuning of the probe lengths helped SPC-EM to outperform other algorithms in their overall convergence process.

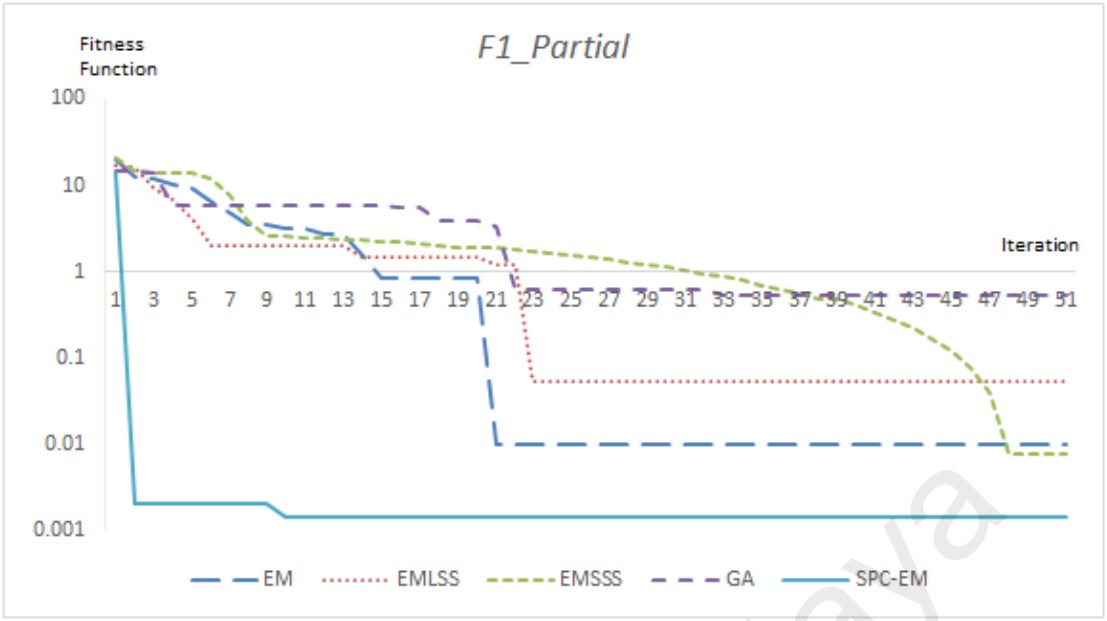


(a)

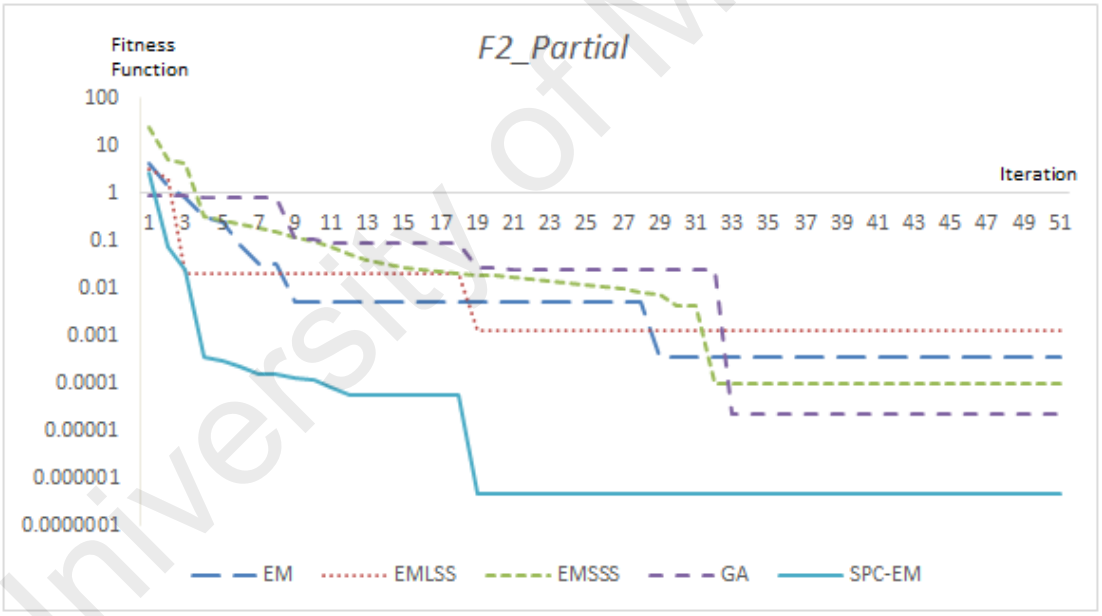


(b)

Figure 4.7: Convergence histories comparison of SPC-EM, conventional EM, EMLSS, EMSSS and GA.

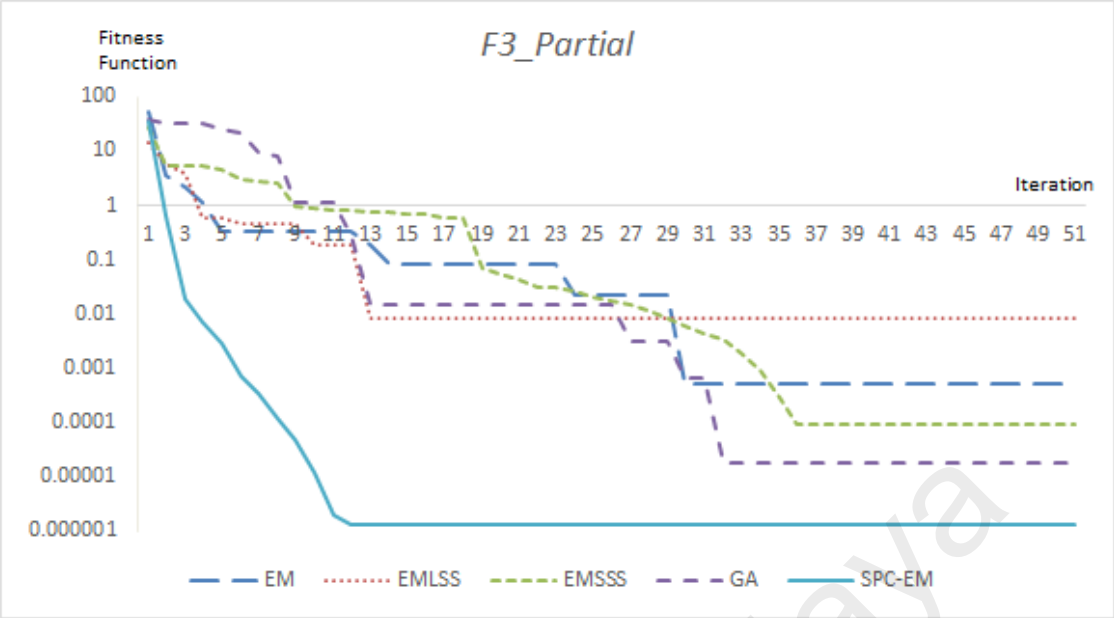


(c)

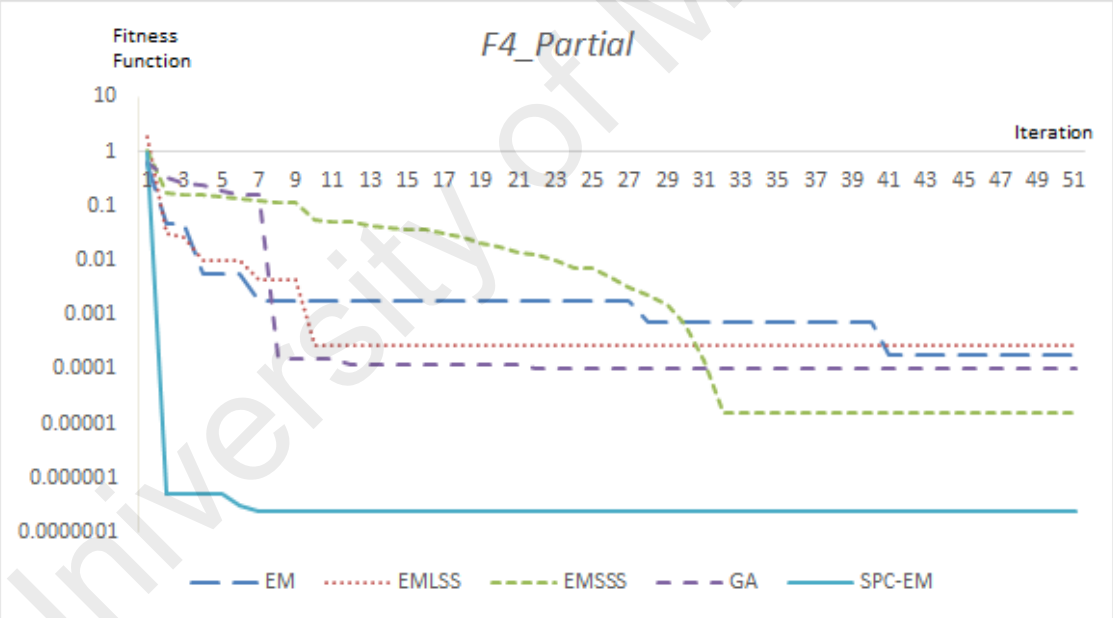


(d)

Figure 4.7, continued: Convergence histories comparison of SPC-EM, conventional EM, EMLSS, EMSSS and GA.

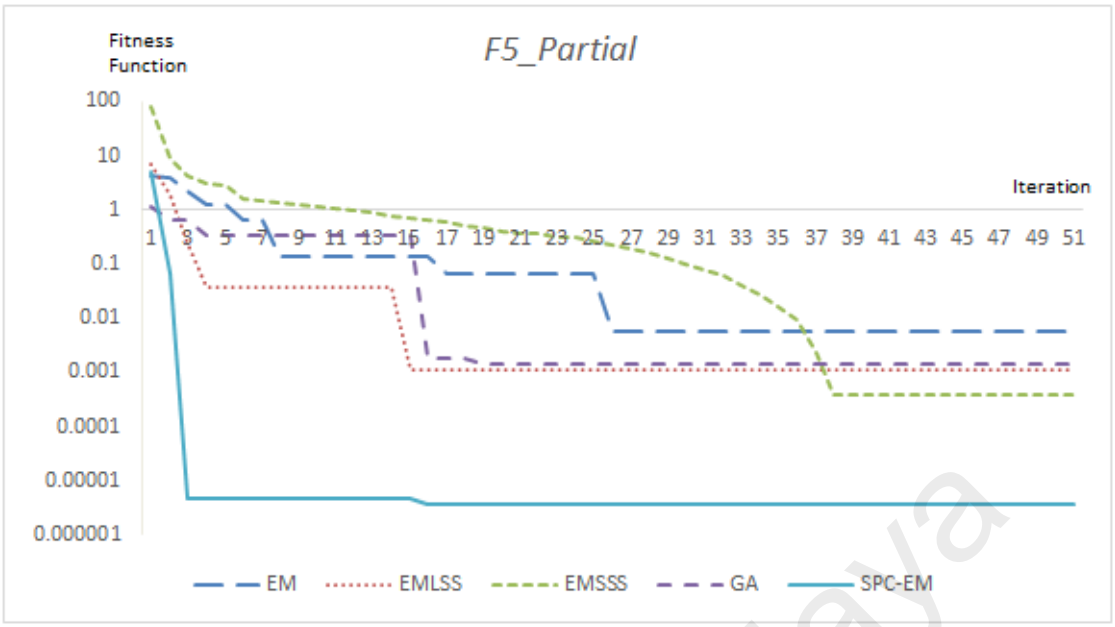


(e)

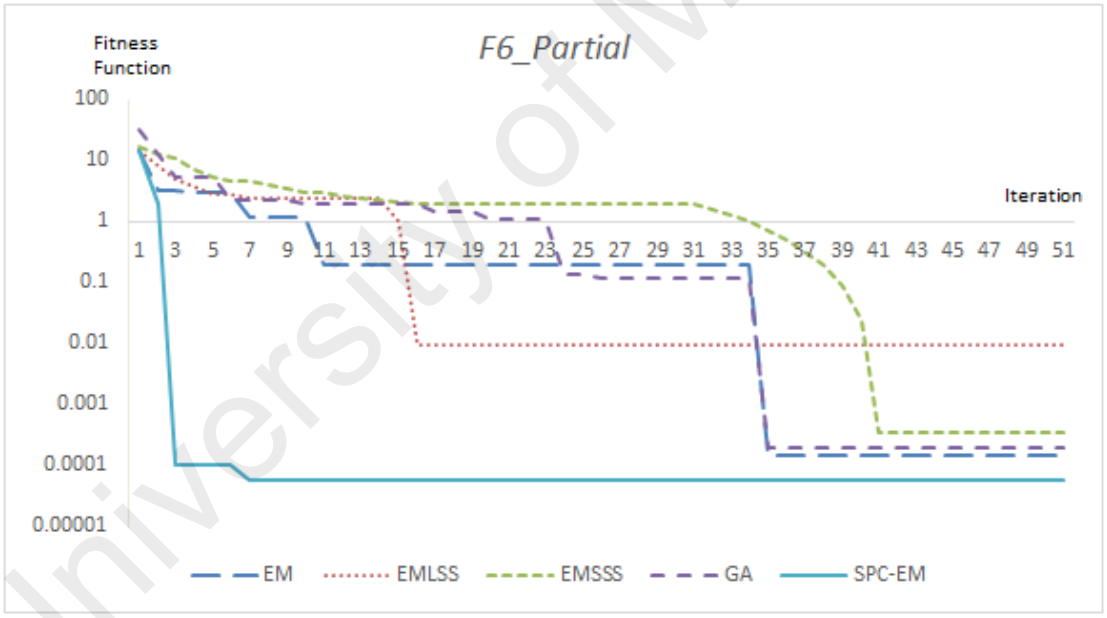


(f)

Figure 4.7, continued: Convergence histories comparison of SPC-EM, conventional EM, EMLSS, EMSSS and GA.

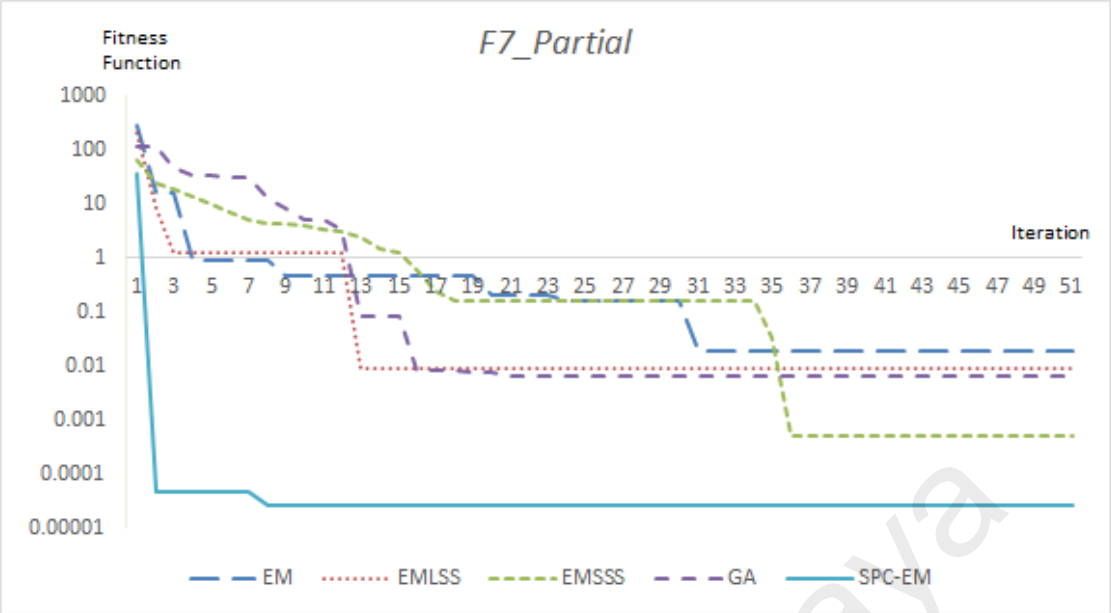


(g)

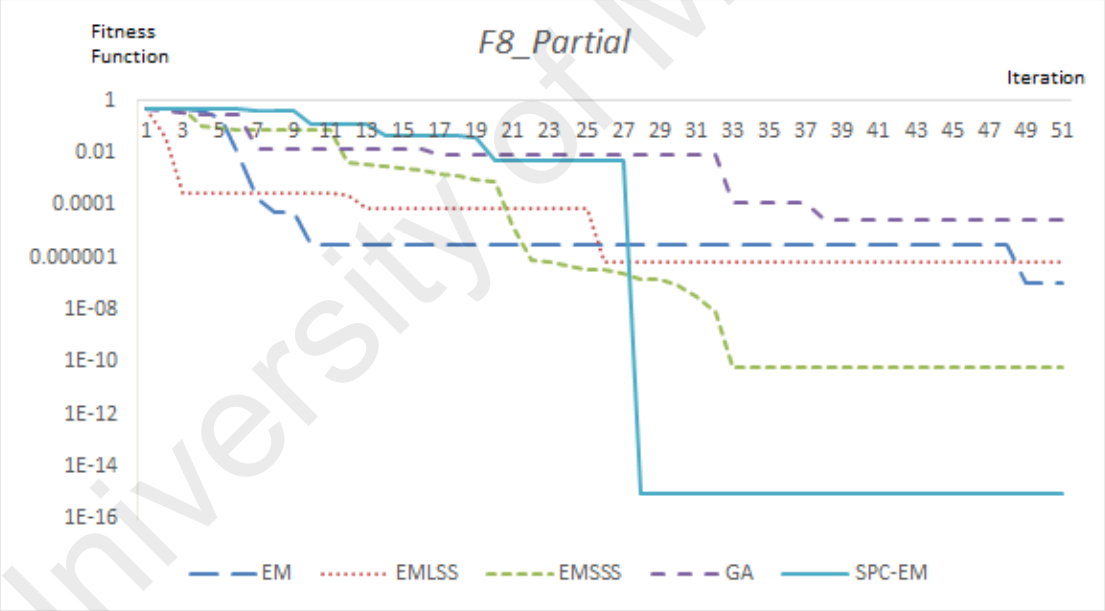


(h)

Figure 4.7, continued: Convergence histories comparison of SPC-EM, conventional EM, EMLSS, EMSSS and GA.

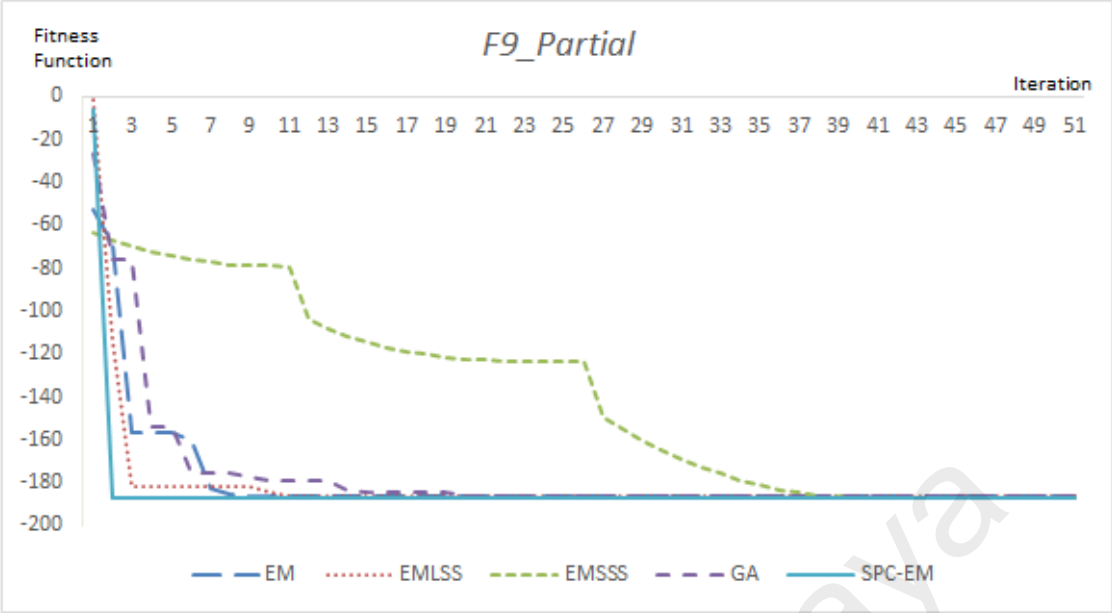


(i)

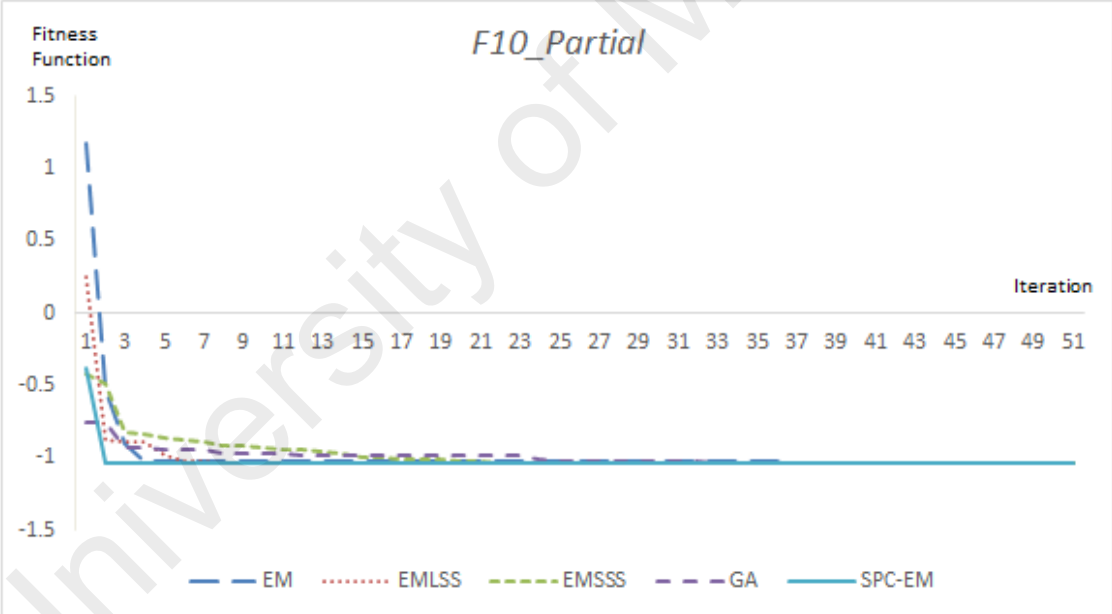


(j)

Figure 4.7, continued: Convergence histories comparison of SPC-EM, conventional EM, EMLSS, EMSSS and GA.

## 4.3 ELEM

The same experiment setup was used to test the proposed ELEM. The experiment for each of the tests were carried out 20 times to avoid stochastic discrepancy. The results obtained by ELEM are compared with the conventional EM, EMLSS, EMSSS and GA in terms of the best solutions, worst solutions, mean values and standard deviations of the 20 independent runs.

### 4.3.1 Performance Benchmarking

Table 4.7 shows the results comparison of ELEM with other algorithms in terms of the best solutions, worst solutions, mean values, and standard deviations of the 20 independent runs. Based on the mean values, ELEM ranks the first place compared to other algorithms. The overall result comparisons reveal the potential of ELEM in achieving optimal solutions with higher accuracies and precisions. ELEM steadily shows better performance in contrast with the conventional EM, EMLSS, EMSSS and GA. EMSSS shows very competitive results on the best solutions achieved in test functions *F2*, *F6*, *F7*, and *F9*. It even outperforms ELEM in the worst value achieved column in *F8*. ELEM shows very promising performance in solving multi-model functions, such as F1, F5, F6, F8, F9, and F10. The strong exploration ability of EM paired with the powerful experience-based exploitation mechanism enabled ELEM to escape local traps and returns with high accuracy solutions.

Table 4.7: Comparison on the best solutions, worst solutions, mean values, and standard deviations generated by ELEM with the other benchmark algorithms.

| | | ELEM | EM | EMLSS | EMSSS | GA |
|---|---|---|---|---|---|---|
| F1 | Best | 2.3785E-04 | 3.5488E-03 | 4.5921E-02 | 3.8573E-03 | 3.0947E-02 |
| | Worst | 9.6410E-04 | 2.7525E-01 | 4.1649E-01 | 1.2121E-02 | 2.6375E+00 |
| | Mean | **8.0935E-04** | 1.0603E-01 | 2.0480E-01 | 7.6152E-03 | 5.9336E-01 |
| | SD | 6.6424E-08 | 5.6446E-03 | 1.5163E-02 | 5.4233E-06 | 5.6891E-01 |
| | Rank | 1 | 3 | 4 | 2 | 5 |
| F2 | Best | 1.7511E-07 | 3.9145E-05 | 2.5787E-04 | 9.5861E-07 | 1.5779E-06 |
| | Worst | 1.6450E-05 | 4.9154E-03 | 3.7381E-03 | 4.6775E-04 | 8.5408E-02 |
| | Mean | **3.0747E-06** | 1.7701E-03 | 1.3424E-03 | 1.6460E-04 | 1.3026E-02 |
| | SD | 1.8329E-11 | 2.5603E-06 | 7.9994E-07 | 2.5631E-08 | 5.5266E-04 |
| | Rank | 1 | 4 | 3 | 2 | 5 |
| F3 | Best | 5.5609E-07 | 1.4551E-05 | 5.4168E-04 | 5.3497E-05 | 1.7997E-05 |
| | Worst | 1.3053E-06 | 9.7606E-03 | 9.3487E-03 | 5.2585E-04 | 2.2922E-02 |
| | Mean | **7.6655E-07** | 3.5775E-03 | 5.1289E-03 | 1.5220E-04 | 1.2109E-02 |
| | SD | 9.9573E-14 | 1.0620E-05 | 6.8173E-06 | 1.2121E-08 | 9.4126E-05 |
| | Rank | 1 | 3 | 4 | 2 | 5 |
| F4 | Best | 1.1096E-07 | 7.9371E-06 | 1.2766E-04 | 2.8497E-06 | 4.0000E-06 |
| | Worst | 1.1162E-07 | 1.2945E-03 | 3.3039E-03 | 2.1470E-05 | 9.0000E-04 |
| | Mean | **1.1106E-07** | 3.7616E-04 | 9.0476E-04 | 1.0529E-05 | 2.6330E-04 |
| | SD | 2.1177E-20 | 1.3192E-07 | 6.0240E-07 | 3.5227E-11 | 5.4418E-08 |
| | Rank | 1 | 4 | 5 | 2 | 3 |
| F5 | Best | 1.6275E-06 | 1.5761E-05 | 1.7194E-04 | 1.1683E-05 | 3.2809E-05 |
| | Worst | 3.5498E-06 | 9.1845E-03 | 9.5083E-03 | 4.6511E-04 | 4.5956E-02 |
| | Mean | **1.9761E-06** | 3.3685E-03 | 4.3701E-03 | 1.9505E-04 | 7.9481E-03 |
| | SD | 3.2895E-13 | 8.8754E-06 | 9.1427E-06 | 1.8427E-08 | 1.4531E-04 |
| | Rank | 1 | 3 | 4 | 2 | 5 |
| F6 | Best | 2.2032E-05 | 1.4493E-04 | 1.8655E-03 | 6.0471E-05 | 1.9855E-04 |
| | Worst | 2.2343E-05 | 3.0677E-02 | 4.9664E-02 | 9.7521E-04 | 1.9884E+00 |
| | Mean | **2.2060E-05** | 1.1116E-02 | 1.9877E-02 | 5.1123E-04 | 2.6310E-01 |
| | SD | 4.6304E-15 | 9.6784E-05 | 2.2039E-04 | 7.4025E-08 | 2.7924E-01 |
| | Rank | 1 | 3 | 4 | 2 | 5 |
| F7 | Best | 1.1120E-05 | 4.8441E-05 | 9.8546E-04 | 4.1846E-05 | 1.4607E-04 |
| | Worst | 2.7677E-05 | 2.8021E-02 | 3.9921E-02 | 1.2764E-03 | 9.0797E-02 |
| | Mean | **1.3260E-05** | 8.4205E-03 | 1.4243E-02 | 4.7670E-04 | 3.3102E-02 |
| | SD | 1.5737E-11 | 5.4449E-05 | 1.3299E-04 | 1.6155E-07 | 9.1038E-04 |
| | Rank | 1 | 3 | 4 | 2 | 5 |
| F8 | Best | 0.0000E+00 | 4.4633E-12 | 1.5314E-07 | 6.4951E-11 | 1.1000E-07 |
| | Worst | 7.5275E-06 | 3.0381E-05 | 2.3740E-05 | 7.1495E-06 | 7.1922E-04 |
| | Mean | **4.2922E-07** | 3.3250E-06 | 4.5667E-06 | 1.8545E-06 | 1.8244E-04 |
| | SD | 2.6611E-12 | 4.6258E-11 | 4.5498E-11 | 6.1744E-12 | 4.7147E-08 |
| | Rank | 1 | 3 | 4 | 2 | 5 |
| F9 | Best | -186.7307 | -186.7259 | -186.7010 | -186.7300 | -186.7299 |
| | Worst | -186.7304 | -186.5277 | -186.3577 | -186.6749 | -169.5802 |
| | Mean | **-186.7306** | -186.6603 | -186.5090 | -186.7030 | -185.3659 |
| | SD | 5.4818E-09 | 3.4926E-03 | 9.7112E-03 | 2.7069E-04 | 1.3925E+01 |
| | Rank | 1 | 3 | 4 | 2 | 5 |
| F10 | Best | -1.03162802 | -1.03162337 | -1.03159788 | -1.03162720 | -1.03162500 |
| | Worst | -1.03162792 | -1.03011631 | -1.03007554 | -1.03152877 | -1.02697000 |
| | Mean | **-1.03162801** | -1.03101462 | -1.03104713 | -1.03157383 | -1.03044870 |
| | SD | 4.9932E-16 | 2.2573E-07 | 1.2621E-07 | 6.3617E-10 | 1.1913E-06 |
| | Rank | 1 | 4 | 3 | 2 | 5 |

### 4.3.2 Convergence Process Analysis

Figures 4.8 graphically present the comparison on typical convergence characteristics between the ELEM, GA, and the variants of EM involved in the benchmarking. It can be clearly observed from the graphs that the ELEM performed well in different complex optimization problems both in terms of the quality of the solution and convergence speed. The gradient analysis of the ELEM and its ability to backtrack the experience of previous searches enable it to perform a well-directed local search. This advantage was balanced by a well-diversified solutions search in the global movement stage of the ELEM, where the particles were moved in accordance to the attraction and repulsion forces influenced by all other particles in the search space. With the combination of the two advantages, the ELEM algorithm converged more rapidly and reached lower objective values than other algorithms, Lower objective values indicate solutions with higher accuracies.

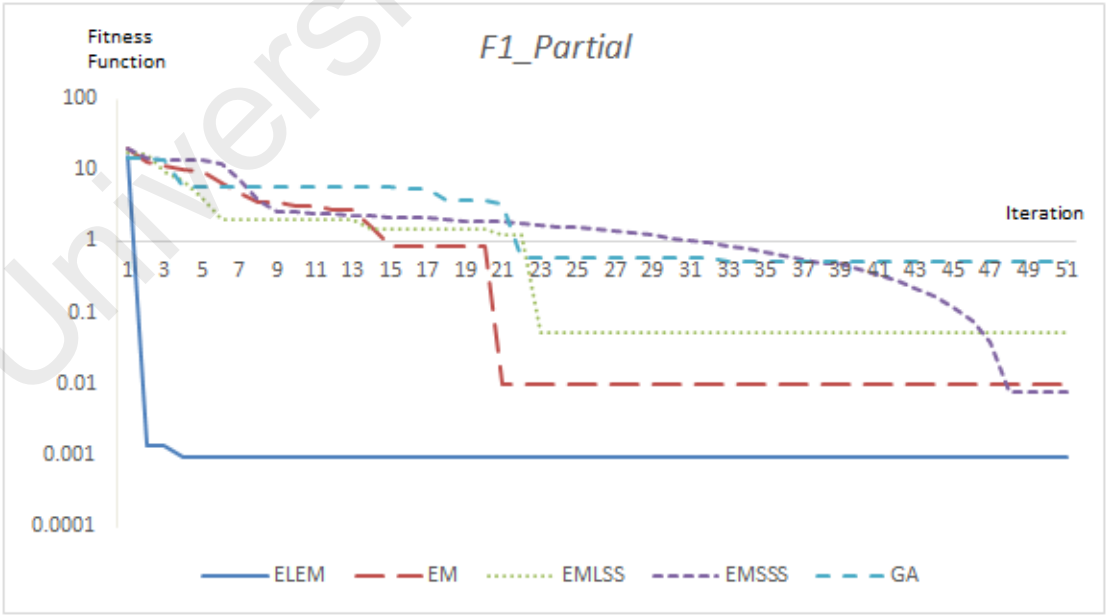


(a)

Figure 4.8, continued: Convergence history comparison of ELEM and other algorithms.

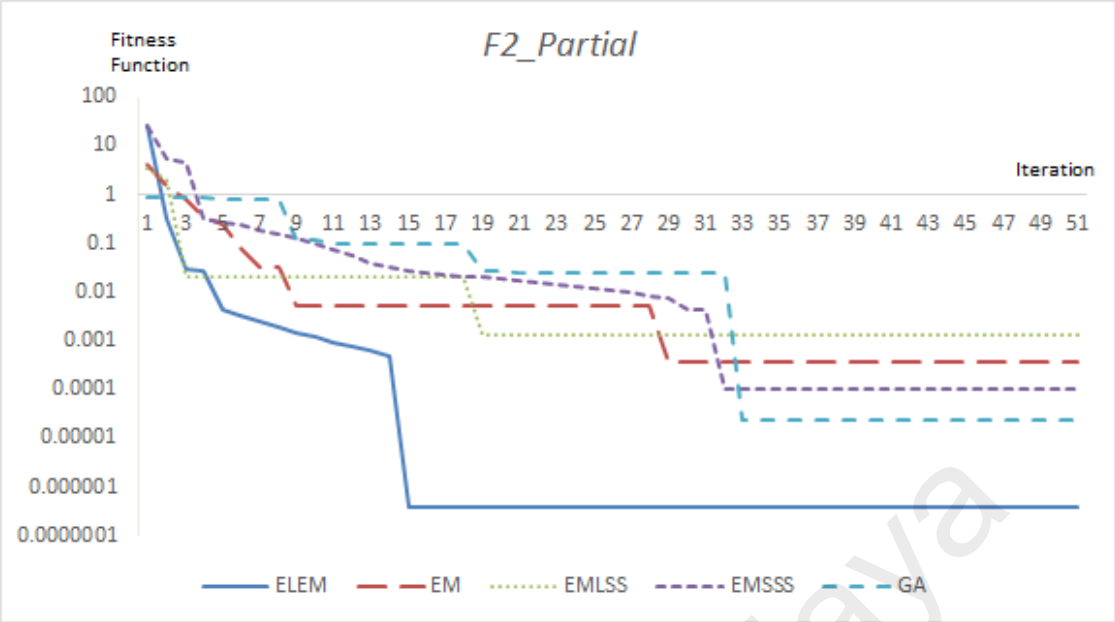


(b)

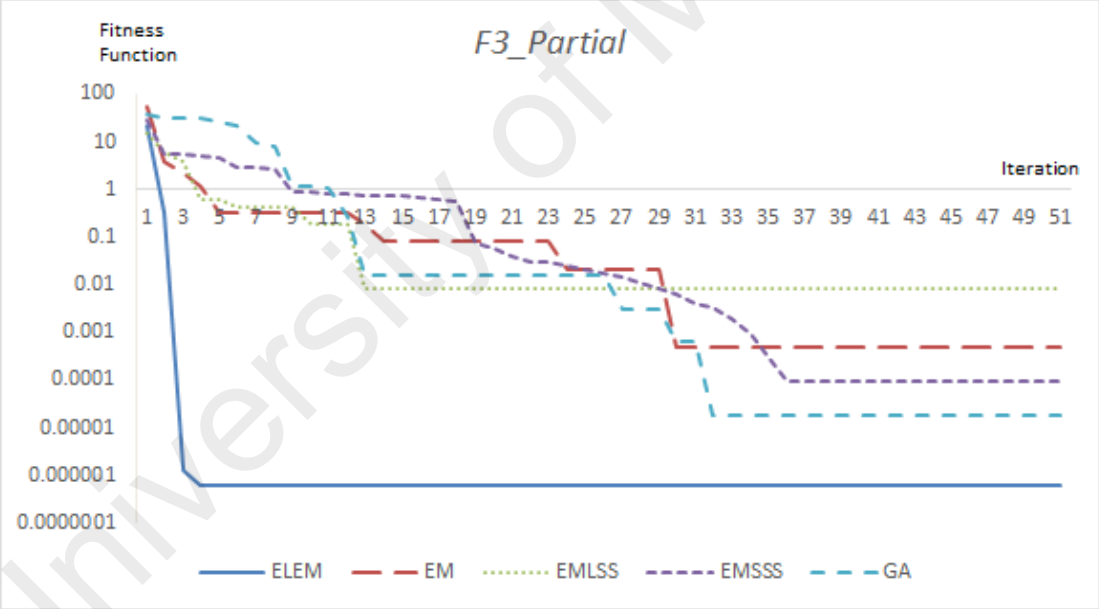


(c)

Figure 4.8, continued: Convergence history comparison of ELEM and other algorithms.

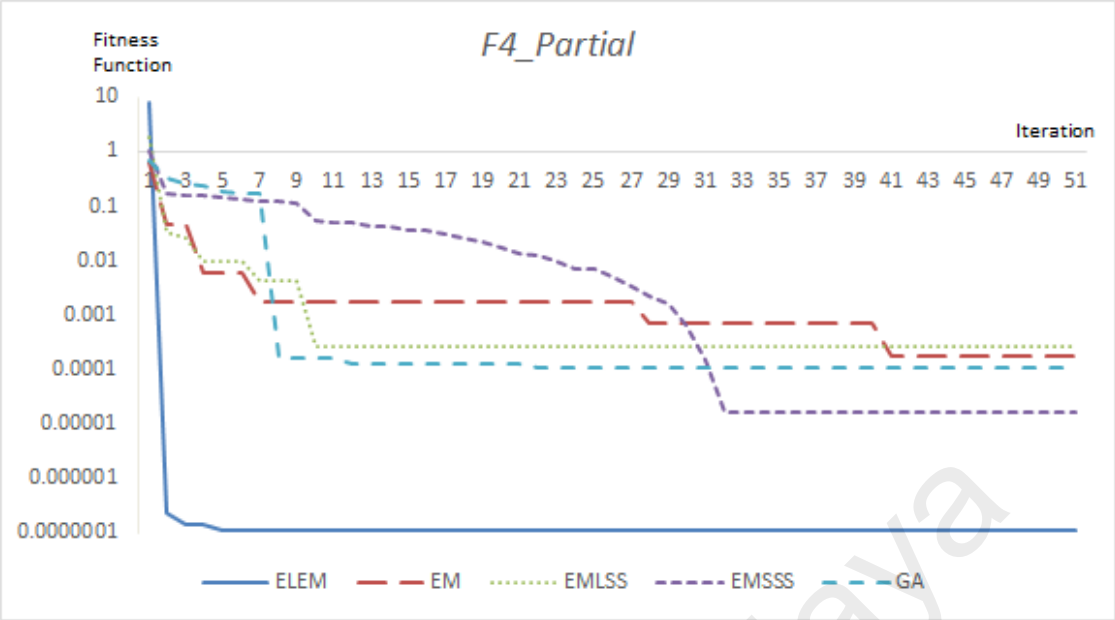


(d)

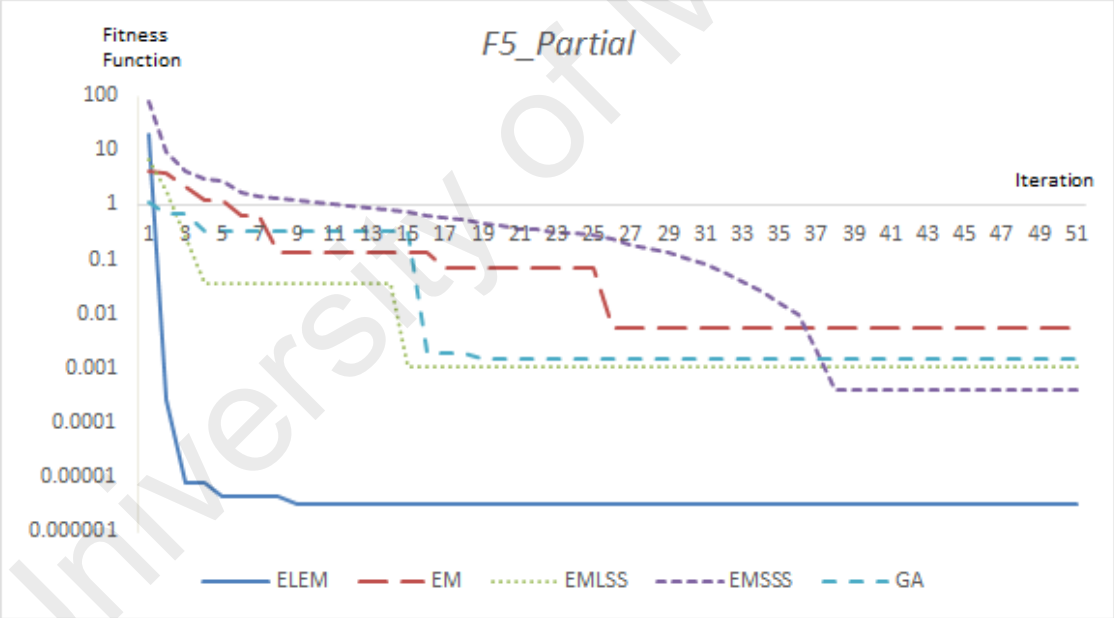


(e)

Figure 4.8, continued: Convergence history comparison of ELEM and other algorithms.

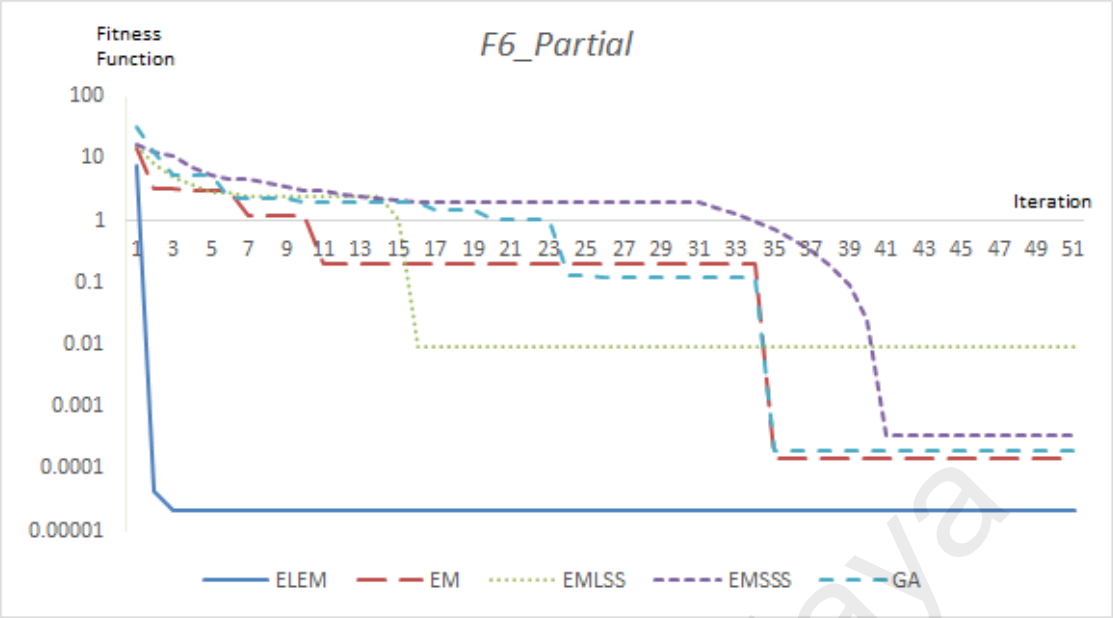


(f)

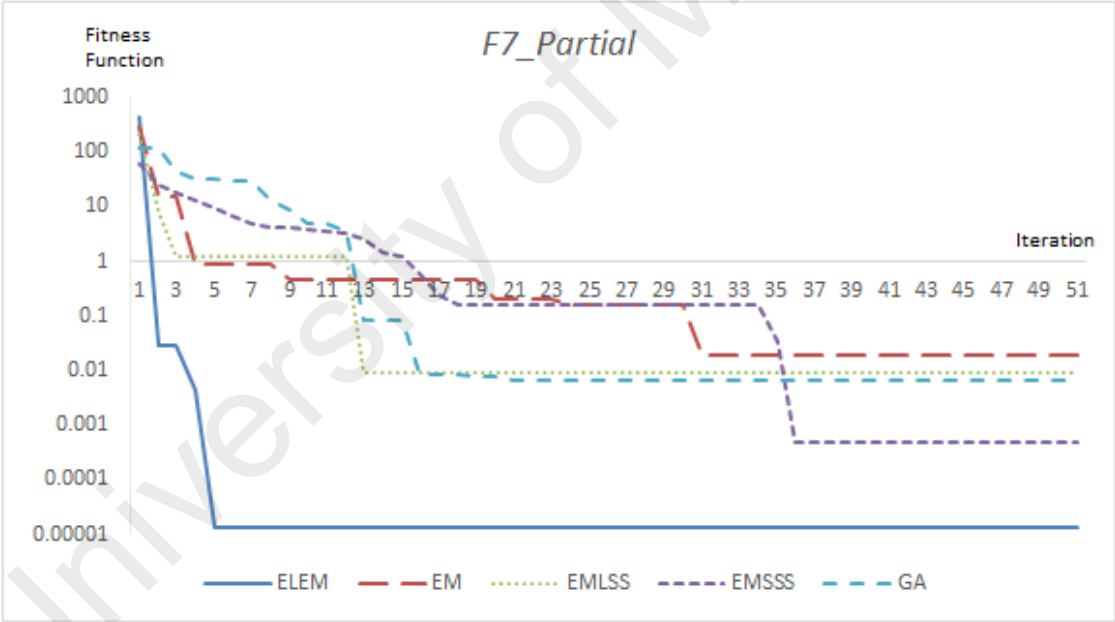


(g)

Figure 4.8, continued: Convergence history comparison of ELEM and other algorithms.

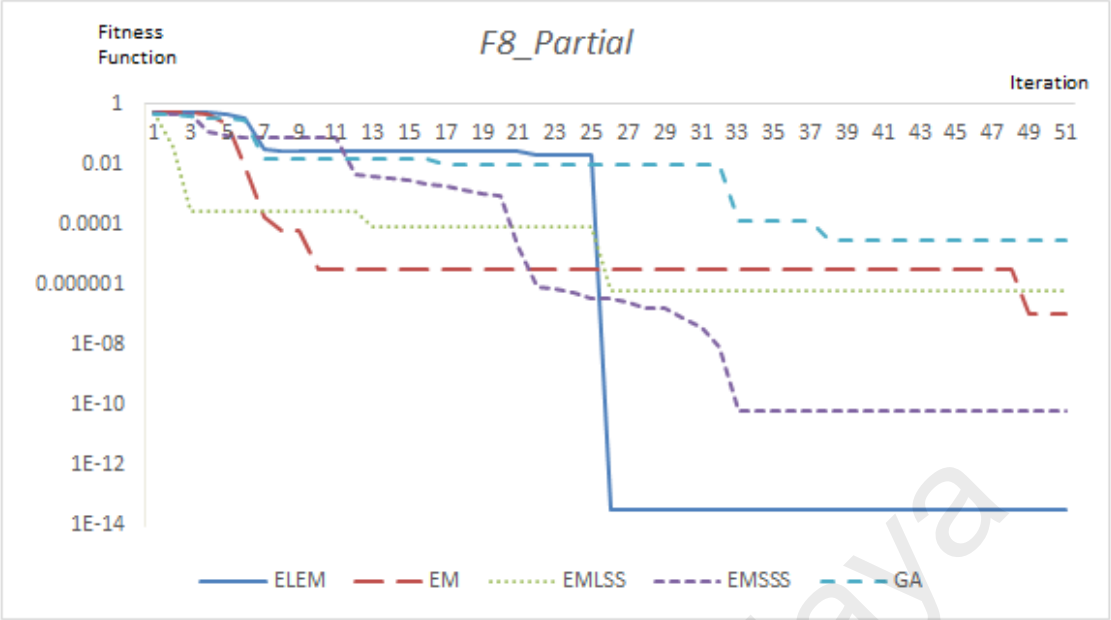


(h)

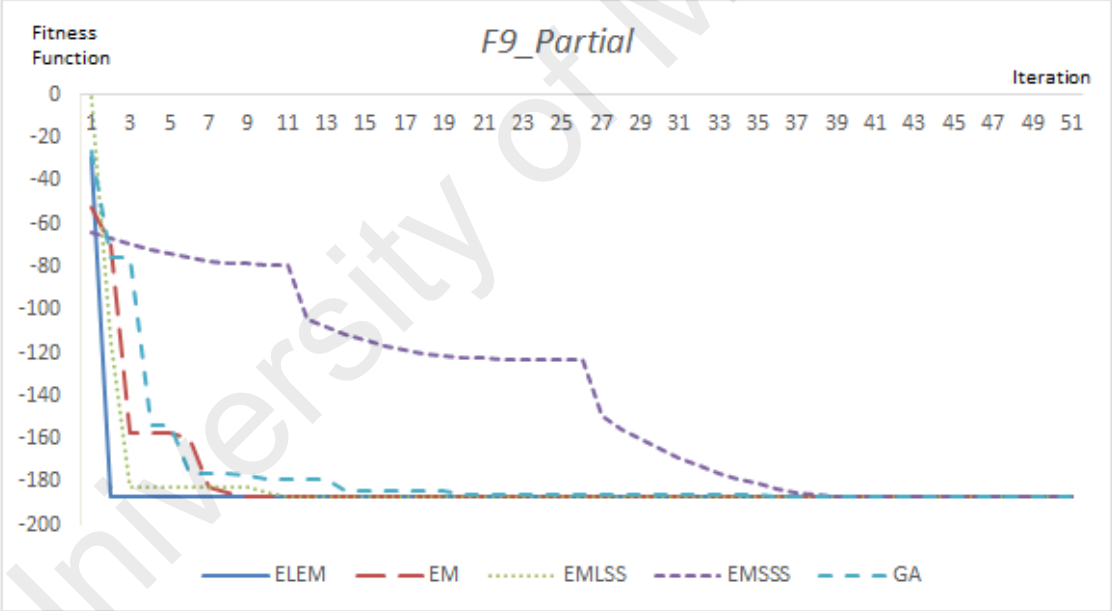


(i)

Figure 4.8, continued: Convergence history comparison of ELEM and other algorithms.

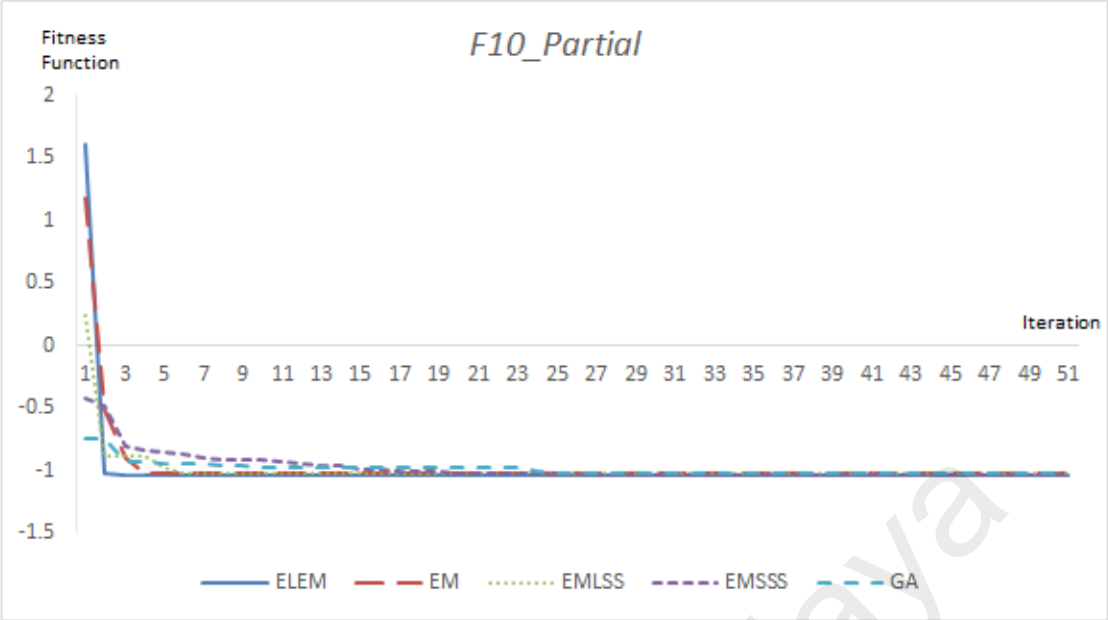


(j)

Figure 4.8, continued: Convergence history comparison of ELEM and other algorithms.

### 4.3.3 Parameter Sensitivity Test

In this section, the effect of $\alpha$ and $\beta$ settings on the performance of the ELEM algorithm is investigated. Simulations were carried out where the algorithm was executed independently 20 times on each benchmark test function with different settings of $\alpha$ and $\beta$. The value of the gain factor, $\alpha$ was limited to vary from 1.1 to 1.5 as it was estimated that a gain too large can generate an out-of-proportion $\lambda$ size. For similar reason, the value of the penalty factor, $\beta$ was limited to vary from 0.5 to 0.9. The mean results generated by pairing increasing $\alpha$ with increasing $\beta$ values are summarized in Tables 4.8, while Table 4.9 shows the outcomes obtained by pairing increasing $\alpha$ with decreasing $\beta$. The best solutions are highlighted in boldface.

Table 4.8: Results generated by pairing increasing $\alpha$ with increasing $\beta$.

| | $\alpha$=1.1<br>$\beta$=0.5 | $\alpha$=1.2<br>$\beta$=0.6 | $\alpha$=1.3<br>$\beta$=0.7 | $\alpha$=1.4<br>$\beta$=0.8 | $\alpha$=1.5<br>$\beta$=0.9 |
|---|---|---|---|---|---|
| F1 | 1.8842E-02 | 3.7731E-03 | 3.1124E-03 | 6.4779E-02 | 3.7888E-02 |
| F2 | 9.6901E-05 | 4.9592E-06 | 9.1646E-05 | 3.1034E-03 | 6.3541E-04 |
| F3 | 9.1630E-04 | 3.1846E-06 | 4.1956E-06 | 3.7929E-05 | 2.4648E-05 |
| F4 | 3.0848E-06 | 9.1750E-07 | 3.8827E-05 | 6.5751E-06 | 6.4104E-04 |
| F5 | 5.0405E-03 | 6.5901E-06 | 3.0366E-05 | 3.4126E-03 | 3.1622E-03 |
| F6 | 3.1954E-02 | 3.2260E-03 | 7.9021E-05 | 3.1645E-02 | 3.0305E-04 |
| F7 | 2.9763E-04 | 7.9311E-04 | 2.9006E-03 | 6.1552E-03 | 2.5645E-04 |
| F8 | 6.0772E-03 | 6.3091E-02 | 1.0979E-05 | 3.3923E-07 | 6.8741E-05 |
| F9 | -186.730133 | -186.730528 | -186.730471 | -186.730241 | -186.730586 |
| F10 | -1.03161688 | -1.03162762 | -1.03162675 | -1.03162432 | -1.03162181 |

Table 4.9: Results generated by pairing increasing $\alpha$ with decreasing $\beta$.

| | $\alpha$=1.1<br>$\beta$=0.9 | **$\alpha$=1.2**<br>**$\beta$=0.8** | $\alpha$=1.3<br>$\beta$=0.7 | $\alpha$=1.4<br>$\beta$=0.6 | $\alpha$=1.5<br>$\beta$=0.5 |
|---|---|---|---|---|---|
| F1 | 6.4644E-03 | **9.3732E-04** | 3.1124E-03 | 9.1788E-02 | 3.9511E-02 |
| F2 | 7.1195E-06 | **3.3910E-06** | 9.1646E-05 | 6.1263E-04 | 6.8411E-05 |
| F3 | 9.1264E-06 | **7.4061E-07** | 4.1956E-06 | 8.0242E-03 | 3.7962E-04 |
| F4 | 6.2338E-06 | **2.5348E-07** | 3.8827E-05 | 3.7121E-06 | 4.3860E-05 |
| F5 | 3.4004E-06 | **3.1928E-06** | 3.0366E-05 | 5.0906E-05 | 2.8377E-04 |
| F6 | 9.8919E-05 | **7.2856E-05** | 7.9021E-05 | 3.1665E-03 | 6.1720E-03 |
| F7 | 6.4407E-04 | **8.1555E-05** | 2.9006E-03 | 3.8337E-02 | 3.0028E-02 |
| F8 | **6.3160E-08** | 9.1616E-07 | 1.0979E-05 | 6.0028E-03 | 6.4552E-05 |
| F9 | -186.730422 | **-186.730601** | -186.730471 | -186.729702 | -186.729288 |
| F10 | -1.03162771 | **-1.03162800** | -1.03162675 | -1.03162391 | -1.03162442 |

The results in Table 4.8 and 4.9 indicate that the setting of parameters $\alpha$ and $\beta$ shows certain impact on the performance of the ELEM. It can be observed from the tables that for most benchmark functions, the ELEM showed the best performance when the gain factor, $\alpha$ was set to 1.2 and the penalty factor, $\beta$ was set to 0.8. When $\alpha$ was set to 1.0, it began to show under gain while any value over 1.2 showed over gain on the step tuning. Over gain led to an oversized search step in the local search procedure, causing it to overstep any better solution within the step. Under gain, on the other hand, caused the search to reach the best solution in relatively later iterations. Similar situations can also be observed for the setting of parameter $\beta$, where 0.9 showed over compensation, while

values under 0.8 caused under compensation. As a whole, ELEM with $\alpha$ = 1.2 and $\beta$ = 0.8 shows the best performance among the tested algorithms.

### 4.3.4 ELEM vs SPC-EM

The SPC-EM and the ELEM both proved improvements compared to the conventional EM. In this section, the performance of the experience-based ELEM is compared with the iteration-based step regulation SPC-EM. Table 4.10 shows the comparison of the results obtained by the ELEM and the SPC-EM. From the table, it can be observed that the ELEM outperformed the SPC-EM in all of the test functions. The SPC-EM shows very competitive solutions in many of the tests, such as *F2*, *F3*, *F4*, *F5*, *F6*, *F7*, and *F9*. However in the end, the ELEM proved to be superior in term of solution accuracies.

Table 4.10: Results comparison of ELEM vs SPC-EM.

| | | **ELEM** | **SPC-EM** |
|---|---|---|---|
| F1 | Best | 2.3785E-04 | 1.4193E-03 |
| | Worst | 9.6410E-04 | 1.4353E-03 |
| | Mean | 8.0935E-04 | 1.4247E-03 |
| | SD | 6.6424E-08 | 2.3926E-11 |
| | Rank | 1 | 2 |
| F2 | Best | 1.7511E-07 | 3.9364E-07 |
| | Worst | 1.6450E-05 | 3.2743E-05 |
| | Mean | 3.0747E-06 | 4.6110E-06 |
| | SD | 1.8329E-11 | 6.1325E-11 |
| | Rank | 1 | 2 |
| F3 | Best | 5.5609E-07 | 1.2472E-06 |
| | Worst | 1.3053E-06 | 2.0052E-06 |
| | Mean | 7.6655E-07 | 1.3958E-06 |
| | SD | 9.9573E-14 | 5.9082E-14 |
| | Rank | 1 | 2 |
| F4 | Best | 1.1096E-07 | 2.4944E-07 |
| | Worst | 1.1162E-07 | 2.4997E-07 |
| | Mean | 1.1106E-07 | 2.4962E-07 |
| | SD | 2.1177E-20 | 2.8795E-20 |
| | Rank | 1 | 2 |
| F5 | Best | 1.6275E-06 | 3.6616E-06 |
| | Worst | 3.5498E-06 | 5.8058E-06 |
| | Mean | 1.9761E-06 | 3.8741E-06 |
| | SD | 3.2895E-13 | 2.1121E-13 |
| | Rank | 1 | 2 |
| F6 | Best | 2.2032E-05 | 4.9526E-05 |
| | Worst | 2.2343E-05 | 5.7421E-05 |
| | Mean | 2.2060E-05 | 5.1338E-05 |
| | SD | 4.6304E-15 | 5.6796E-12 |
| | Rank | 1 | 2 |
| F7 | Best | 1.1120E-05 | 2.4945E-05 |
| | Worst | 2.7677E-05 | 2.8149E-05 |
| | Mean | 1.3260E-05 | 2.5914E-05 |
| | SD | 1.5737E-11 | 8.6973E-13 |
| | Rank | 1 | 2 |
| F8 | Best | 0.0000E+00 | 1.1102E-16 |
| | Worst | 7.5275E-06 | 2.0630E-05 |
| | Mean | 4.2922E-07 | 1.4542E-06 |
| | SD | 2.6611E-12 | 2.0079E-11 |
| | Rank | 1 | 2 |
| F9 | Best | -186.7307 | -186.7304 |
| | Worst | -186.7304 | -186.7303 |
| | Mean | -186.7306 | -186.7303 |
| | SD | 5.4818E-09 | 5.4656E-10 |
| | Rank | 1 | 2 |
| F10 | Best | -1.03162802 | -1.03162780 |
| | Worst | -1.03162792 | -1.03162745 |
| | Mean | -1.03162801 | -1.03162749 |
| | SD | 4.9932E-16 | 5.2578E-15 |
| | Rank | 1 | 2 |

The sampled convergence processes of the ELEM are also compared with that of the SPC-EM in Figure 4.9. Since it is not feasible to show F9 and F10 in algorithmic axis, the graphs are shown without taking the initialization iteration values as the scales of the movements after the initialization stage are relatively too small to be visible. The ELEM achieves comparatively lower solution values in most of the sampled convergence, except for F8. Given the nature of the graph shape in Schaffer N2 test, the sharp spikes pose many local optima traps, rendering differential type local search mechanism to show limitations. In problems as such, the exploration ability of the algorithm plays a more important role in diversifying the search for other optima points. In term of convergence rate, it can be observed from the all the comparisons that both algorithms are equally rapid in most of the test functions. In some of the tests, such as *F3* and *F6*, ELEM shows slightly quicker convergence.

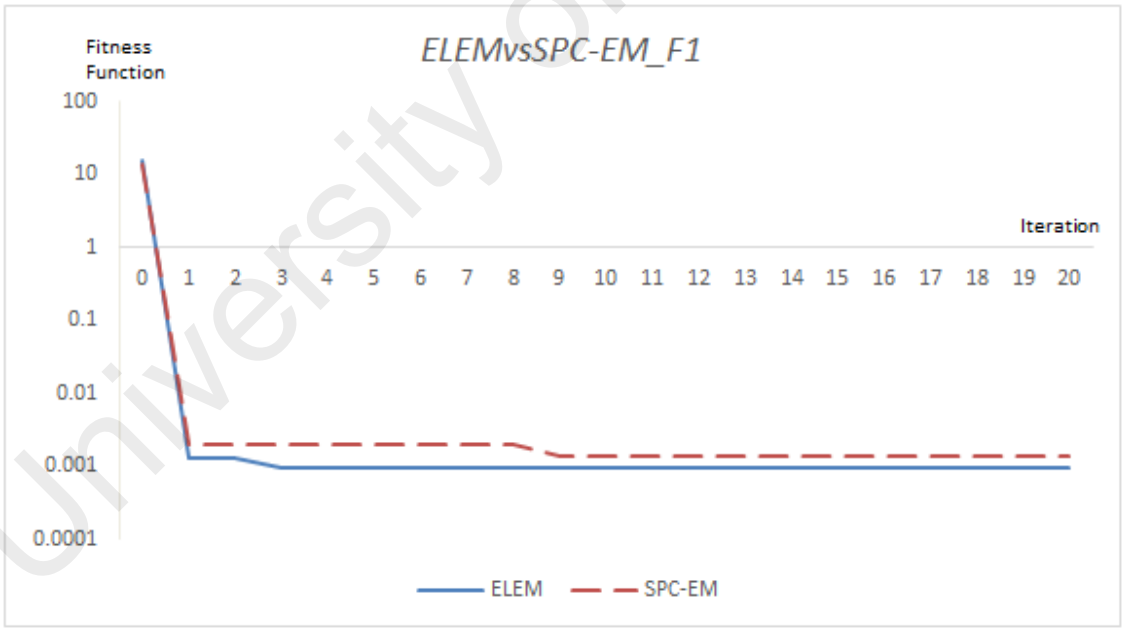


(a)

Figure 4.9: Convergence rate comparisons of ELEM vs SPC-EM.

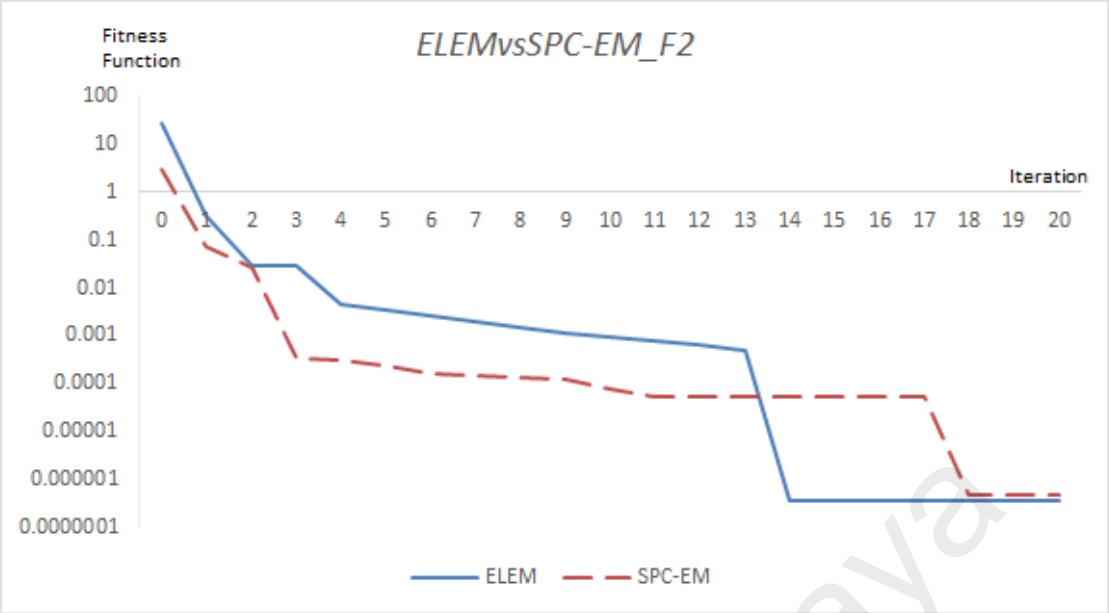


(b)

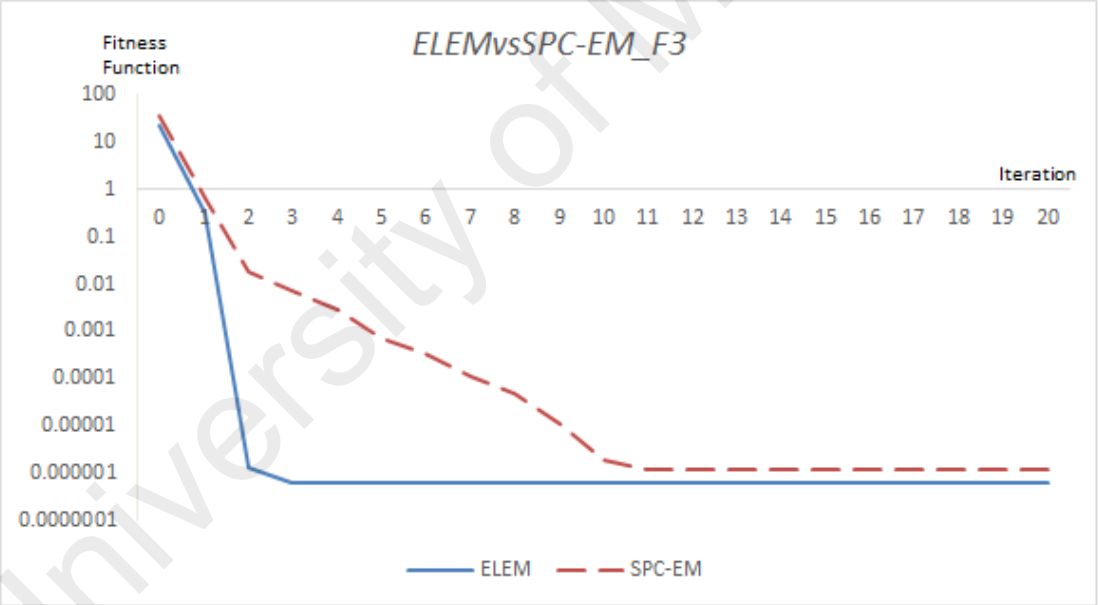


(c)

Figure 4.9, continued: Convergence rate comparisons of ELEM vs SPC-EM.

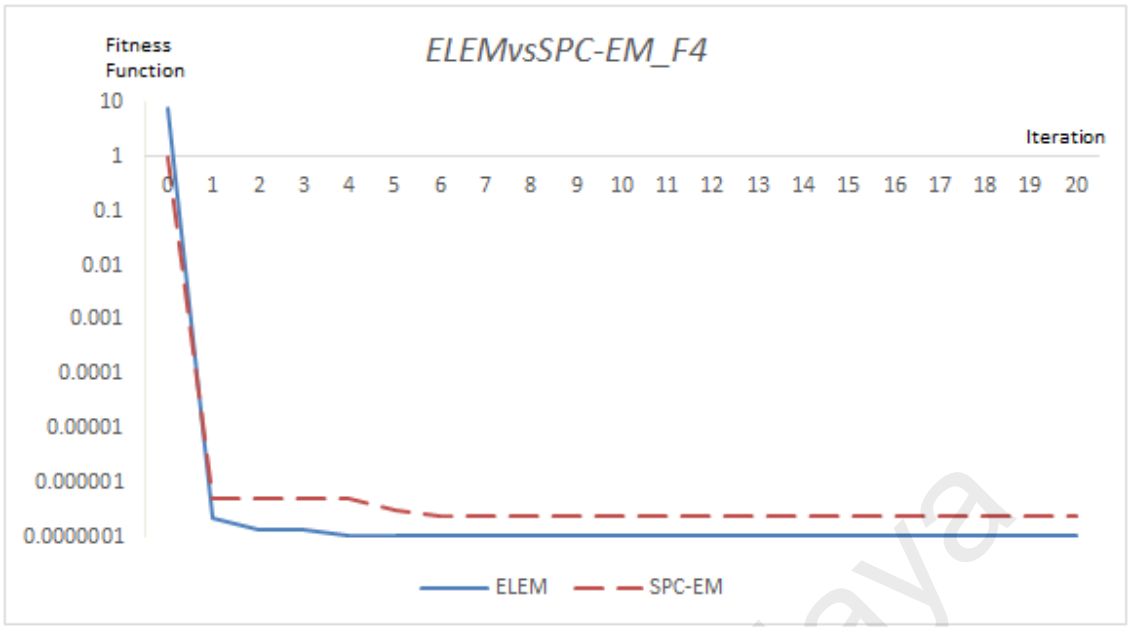


(d)

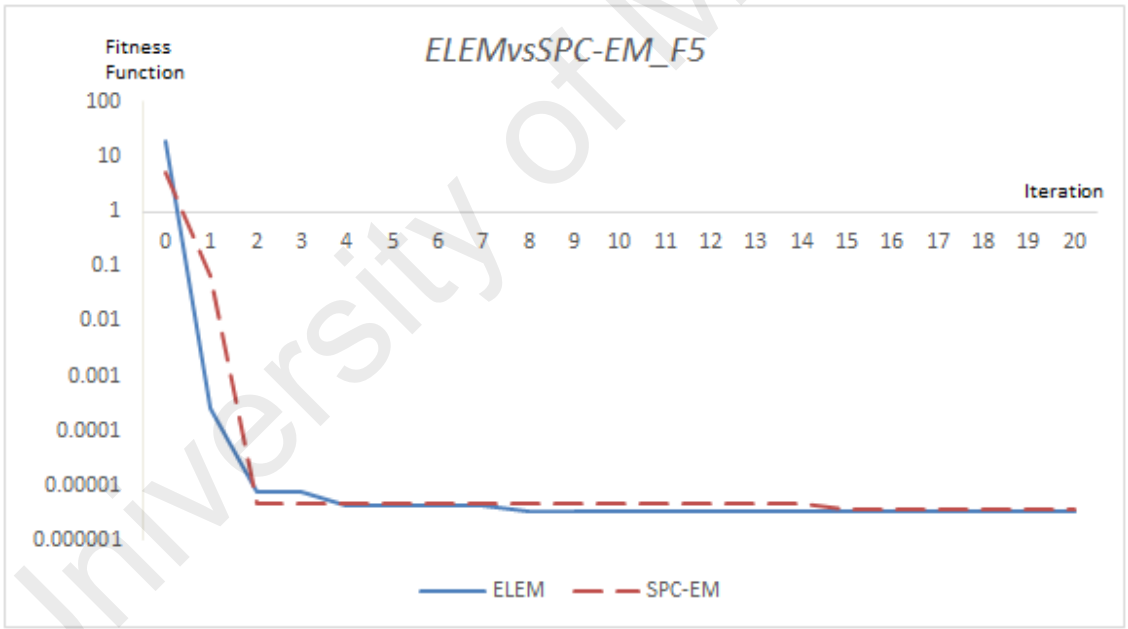


(e)

Figure 4.9, continued: Convergence rate comparisons of ELEM vs SPC-EM.

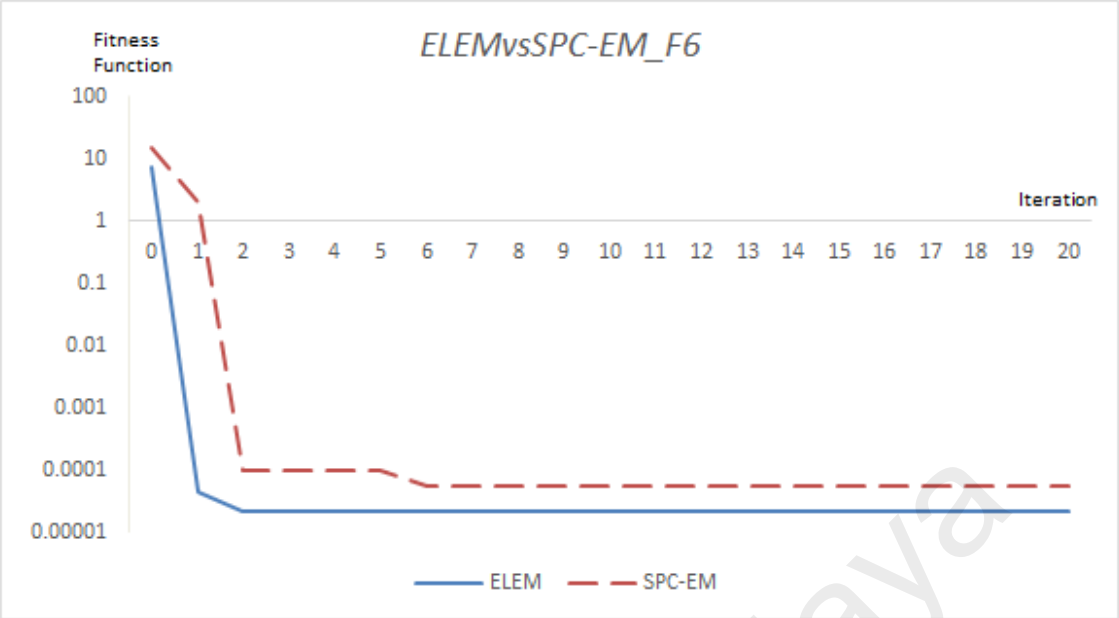


(f)

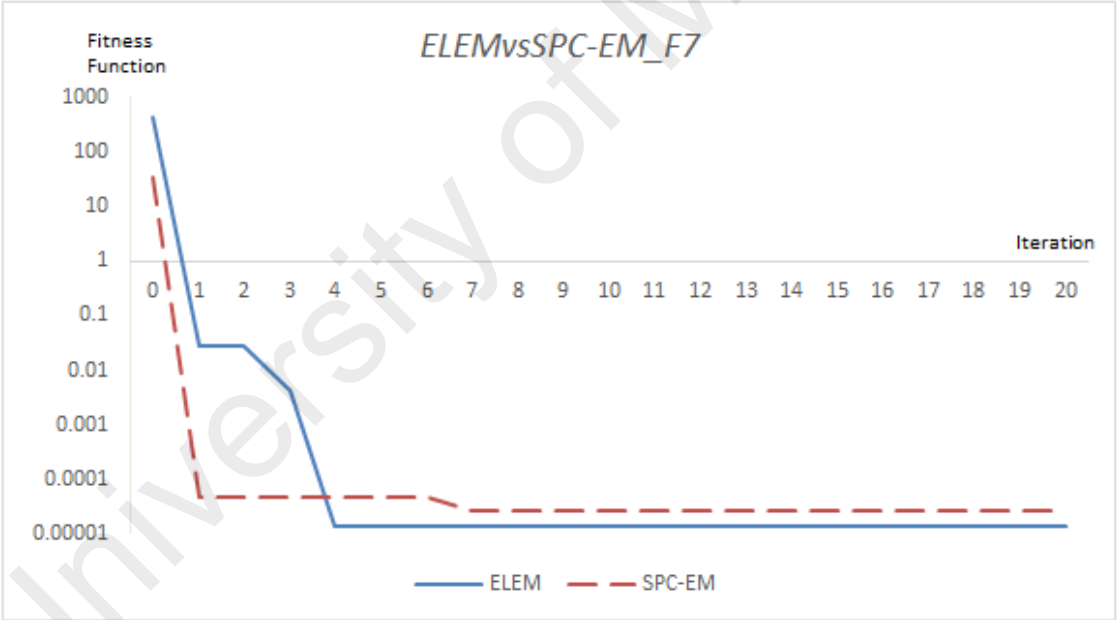


(g)

Figure 4.9, continued: Convergence rate comparisons of ELEM vs SPC-EM.

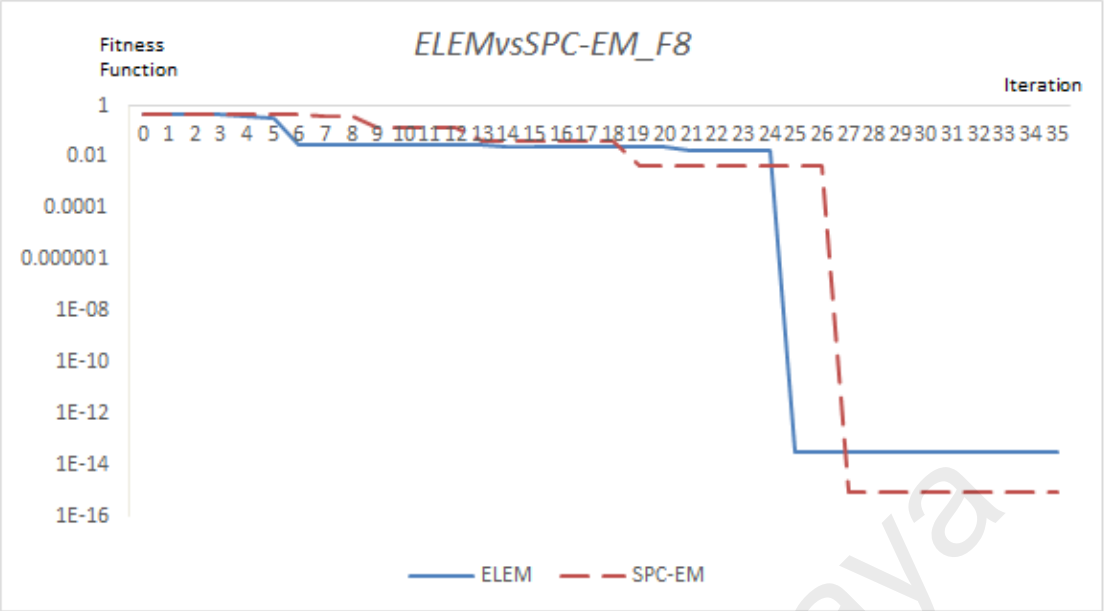


(h)

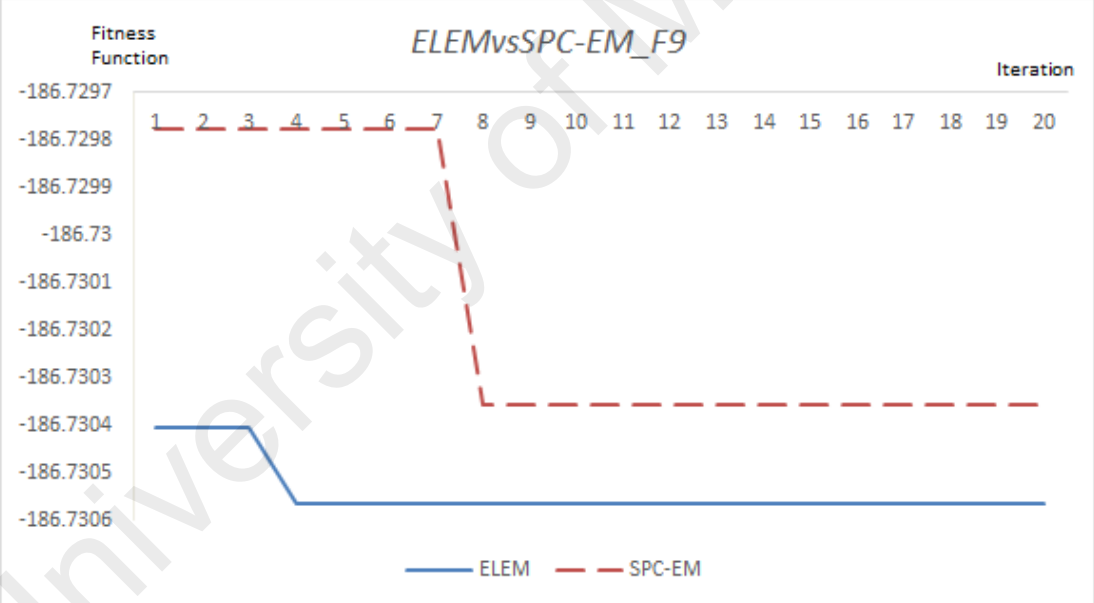


(i)

Figure 4.9, continued: Convergence rate comparisons of ELEM vs SPC-EM.

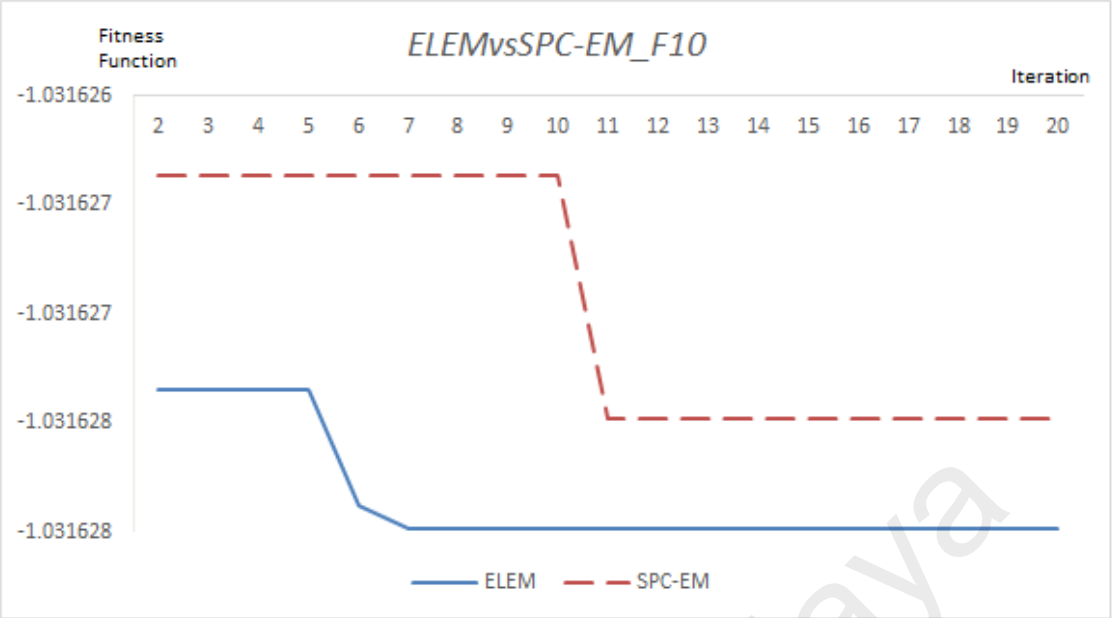


(j)

Figure 4.9, continued: Convergence rate comparisons of ELEM vs SPC-EM.



### 4.4 EM in MPPT

To test the performance of the enhanced EM in solving engineering optimization problems, the proposed ELEM was implemented in the simulation to track the MPP of a PV solar harvesting system. First, ELEM was tested to track the MPP of 3 serial-connected BP Solar MSX-120W PV panels under ideal and uniform irradiance. As mentioned in Chapter 3, the Power-Voltage behaviour of the simulated PV array under ideal and uniform irradiance is as shown in Figure 4.10.

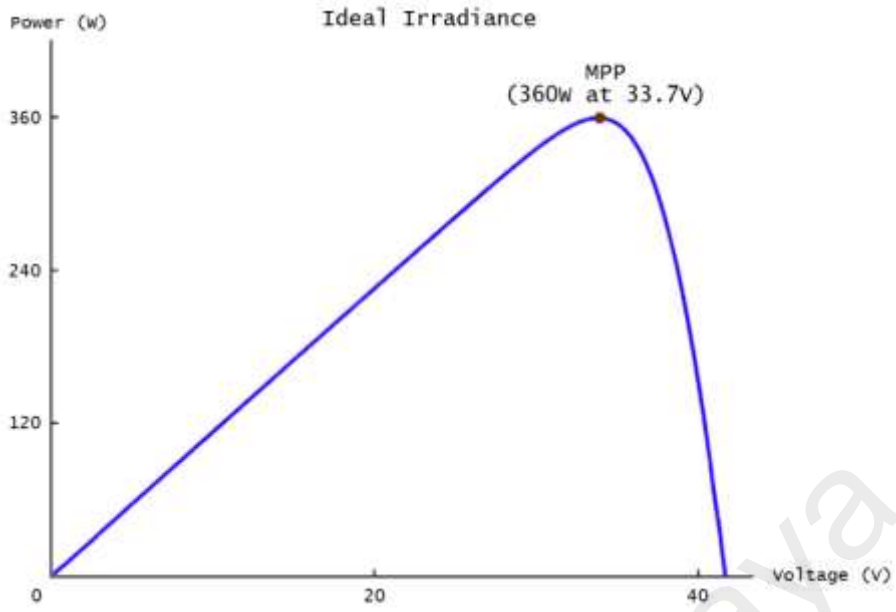


Figure 4.10: P-V curve of the serial-connected arrays under ideal irradiance.

### 4.4.1 Ideal Irradiance

Simulations were carried out 20 times and some results were sampled and analysed. Figure 4.11 shows an example of the convergence of the ELEM in the MPPT simulation under uniform insolation. The modified ELEM was quick in locating the MPP as the single peak P-V characteristic of the PV array under uniform irradiance required relatively easier convergence process.

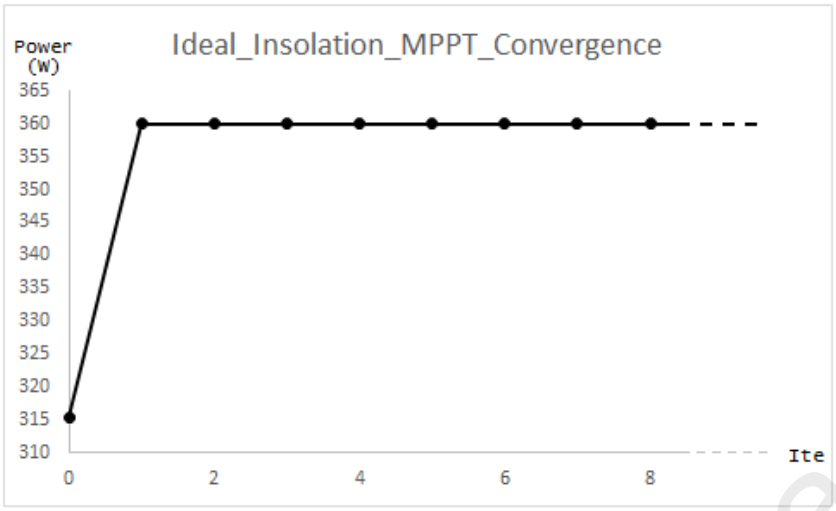


Figure 4.11: MPPT convergence of the ELEM under ideal irradiance.

Table 4.11 shows an example of the particle movement in search of the MPP under the enhanced exploitation procedure proposed in the ELEM. Figure 4.12 gives a better illustration of the movements in the form of a Power vs Voltage graph. It can be observed from Figure 4.12 that the best particle began the search procedure in the initial position marked in the graph. It then moved in search for a higher power point towards the peak of the P-V curve (refer Figure 4.11) until it finally hit the MPP of 360W at 33.7V. Figure 4.13 shows the sampled local search convergence process.

Table 4.11: Example of local search particle displacement of the ELEM in tracking the MPP.

| Ite | Voltage (V) | Power (W) |
|---|---|---|
| 0 | 30.08889 | 324.9600 |
| 1 | 30.97778 | 334.5600 |
| 2 | 31.86667 | 344.1600 |
| 3 | 32.75556 | 355.4492 |
| 4 | 33.64444 | 359.9844 |
| 5 | 33.70000 | 360.0000 |
| 6 | 33.70000 | 360.0000 |
| 7 | 33.70000 | 360.0000 |
| - | - | - |
| - | - | - |
| - | - | - |

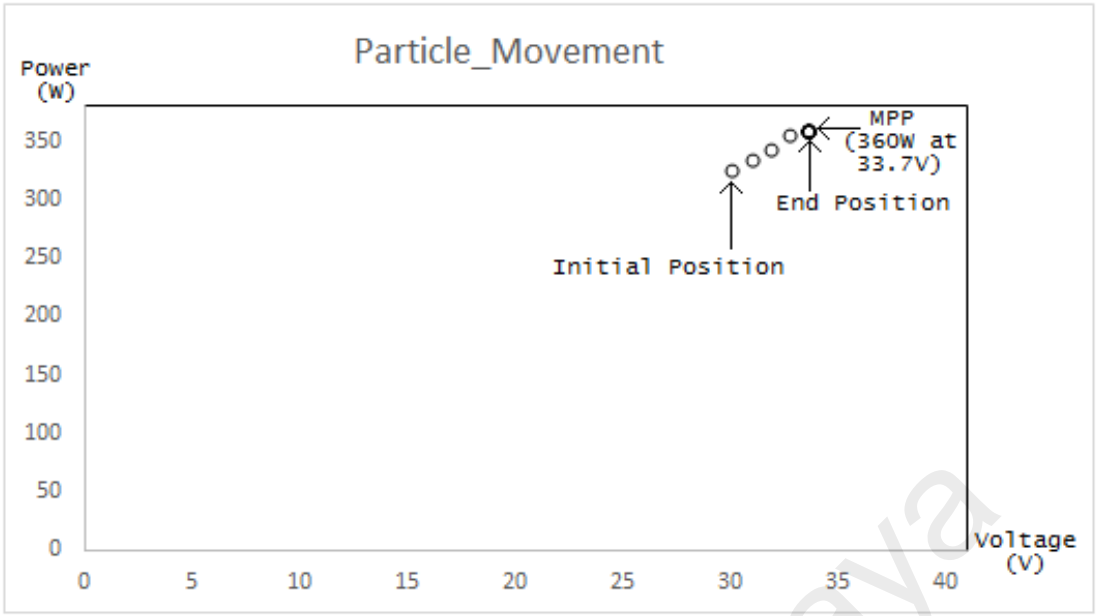


Figure 4.12: Particle movement in search for the MPP under ideal irradiance condition.

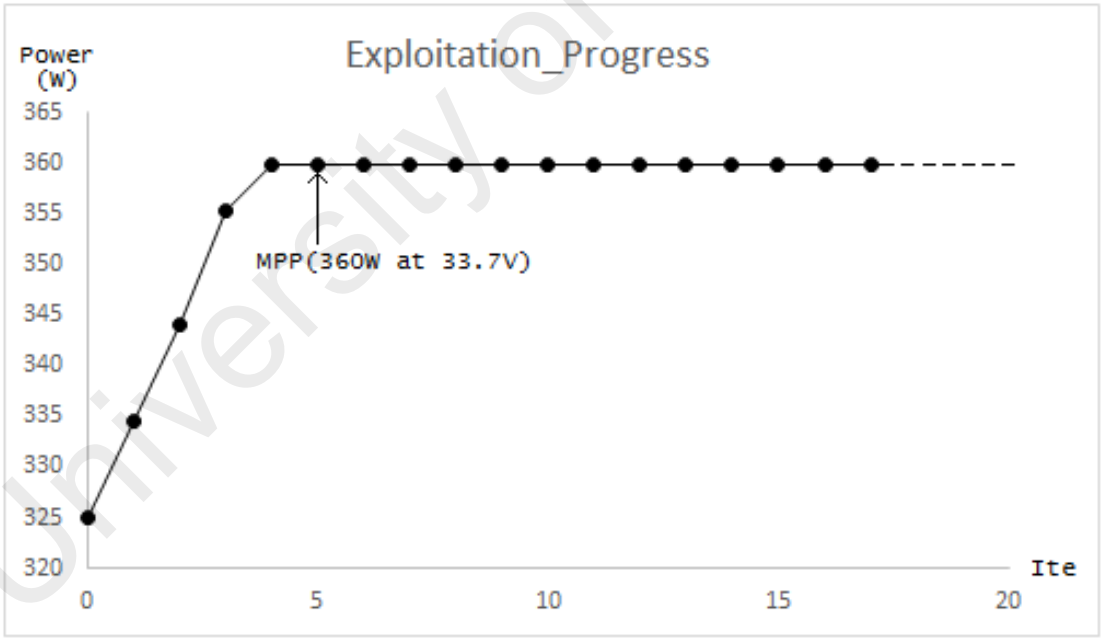


Figure 4.13: The exploitation progress in search of the MPP under ideal irradiance condition.

### 4.4.2 Partial Shaded Condition

In practical applications, the solar irradiance onto the PV arrays is seldom uniform. Shadows of clouds, buildings and accumulated dust can disturb the insolation of the PV arrays, causing non-uniform irradiance to the PV arrays (Boukenoui, 2016). The rapidly changing shading pattern makes it even harder for the PV system to perform effectively. To simulate challenging partial shading conditions as such, the algorithm was tested to track for the MPP under 3 changing shading patterns, as shown in Figure 4.14. In the simulation, the P-V curve of the shading pattern was as shown in Figure 4.14 (a) during the first second. Then, in the following second, the P-V curve changed into Pattern 2, representing changes in the shading pattern on the PV array. In the third second, the shading pattern changed again into pattern 3 with the P-V curve as shown in Figure 4.14 (c).

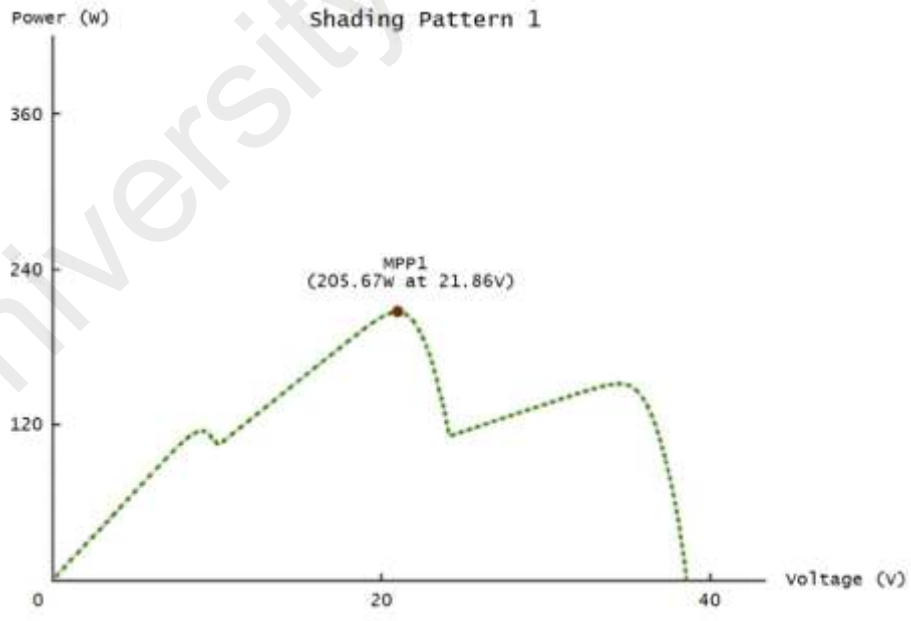


Figure 4.14 (a): Simulated pattern 1 of shading condition.

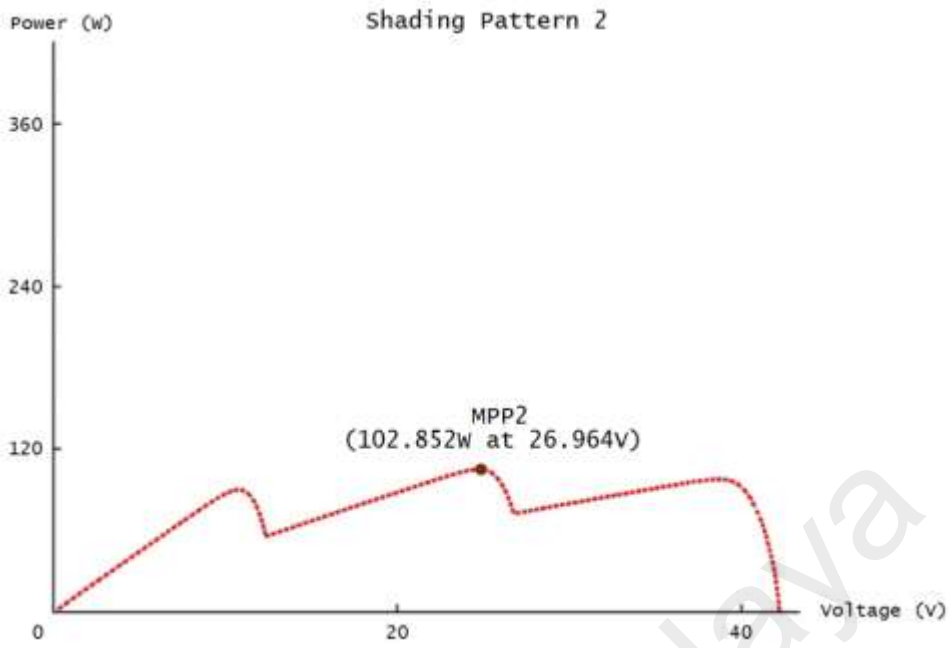


Figure 4.14 (b): Simulated pattern 2 of shading condition.

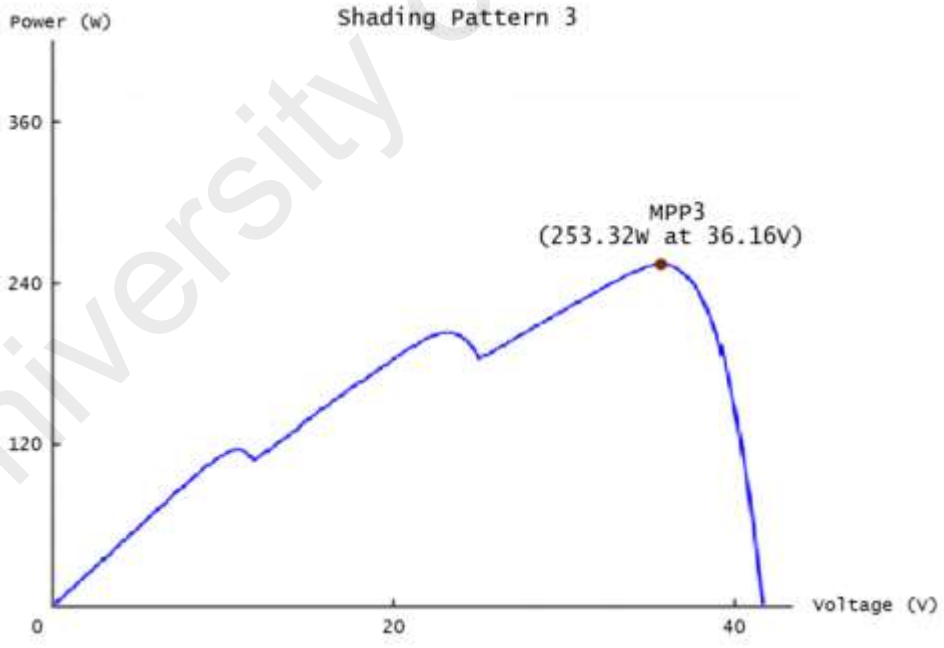


Figure 4.14 (c): Simulated pattern 3 of shading condition.

Simulations were carried out 20 times and some results were sampled and analysed. Figure 4.15 shows an example of the result obtained by implementing ELEM in the MPPT of the PV system under varying shading condition. It can be observed that the algorithm successfully found the MPP under the first shading pattern (MPP1). The operating voltage remained at 21.86V until the shading condition changed to the second shading pattern. The algorithm carefully tracked the MPP as it dropped to MPP2 at 102.852W. When the shading pattern changed again to pattern 3, the algorithm followed and tracked the MPP to 253.32W. It can be concluded from this observation that the ELEM successfully tracked the MPP as it moved under different PSC patterns.

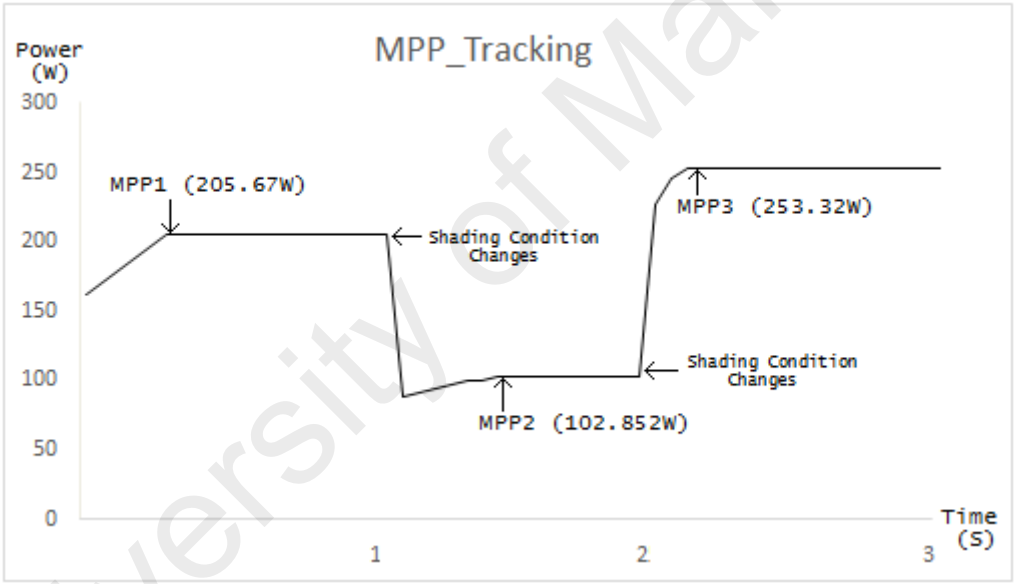


Figure 4.15: The MPPT successfully performed by ELEM under changing PSCs from pattern 1 to pattern 2 and then to pattern 3.

Figure 4.16 (a), (b), and (c) show some sampled movements of the particles in tracking the MPPs under shading pattern 1, 2, and 3 respectively. These movements gives a clear picture on how the algorithm tracks the MPP by adjusting the Voltage.

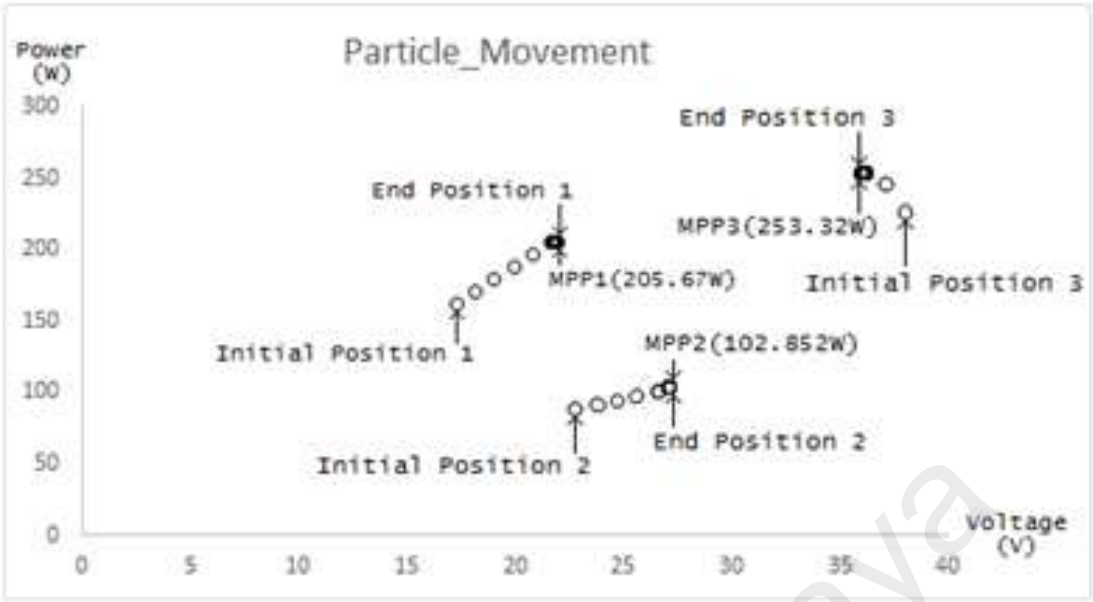


Figure 4.16: Particle movement in search of the MPPs in PSC pattern 1, pattern 2 and pattern 3.

Literature study shows that the P&O is one of the most commonly applied algorithms in the MPPT of a PV system. Thus, the performance of the ELEM is also compared with a conventional P&O with random perturbation length setting. Simulations with P&O were also carried out 20 times. Result was sampled and shown in Figure 4.17. It can be observed that in this example that in shading pattern 1 and 3, P&O was trapped in the local optima for some time before managed to escape them. It is important for an MPPT algorithm to avoid local MPP traps as they can cause unnecessary loss of energy.

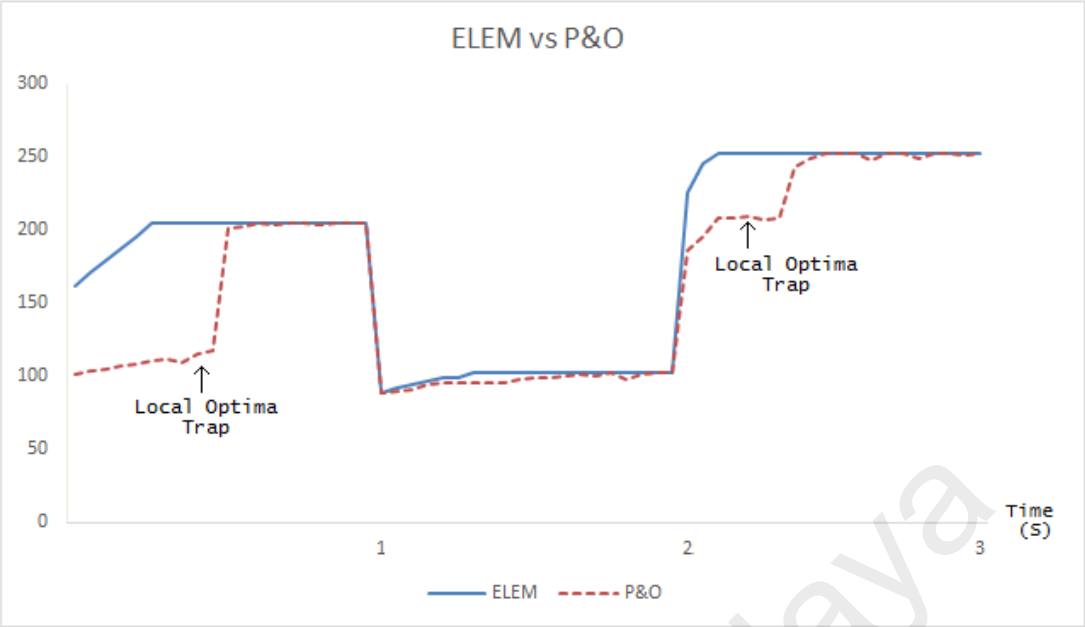


Figure 4.17. Performance comparison of ELEM vs P&O.

In the case of a PV solar energy harvesting system, the main challenge of the MPPT mechanism is to adjust the output Voltage in order to optimize the output power under different irradiance conditions. The simulation results in this section indicate that ELEM is successful in tracking the maximum power point of a PV solar harvesting system under uniform irradiance, non-uniform irradiance, and varying shading conditions.

# CHAPTER 5: CONCLUSION

The Electromagnetism-like Mechanism algorithm is a population based meta-heuristic search method. Mimicking the attraction and repulsion mechanisms in the electromagnetism theorem, the EM is designed to search for the global optimum point in a continuous search space. In this research, extensive studies have been carried out to learn the behaviour of this algorithm. Modifications and improvements are proposed to further enhance the performance of it. The enhanced EM is then tested to solve engineering optimization problem.

The effect of the search step size setting on the convergence performance of the EM was investigated by modifying a conventional EM to search in two different extreme sets of step size settings. EMLSS was set to search in relatively larger steps, while EMSSS conducted the search in smaller search step setting. Experimental results showed that larger and smaller search step size settings both have their respective advantages and disadvantages. Larger step settings speeded up the convergence process, but the final results returned by the algorithm is comparatively less accurate. Smaller step settings, on the other hand, yielded results with higher accuracies. The trade off, however, was that the algorithm required significantly more iterations before it obtained the final outcome, which in turn rendered the overall convergence process to be slower.

In order to acquire the advantages from both large and small search step settings, a local search scheme with a dynamic tuning mechanism, known as the Split, Probe and

Compare mechanism was developed for the EM in this research. The SPC mechanism is a solution exploitation scheme created to replace the entire local search segment of a conventional EM. This search scheme enhances the EM with the ability to hit a more accurate solution without heavily slowing down the entire convergence process. The search mechanism probes for better solutions in split directions in the dimension. A nonlinear equation has been designed to systematically and dynamically adjust the length of the probes based on the outcome of the Compare segment in each iteration. The general concept of the tuning strategy is to begin the search with relatively longer probes and dynamically tune the probe lengths as iterations go. Experiments on 10 different test problems reveal that the modified algorithm performed well in solving numerical optimization problems. The proposed modification onto the algorithm brought significant improvements especially in term of solutions exploitation.

Besides SPC-EM, an experience-based search strategy has also been successfully developed and introduced into the EM. The Experiential-Learning EM is enhanced with the ability to learn from previous search experience and adjust the scale and direction of the following search iterations. A trail memory was generated as iterations went on, allowing the algorithm to remember and backtrack previous search results and improvement rates. In addition, the ELEM employed a more directional search approach instead of a random line search in a conventional EM. This approach significantly improved the exploitation ability of the algorithm. Combining with the powerful exploration mechanism of the EM, the proposed ELEM stroke a good balance in searching for well diversified solutions and accurately exploited results. In the experiment of 10 complex optimization problems, the ELEM showed significant superiority in terms of solution accuracies and convergence efficiencies compared to all other algorithms

involved in the benchmarking. The ELEM also proved to outperform the SPC-EM in the same test suite.

The ELEM was implemented in the simulation to track the maximum power point of a PV solar energy harvesting system. Experiment on a PV array with 3 serial-connected PV panels was carried out. Simulations of changing shading patterns were carried out to mimic the challenging shading conditions in the actual applications. The algorithm was tested to track the moving MPP caused by the changing shading conditions. Results showed that the enhanced EM was successful in tracking the MPP under uniform irradiance, non-uniform irradiance, and rapid changing shading conditions with moving MPPs. A maximum power point tracking scheme for a PV system adopting the advantages of the ELEM has been successfully developed. The achievement of the ELEM in this experiment also proved the capability of it in solving actual engineering optimization problems.

As a conclusion, all the aims and objectives of this research are successfully achieved. In the future, inter-particle experience sharing feature can be considered for the betterment of the EM. Sharing local information with immediate neighbours can be very helpful in speeding up the local search procedure. Furthermore, there is also possibility to apply the experience-learning feature into the exploration segment of the EM to further enhance the diversification of the solutions. The proposed SPC and Experiential Learning features can also be introduced into other population-based global optimization algorithms, such as particle swarm optimization, ant colony optimization, and artificial bee colony in the future work. The ability to learn from previous experience can be very useful in enhancing the convergence performance of these algorithms. It is also suggested

that in time to come, the implementation of the ELEM can be extended to track the global MPPs of other energy harvesting systems with multiple local peaks, as well as other engineering optimization problems with the need of global optima searching.

## REFERENCES


Abdelsalam Ahmed K, Massoud Ahmed M, Shehab Ahmed, Enjeti Prasad N (2011). High performance adaptive perturb and observe MPPT technique for photovoltaic-based micro grids. IEEE Trans Power Electron, 26(4):1010–21.

Ahmed Jubaer, Salam Zainal (2015). An improved perturb and observe (P&O) maximum power point tracking (MPPT) algorithm for higher efficiency. Appl Energy, 150:97108.

Alabedin AMZ, El-Saadany EF, Salama MMA (2011). Maximum power point tracking for photovoltaic systems using fuzzy logic and artificial neural networks. IEEE Power Energy Soc Gen Meet, 1–9.

Alajmi BN, Ahmed KH, Finney SJ, Williams BW (2013). A maximum power point tracking technique for partially shaded photovoltaic systems in microgrids. IEEE Trans Ind Electron, 60:1596–606.

Al-Amoudi A, Zhang L (1998). Optimal control of a grid-connected PV system for maximum power point tracking and unity power factor. In:Proceedings of the 7th international conference on power electronics variable speed drives, p.80–85.

Al-Amoudi A, Zhang L (2000). Application of radial basis function networks for solar array modelling and maximum power-point prediction. In:IEEE Proceedings of the Generation, Transmission and Distribution, IET, p.310–6.

Ali Sharifi, Vahid Noroozi, Masoud Bashiri, Ali B. Hashemi, Mohammad Reza Meybodi (2012). Two Phased Cellular PSO: A New Collaborative Cellular Algorithm for Optimization in Dynamic Environments. WCCI 2012 IEEE World Congress on Computational Intelligence, Brisbane, Australia.

Amrouche B, Guessoum A, Belhamel M (2012). A simple behavioural model for solar module electric characteristics based on the first order system step response for MPPT study and comparison. Appl Energy, 91:395–404.

Ansari F, Iqbal A, Chatterji S, Afzal A (2009). Control of MPPT for photovoltaic systems using advanced algorithm EPP. In: Proceedings of international conference on power systems ICPS, 1:6, p. 27-9.

Arcidiacono V, Corsi S, Lambri L (1982). Maximum power point tracker for photovoltaic power plants. In: Proc IEEE photovoltaic spec conf, p. 507–12.

Armstrong S, Hurley WG (2010). A new methodology to optimize solar energy extraction under cloudy conditions. Renewable Energy, 35:780–7.

Arora, J.S., Elwakeil, O.A., & Chahande, A.I. (1995). Global optimization methods for engineering applications: a review. *Structural Optimization, 9*, 137-159.

Ashiru I., Czanecki C., Routen T. (1995). Intelligent operators and optimal genetic-based path planning for mobile robots, Proceedings of the International Conference on Recent Advances in Mechatronics, Istanbul, Turkey, August, pp. 1018–1023.

Bagis Aytekin (2008). Fuzzy rule base design using tabu search algorithm for nonlinear system modeling. ISA Trans, 47:32–44.

Bahgat A, Helwa N, Ahmad G, El Shenawy E (2005). Maximum power point tracking controller for PV systems using neural networks. Renew Energy, 30:1257–68.

Bakirci K (2009). Models of solar radiation with hours of bright sunshine: a review. Renewable and Sustainable Energy Reviews, 13:2580–8.

Barr A, Feigenbaum EA (1981). The handbook of artificial intelligence, vol. 1. Los Altos, CA: Morgan Kaufmann.

Beasley D, Bull DR, Martin RR (1993). An overview of genetic algorithms:Part 1, fundamentals. University Computing, 15(2):58–69.

Birbil S. I. and Fang S. C. (2003). "An electromagnetism-like mechanism for global optimization," *Journal of Global Optimization*, vol. 25, no.3, pp. 263-282.

Bodur M, Ermis M (1994). Maximum power point tracking for low power photovoltaic solar panels. In: Proc 7th Mediterranean electrotechnical conf, p. 758–61.

Boukenoui R., Salhi H., Bradai R., Mellit A. (2016). A new intelligent MPPT method for stand-alone photovoltaic systems operating under fast transient variations of shading patterns. Solar Energy, 124:124–142.

Bratton D., Kennedy J. (2007). Defining a standard for particle swarm optimization, *Proceedings of the 2007 IEEE Swarm Intelligence Symposium*, 120 - 127.

Burke EK, Kendall G (2005). Search methodologies: Introductory Tutorials in Optimization and Decision Support Techniques. New York: Springer-Verlag.

Cacciato M, Consoli A, Attanasio R, Gennaro F (2010). Soft-switching converter with HF transformer for grid-connected photovoltaic systems. IEEE Trans Ind Electron, 57(5):1678–86.

Carrano EG, Guimarães FG, Takahashi RH, Neto OM, Campelo F (2007). Electric distribution network expansion underload-evolution uncertainty using an immune system inspired algorithm. IEEE Trans Power Sys,22:851–61.

Chandel SS, Aggarwal RK, Pandey AN (2005). New correlation to estimate global solar radiation on horizontal surfaces using sunshine hour and temperature data for Indian sites. Journal of Solar Energy Engineering, 127 (3):417–20.

Chang Y (2010). Optimal the tilt angles for photovoltaic modules using PSO method with nonlinear time-varying evolution. Energy, 35:1954–63.

Charniak E, McDermott D (1985). Introduction to artificial intelligence. Reading, MA: Addison Wesley.

Chee Wei T, Green TC, Hernandez-Aramburo CA (2007). A current mode controlled maximum power point tracking converter for building integrated photo- voltaics. In: Proceedings of European conference on power electronics and applications.

Chelouah R, Siarry P (2005). A hybrid method combining continuous tabu search and Nelder–Mead simplex algorithms for the global optimization of multi minima functions. Eur.J.Oper.Res, 161:636–54.

Chen LR, Tsai CH, Lin YL, Lai YS (2010). A biological swarm chasing algorithm for tracking the PV maximum power point. IEEE Trans Energy Convers, 25:484–93.

Chen YM, Lee CH, Wu HC (2005). Calculation of the optimum installation angle for fixed solar-cell panels based on the genetic algorithm and the simulated annealing method.IEEE Trans Energy Conversion, 20 (2):467–73.

Chen Z (2000). Computational intelligence for decision support. Boca Raton, FL: CRC Press.

Chian-Song C (2010). T–S fuzzy maximum power point tracking control of solar power generation systems. IEEE Trans Energy Convers, 25:1123–32.

Cho B.J., Hong S.C., Okoma S. (1996). Job shop scheduling using genetic algorithm, Proceedings of the Third World Congress on Expert Systems, Seoul, Korea, February, pp. 351–358.

Chowdhury SR, Saha H (2010). Maximum power point tracking of partially shaded solar photovoltaic arrays. Sol Energy Mater Sol Cells, 94:1441–7.

Čongradac V, Prica M, Paspalj M, Bojanič D, Čapko D (2012). Algorithm for blinds control based on the optimization of blind tilt angle using a genetic algorithm and fuzzy logic. Solar Energy, 86:2762–70.

Cuevas E., Oliva D., Zaldivar D., Perez-Cisneros M., Sossa H. (2012). Circle detection using electro-magnetism optimization, Information Sciences,182(1)40–55.

D'Souza NS, Lopes LAC, Liu X (2005). An intelligent maximum power point tracker using peak current control. In:Proceedings of 36th annual IEEE power electronics specialists conference, p.172–7.

Daraban S,Petreus D,Morel C (2014). A novel MPPT (maximum power point tracking) algorithm based on a modified genetic algorithm specialized on tracking the global maximum power point in photovoltaic systems affected by partial shading Energy.

Davis L. (1991). Handbook of Genetic Algorithms. Van Nostrand, New York, NY.

De Carvalho PCM, Pontes RST, Oliviera Jr DS, Riffel DB, De Oliviera RGV, Mesquita SB (2004). Control method of a photovoltaic powered reverse osmosis plant without batteries based on maximum power point tracking. In: Proc IEEE PES transmiss distrib conf & expo. Latin, America, p. 137–42.

Deepak Verma, Savita Nema, A.M. Shandilya, Soubhagya K. Dash (2016). Maximum power point tracking (MPPT) techniques: Recapitulation in solar photovoltaic systems. Renewable and Sustainable Energy Reviews 54 :1018–1034.

Demain C, Journée M, Bertrand C (2013). Evaluation of different models to estimate the global solar radiation on inclined surfaces. Renewable Energy, 50:710–21.

Deyi L, Yi D (2007). Artificial intelligence with uncertainty. first ed. London: Chapman & Hall/CRC.

Di Piazza MC, Vitale G (2012). Photovoltaic field emulation including dynamic and partial shadow conditions. Appl Energy, 87:814–23.

Dorigo M. (1992). Optimization, Learning and Natural Algorithms (PhD thesis) Politecnicodi Milano, Italy.

Dorigo M., Stützle T. (2004). Ant Colony Optimization, Bradford books, Cambridge, MA.

Drake P.R., Choudhry I.A. (1997). From apes to schedules, Manuf. Eng. 76:43 45.

Eberhart RC, Shi Y (2001). Tracking and optimizing dynamic systems with particle swarms. IEEE International Conference on Evolutionary Computation , 94–100.

El-Sebaii AA, Al-Hazmi FS, Al-Ghamdi AA, Yaghmour SJ (2010). Global, direct and diffuse solar radiation on horizontal and tilted surfaces in Jeddah, Saudi Arabia.Applied Energy, 87:568–76.

El-Tamaly HH, Elbaset MA (2006). Impact of interconnection photovoltaic/ wind system with utility on their reliability using a fuzzy scheme. Renew Energy, 31:2475–91.

Esram T, Kimball JW, Krein PT, Chapman PL, Midya P (2006). Dynamic maximum power point tracking of photovoltaic arrays using ripple correlation control. IEEE Trans Power Electron, 21:1282–91.

Esram Trishan, Chapman Patrick L (2007). Comparison of photovoltaic array maximum power point tracking techniques. IEEE Trans Energy Convers, 22 (2):439–49.

Fangrui L,et al (2008). A variable step size INCMPPT method for PV systems. IEEE Transactions on Industrial Electronics, 55(7):2622–8.

Femia N, Petrone G, Spagnuolo G, Vitelli M (2005). Optimization of perturbs and observe maximum power point tracking method. IEEE Trans Power Electron, 20(4):963–73.

Filipovi´c V. (2011). An electromagnetism metaheuristic for the uncapacitated multiple allocation hub location problem, Serdica Journal on Computing 5(3):261–272.

Filipovic, V., Kartelj, A., Matic, D. (2013). An electromagnetism metaheuristic for solving the Maximum Betweenness Problem. *Applied Soft Computing,* 13: 1303 1313.

Floudas, C. A., & Gounaris, C. E. (2009). A review of recent advances in global optimization. *Journal of Global Optimization*, *45,* 3–38.

Forrest S. (1993). Genetic algorithms: principles of natural selection applied to computation, Science, 261:872–878.

Gholamalizadeh, E., Kim, M.H. (2014). Thermo-economic triple-objective optimization of a solar chimney power plant using genetic algorithms. *Energy,* 70:204 211.

Glover F, Laguna M (1997). Tabu search. Boston:Kluwer Academic Publishers.

Goldberg D.E. (1989). Genetic Algorithms in Search, Optimisation and Machine Learning. Addison Wesley, Reading, MA.

Goldberg D.E., Holland J.H. (1988). Genetic algorithms and machine learning, Mach. Learn,3:95–99.

Haas A (1995). The value of photovoltaic electricity for society. Sol Energy, 5(4):25–31.

Hadavandi E. (2010). Developing a time series model based on particle swarm optimization for gold price forecasting, Proceedings of the Third International Conference on Business Intelligence and Financial Engineering, IEEE press, New York, NY, pp. 337–340.

Hadjer Bounechba, Aissa Bouzid, Hamza Snani, Abderrazak Lashab (2016). Real time simulation of MPPT algorithms for PV energy system. Electrical Power and Energy Systems, 83:67–78.

Han X, Wang Y, Zhu L (2011). Electrical and thermal performance of silicon concentrator solar cells immersed in dielectric liquids. Appl Energy, 88(12):4481–9.

Hart GW, Branz HM, Cox CH (1984). Experimental tests of open-loop maximum power- point tracking techniques. Sol Cells, 13:185–95.

Hashimoto O, Shimizu T, Kimura G (2000). A novel high performance utility interactive photovoltaic inverter system. In:Proceedings of conference record of 2000 IEEE industry applications conference, p.2255–60.

Herna´ deza JCN, Medinaa A, Juradob F (2007). Optimal allocation and sizing for profitability and voltage enhancement of PV systems on feeders. Renew Energy, 32:1768–89.

Hiren Patel, Vivek Agarwal (2008). Maximum power point tracking scheme for PV systems operating under partially shaded conditions. IEEE Trans Ind Electron, 55(4):1689–98.

Hiyama T, Kouzuma S, Imakubo T, Ortmeyer T (1995). Evaluation of neural network based real time maximum power tracking controller for PV system. IEEE Trans Energy Convers, 10:543–8.

Holland J.H. (1975). *Adaptation in Natural and Artificial Systems*. The University of Michigan Press, Ann Arbor, MI.

Ioulia T, Purvins PA (2012). Mathematical and graphical approach for maximum power point modeling. Appl Energy, 91:59–66.

Irisawa Kei, Saito Takeshi, Takanolchiro, Sawada Yoshio (2000). Maximum power point tracking control of photovoltaic generation system under non-uniform insolation by means of monitoring cells. In:Proceedings of the IEEE conference on photovoltaic specialist, p.1707–1710.

Ishaque K, Salam Z (2013). A deterministic particle swarm optimization maximum power point tracker for photovoltaic system under partial shading condition. IEEE Trans Ind Electron, 60:3195–206.

Ishaque K, Salam Z, Amjad M, Mekhilef S (2012). An improved particle swarm optimization (PSO)–based MPPT for PV with reduced steady-state oscillation. IEEE Trans Power Electron, 27:3627–38.

Ishaque K, Salam Z, Shamsudin A, Amjad M (2012). A direct control based maximum power point tracking method for photovoltaic system under partial shading conditions using particle swarm optimization algorithm. Appl Energy, 99:414–22.

Ishaque K, Salam Z, Taheri H (2011). A comprehensive MATLAB Simulink PV system simulator with partial shading capability based on two-diode mode. Sol Energy, 85:2217–27.

Jainand S, Agarwal V (2004). A new algorithm for rapid tracking of approximate maximum power point in photovoltaic systems. IEEE Power Electron Lett, 2(1):16–9.

Jianga LL, Maskell DL, Patra JC (2013). A novel ant colony optimization-based maximum power point tracking for photovoltaic systems under partially shaded conditions. Energy Build, 58:227–36.

Jie L, Ziran C (2011). Research on the MPPT algorithms of photovoltaic system based on PV neural network. In: Chinese control and decision conference.

Jinbang X, Shen A, Yang C, Rao W, Yang X (2011). ANN based on IncCond algorithm for MPP tracker. In: Bio-inspired computing: theories and applications (BIC-TA). Sixth international conference on, p. 129–34.

Joyce A, Rodriguesa C, Mansob R (2001). Modelling PV system. Renew Energy, 22:275–80.

Junjie MA, Yulong W, Yang L. Size and location of distributed generation in distribution system based on immune algorithm (2012). Syst Eng Procedia, 4:124–32.

Kalogirou SA (2003). Artificial intelligence for the modeling and control of combustion processes: a review. Prog Energy Combust Sci, 29:515–66.

Kalogirou SA (2007). Artificial intelligence in energy and renewable energy systems, Nova Publisher, [Chapters 2 and 5].

Kamejima T, Phimmasone V, Kondo Y, Miyatake M (2011). The optimization of control parameters of PSO based MPPT for photovoltaics. In:Proceedings of the IEEE ninth international conference on power electronics and drive systems (PEDS), p.881–3.

Karatepe E, Boztepe M, Colak M (2006). Neural network based solar cell model. Energy Convers Manage, 47:1159–78.

Karatepe E, Hiyama T, Boztepe M, Colak M (2008). Voltage based power compensation system for photovoltaic generation system under partially shaded insolation conditions. Energy Convers Manag, 49:2307–16.

Kasa N,Iida T, Chen L (2005). Fly back inverter controlled by sensor less current MPPT for photovoltaic power system. IEEE Transactions on Industrial Electronics, 52(4):1145–52.

Kennedy J., Eberhart R.C. (1995). Particle swarm optimization, Proceedings of the IEEE International Conference on Neural Networks, vol.4, IEEE press, p.1942–1948.

Keyrouz F, Hamad M, Georges S (2012). Bayesian fusion for maximum power output in hybridwind-solarsystems. In: Proceedings of the 2012 3rd IEEE international symposium on power electronics for distributed generation systems (PEDG), p.393–97.

Keyrouz F,Georges S (2011). Efficient multidimensional maximum power point tracking using Bayesian fusion. In:Proceedings of the 2011 2nd international conference on electric power and energy conversion systems(EPECS), p. 1–5.

Khaehintung N, Wiangtong T, Sirisuk P. (2006) FPGA Implementation of MPPT using variable step-size P&O algorithm for PV applications. In: Proceedings of the IEEE International Conference on ISCIT; 2006. p. 212–215.

Kilic O, Nguyen QM (2010). Application of artificial immune system algorithm to electromagnetics problems. Prog Electro Res, 20:1–17.

Kim IS (2006). Sliding mode controller for the single-phase grid-connected photovoltaic system. Appl Energy, 83:1101–15.

Kim Y, Jo H, Kim D (1996). A new peak power tracker for cost-effective photovoltaic power system. In:Proceedings of 31st intersociety energy conversion engineering conference, p.1673–8.

Kitano T, Matsui M, Xu DH (2001). Power sensor-less MPPT control scheme utilizing power balance at DC link-system design to ensure stability and response. In: Proc 27th annual conf IEEE Indust Electron Soc, p. 1309–14.

Kobayashi K, Takano I, Sawada Y (2003). A study on a two stage maximum power point tracking control of a photovoltaic system under partially shaded irradiance conditions. IEEE Power Eng Soc Gen Meet, 2612–7.

Kobayashi K. Matsuo H, Sekine Y (2004). A novel optimum operating point tracker of the solar cell power supply system. In: 35th Power electron spec conf, vol. 3, p. 2147–51.

Kolb, D. (1984). Experiential learning. Prentice-Hall, Englewood Cliffs, NJ.

Konar A (1999). Artificial intelligence and soft computing behavioural and cognitive modeling of the human brain. Boca Raton, FL: CRC Press, [Chapter 1].

Koutroulis E, Kalaitzakis K, Voulgaris NC (2001). Development of a microcontroller based photovoltaic maximum power point tracking control system. IEEE Trans Power Electron, 16(21):46–54.

Koutroulis E, Kolokotsa D, Potirakis A, Kalaitzakis K (2006). A methodology for optimal sizing of stand-alone photovoltaic/wind generator systems using genetic algorithms. Sol Energy, 80: 1072–88.

Krebs FC (2009). Fabrication and processing of polymer solar cells: a review of printing and coating techniques. Sol Energy Mater Sol Cells, 93(4):394–412.

Krishnamoorthy CS, Rajeev S (1996). Artificial intelligence and expert systems for engineers. LLC: CRC Press.

Kulaksız AA, Akkaya R (2012). A genetic algorithm optimized ANN-based MPPT algorithm for a stand-alone PV system with induction motor drive. Solar Energy, 86:2366–75.

Kumar Kollimalla Sathish, Kumar Mishra Mahesh (2014). Variable perturbation size adaptive P&O MPPT algorithm for sudden changes in irradiance. IEEE Trans Sustain Energy, 5(3):718–28.

Kumar P., Jain, G., Palwalia, D.K. (2015). Genetic algorithm based maximum power tracking in solar power generation. 2015 International Conference on Power and Advanced Control Engineering (ICPACE), 1-6.

Kuo C. L., Chu C. H., Li Y., Li X. Y., Gao L. (2015). Electromagnetism-like algorithms for optimized tool path planning in 5-axis flank machining, *Computers & Industrial Engineering,* 84:70–78.

Kuo YC, Liang TJ, Chen JF (2001). Novel maximum-power-point-tracking controller for photovoltaic energy conversion system. IEEE Trans Ind Electron, 48(3):594–601.

Kuo Yeong-Chau, Liang Tsorng-Juu, Chen Jiann-Fuh (2001). Novel maximum power point tracking controller for photovoltaic energy conversion system. IEEE Trans Ind Electron, 48(3):594–601.

Larbes C, Aït Cheikh SM, Obeidi T, Zerguerras A (2009). Genetic algorithms optimized fuzzy logic control for the maximum power point tracking in photovoltaic system. Renew Energy, 34:2093–100.

Lee C. H. and Chang F. K. (2008). "Recurrent fuzzy neural controller design for nonlinear systems using electromagnetism-like algorithm," *Far East Journal of Experimental and Theoretical Artificial Intelligence*, vol. 1, no. 1, pp. 5-22.

Letting LK, Munda JL, Hamam A (2010). Particle swarm optimized TS fuzzy logic controller for maximum power point tracking in a photovoltaic system. In: IPEC, 2010 conference proceedings:IEEE, p.89–94.

Lin B, Miller DC (2004). Solving heat exchange network synthesis problem with tabu search. Comput.Chem.Eng, 28:1451–64.

Lin CH, Huang CH, Du YC, Chen JL (2011). Maximum photovoltaic power tracking for the PV array using the fractional-order incremental conductance method. Appl Energy, 88:4840–7.

Liu F, Kang Y, Zhang Y, Duan S (2008). Comparison of P&O and hill climbing MPPT methods for grid-connected PV generator. In:Proceedings of the 3rd IEEE conference on industrial electronics and application, p.3–5.

Liu YH, Huang SC, Huang JW, Liang WC (2012). A particle swarm optimization-based maximum power point tracking algorithm for PV systems operating under partially shaded conditions. IEEE Trans Energy Convers, 27:1027–35.

Luger GF, Stubblefield WA (1993). Artificial intelligence: structures and strategies for complex problem solving. Menlo Park, CA: Benjamin/ Cummings.

Marcelo Gradella Villalva JRG, Ernesto Ruppert Filho (2009). Analysis and simulation of the P&O Algorithm Using A Linearized PV array model. In:Proceedings of industrial electronics conference, IECON' 09, p.231–6.

Masoum MAS, Dehbonei H, Fuchs EF (2002). Theoretical and experimental analyses of photovoltaic systems with voltage and current-based maximum power-point tracking. IEEE Trans Energy Convers, 17(4):514–22.

Meissner M., Schmuker M., Schneider G. (2006). Optimized Particle Swarm Optimization (OPSO) and its application to artificial neural network training, BMC Bioinformatics 7.

Mellit A (2006). Artificial intelligence based-modelling for sizing of a standalone photovoltaic power system: proposition for a new model using neuro-fuzzy system (ANFIS). In: Proceedings of the third international IEEE conference on intelligent systems, UK, vol. 1, p. 605–11.

Mellit A (2006). Artificial intelligence techniques for sizing and simulation of photovoltaic system. PhD thesis, Faculty of electronics & computer sciences, USTHB (Algiers), Algeria.

Mellit A, Benghanem M, Hadj Arab A, Guessoum A (2003). Modeling of sizing the photovoltaic system parameters using artificial neural network. In: Proceedings of IEEE conference on control application, vol. 1, p. 353–7.

Mellit A, Benghanem M, Hadj Arab A, Guessoum A, Moulai K (2004). Neural network adaptive wavelets for sizing of stand-alone photovoltaic systems. In: Second IEEE international conference on intelligent systems, vol. 1, p. 365–70.

Mellit A, Kalogirou SA (2006). Application of neural networks and genetic algorithms for predicting the optimal sizing coefficient of photovoltaic supply (PVS) systems. In: Proceedings of the world renewable energy congress IX and exhibition, 19–25 August 2006, (on CD ROM).

Messai A, Mellit A, Guessoum A, Kalogirou S (2011). Maximum power point tracking using a GA optimized fuzzy logic controller and its FPGA implementation. Solar Energy, 85:265–77.

Midya P, Krein PT, Turnbull RJ, Reppa R, Kimball J (1996). Dynamic maximum power point tracker for photovoltaic applications. In: Proc 27th annu IEEE power electron spec conf, p. 1710–6.

Mitchell M. (1999). An introduction to Genetic Algorithms. Fifth ed., MIT Press.

Miyatake M, Veerachary M, Toriumi F, Fujii N, Ko H (2011). Maximum power point tracking of multiple photovoltaic arrays: a PSO approach. IEEE Trans Aerosp Electron Syst, 47:367–80.

Mohajeri HR, Moghaddam MP, Shahparasti M, Mohamadian M (2012). Development a new algorithm for maximum power point tracking of partially shaded photovoltaic arrays. In:Proceedings of the 2012 20th Iranian conference on electrical engineering (ICEE), IEEE, p.489–94.

Mohammad Faridun Naim T, Shahrin MA, Zainal S, Mohd Sazli S (2013). Evolutionary based maximum power point tracking technique using differential evolution algorithm.

Mohammadi N., Mirabedini S.J. (2014). Comparison of particle swarm optimization and back propagation algorithms for training feedforward neural network, J.Math. Computer Sci, 12:113–123.

Muhtazaruddin MN, Jamian JJ, Fujita G, Baharudin MA,Wazir MW, Mokhlis H (2014). Distribution network loss minimization via simultaneous distributed generation coordination with network reconfiguration. Arab J Sci Eng,39:1–11.

Naderi B., Tavakkoli-Moghaddam R., Khalili M. (2010). Electromagnetism-like mechanism and simulated annealing algorithms for flowshop scheduling problems minimizing the total weighted tardiness and makespan, *Knowledge-Based Systems*, 23:77–85.

Naji-Azimi Z., Toth P., Galli L. (2010). An electromagnetism metaheuristic for the unicast set covering problem, European Journal of Operational Research, 205(2):290–300.

Nearchou A.C., Aspragathos N.A. (1997). A genetic path planning algorithm for redundant articulated robots, Robotica 15:213–224.

Neto, R.F.T., & Filho, M.G. (2013). Literature review regarding Ant Colony Optimization applied to scheduling problems: Guidelines for implementation and directions for future research. *Engineering Applications of Artificial Intelligence, 26,* 150–161.

Newell A, Shaw JC, Simon HA (1963). Empirical explorations with the logic theory machine: a case study in heuristics. In: Feigenbaum EA,Feldman J, editors. Computers and thought. New York: McGraw-Hill.

Ngan Mei Shan, Tan Chee Wei (2011). A study of maximum power point tracking algorithms for stand-alone photovoltaic systems. In:Proceedings of 2011 IEEE applied power electronics colloquium(IAPEC), p.22–7.

Nilsson N (1998). Artificial intelligence: a new synthesis. Los Altos, CA: Morgan Kaufmann.

Nocedal J., Wright S.J. (2000). Numerical Optimization,seconded.,Springer.

Noguchi T, Togashi S, Nakamoto R (2000). Short-current pulse based adaptive maximum power point tracking for photovoltaic power generation system. In: IEEE Int Symp Indust Electron, p.157–62.

Noh HJ, Lee DY, Hyun DS (2002). An improved MPPT converter with current compensation method for small scaled PV-applications. In: Proc 28th annu conf Indust Electron Soc, p.1113–8.

Ohsawa Y, Emurd S, Arai K (1993). Optimal operation of photovoltaic/ diesel power generation system by neural network. In: Proceedings of the second international forum on applications of neural networks to power systems, ANNPS 93.

Pan CT, Chen JY, Chu CP, Huang YS (1999). A fast maximum power point tracker for photovoltaic power systems. In: Proc 25th annu conf IEEE ind electron soc, p. 390–3.

Papadimitriou C.H. and Steiglitz K. (1998). Combinatorial Optimization: Algorithms and Complexity. Dover, New York.

Parida B, Iniyan S, Goic R (2011). A review of solar photovoltaic technologies. Renew Sust Energy Rev, 15:1625–36.

Patcharaprakiti N, Premrudeepreechacharn S (2002). Maximum power point tracking using adaptive fuzzy logic control for grid-connected photovoltaic system. Power Eng Soc Winter Meet IEEE, 1:372–7.

Perez R, Reed R, Ho T (2004). Validation of a simplified PV simulation engine. Sol Energy, 77:357–62.

Petrone Giovanni, Spagnuolo Giovanni, Massimo Vitelli (2011). A multivariable perturb-and observe maximum power point tracking applied to a single-stage photovoltaic inverter. IEEE Trans Ind Electron, 58(1):76–83.

Pham D.T., Karaboga D. (1994). Some variable mutation rate strategies for genetic algorithms, Proceedings of IMACS International Symposium on Signal Processing, Robotics and Neural Networks (SPRANN '94), pp. 73–96.

Pham D.T., Yang Y. (1993). A genetic algorithm based preliminary design system, Proc. IMechE, Part D: J. Automobile Eng., 207:127–133.

Phimmasone V, Kondo Y, Kamejima T, Miyatake M (2011). Verification of efficacy of the improved PSO-based MPPT controlling multiple photovoltaic arrays. In: Proceedings of the 2011 IEEE ninth international conference on power electronics and drive systems (PEDS), p.1015–19.

Ramaprabha R, Gothandaraman V, Kanimozhi K, Divya R, Mathur BL (2011). Maximum power point tracking using GA-optimized artificial neural network for Solar PV system. In: 1st Int conf on elec energy sys IEEE, p. 264–8.

Ratnaweera A., Halgamuge S., Watson H.C. (2004). Self-organizing hierarchical particle swarm optimizer with time-varying acceleration coefficients, IEEE Trans. Evol. Comput, 8:240–255.

Rich E, Knight K (1996). Artificial intelligence. New York: McGraw-Hill.

Rosell JI, Ibanez M (2006). Modeling power output in photovoltaic modules for outdoor operating conditions. Energy Convers Manage,472424–30.

Rtiz-Rivera EI, Peng F (2004). A novel method to estimate the maximum power for a photovoltaic inverter system. In: Proc 35th annu IEEE power electron spec conf, p. 2065–9.

Russel S, Norvig P (1995). Artificial intelligence: a modern approach. Englewood Cliffs, NJ: Prentice-Hall.

Salam Z, Ahmed J, Merugu BS (2013). The application of soft computing methods for MPPT of PV system: a technological and status review. Appl Energy, 107:135–48.

Saravanan S, Ramesh Babu N (2015). Incremental conductance based MPPT for PV system using boost and SEPIC converter. ARPNJ Eng Appl Sci, 10(7):2914–9.

Saravanan S, Ramesh Babu N (2015). Performance analysis of boost and cuk converter in MPPT based PV system. In:Proceedings of the international conference on circuit, power and computer technology, p.1–6.

Schalkoff J, Culberson J, Treloar N, Knight B (1992). A world championship caliber checkers program. Artif Intell, 53(2–3):273–89.

Seals R.C., Whapshott G.F. (1994). Design of HDL programmes for digital systems using genetic algorithms, Artif. Intell. Eng., 9:331–338.

Senjyua T, Hayashia D, Yonaa A, Urasakia N, Funabashib T (2007). Optimal configuration of power generating systems in isolated island with renewable energy. Renew Energy, 32:1917–33.

Sera D, Teodorescu R, Rodriguez P (2007). PV panel model based on data sheet values. In: Proceedings of the IEEE international symposium on industrial electronics, p.2392–2398.

Seyedmahmoudian M., Horan B., Kok Soon T., Rahmani R., Muang Than Oo A., S. Mekhilef S., Stojcevski A. (2016). State of the art artificial intelligence-based MPPT techniques for mitigating partial shading effects on PV systems – A review. Renewable and Sustainable Energy Reviews 64, p 435–455.

Shaiek Y, Ben Smida M, Sakly A, Mimouni MF (2013). Comparison between conventional methods and GA approach for maximum power point tracking of shaded solar PV generators. Solar Energy, 90:107–22.

Shannon CE (1950). Programming a computer for playing chess. Philos Mag Series 7, 41:256 75.

Shi Y, Eberhart RC (1998). A modified particle swarm optimizer. IEEE International Conference on Evolutionary Computation, 69–73.

Shi Y, EberhartRC (1995). Empirical study of particle swarm optimization. IEEE International Conference on Evolutionary Computation, 1945–50.

Shmilovitz D (2005). On the control of photovoltaic maximum power point tracker via output parameters. IEE Proc Electr Power Appl, 239–48.

Shojaee, K.G., Behnam, M.T., Shakouri, H.G., & Rezaei, M. (2010). Enhancement of SA Algorithm by Intelligent Time Schedule. *Proceedings of the 29th Chinese Control Conference*, 1768-1774.

Simoes MG, Franceschetti NN, Friedhofer M (1998). A fuzzy logic based photovoltaic peak power tracking control. In: Proce of Indust Electron IEEE Int Symp, vol. 1, p. 300–5.

Sivanandam SN, Deepa SN (2008). Introduction to genetic algorithms. NewYork: Springer Verlag Berlin Heidelberg.

Solodovnik EV, Liu S, Dougal RA (2004). Power controller design for maximum power tracking in solar installations. IEEE Trans Power Electron, 19(5):1295–304.

Soon TeyKon, Mekhilef Saad (2014). Modified incremental conductance algorithm for photovoltaic system under partial shading conditions and load variation. IEEE Trans Ind Electron, 61(10):5384–92.

Storn R, Price K (1995). Differential evolution- a simple and efficient adaptive scheme for global optimization over continuous spaces:ICSI Berkeley.

Storn R, Price K (1997). Differential evolution – a simple and efficient Heuristic for global optimization over continuous spaces. J Global Optim, 11:341–59.

Su C., Lin H.(2011). Applying electromagnetism-like mechanism for feature selection, Information Sciences, 181(5):972–986.

Sugimoto H, Dong H (1997). A new scheme for maximum photovoltaic power tracking control. In: Proc IEEE power conv conf, p. 691–6.

Taheri H, Salam Z, Ishaque K (2010). A novel maximum power point tracking control of photovoltaic system under partial and rapidly fluctuating shadow conditions using differential evolution. In:Proceedings of the 2010 IEEE symposium on industrial electronics and applications (ISIEA),IEEE, p.82–7.

Tajuddin MFN, Ayob SM, Salam Z (2012). Tracking of maximum power point in partial shading condition using differential evolution(DE). Power Energy ((PECon)), 384–9.

Talebizadeha P, Mehrabiana MA, Abdolzadehb M (2011). Prediction of the optimum slope and surface azimuth angles using the Genetic Algorithm. Energy and Buildings, 43:2998-3005.

Tan Jian-Ding, Dahari Mahidzal, Koh Siaw-Paw, Koay Ying-Ying, Abed Issa Ahmed (2016). An improved electromagnetism-like algorithm for numerical optimization. Theoretical Computer Science 641:75–84.

Tawanda H (2000). A method for predicting long-term average performance of photovoltaic systems. Renew Energy, 21:207–29.

Teulings WJA, Marpinard JC, Capel A, O' Sullivan D (1993). A new maximum power point tracking system. In:Proceedings of the 24th annual IEEE conference on power electronics specialists PESC, p.833–38.

Tsou C. S., Kao C. H. (2007). Multi-objective inventory control using electromagnetism-like meta-heuristic, *International Journal of Production Research*, p. 1–16.

Valenciaga F, Puleston PF, Battaitto PE (2001). Power control of a photovoltaic array in a hybrid electric generation system using sliding mode techniques. Proc IEEE, 148(6):448–55.

Veerachary M, Senjyu T, Uezato K (2001). Maximum power point tracking control of IDB converter supplied PV system. In:IEEE proceedings of electric power applications, p.494–502.

Veerachary M, Senjyu T, Uezato K (2003). Neural-network-based maximum power-point tracking of coupled-inductor interleaved-boost-converter supplied PV system using fuzzy controller. IEEE Trans Ind Electron, 50(4):749–58.

Veerachary M,Yadaiah N (2000). ANN based peak power tracking for PV supplied DC motors. Solar Energy, 69:343–50.

Wang J.-C., Su Y.-L., Shieh J.-C., Jiang J.-A. (2011). High-accuracy maximum power point estimation for photovoltaic arrays. Sol. Energy Mater. Sol. Cells, 95:843 851.

Wilde P., Shellwat H. (1997). Implementation of a genetic algorithm for routing an autonomous robot, Robotica 15:207–211.

Winston PH (1994). Artificial intelligence. 2nd ed. Reading, MA: Addison-Wesley.

Wu G., Pedrycz W., Li H., Qiu D., Ma M., Liu J. (2013). Complexity reduction in the use of evolutionary algorithms to function optimization: a variable reduction strategy,Sci.World J, 1–8.

Wu TF, Yang CH, Chen YK, Liu R (1999). Photovoltaic inverter systems with self-tuning fuzzy control based on an experimental planning method. In: 34th indust app annu meet conf IEEE, vol. 3, p. 1887–94.

Wu Wenkai, Pongratananuku lN, Qiu Weihong, Rustom K, Kasparis T, Batarseh I (2003). DSP based multiple peak power tracking for expandable power system. In: Proceedings of the 18th Annual IEEE conference on applied power electronics, p.525–530.

Xiao Weidong, Dunford WG (2004). A modified adaptive hill climbing MPPT method for photovoltaic power systems. In:Proceedings of the IEEE 35th annual conference on power electronics specialists, p.1957-63.

Xiao Weidong, Dunford William G, Palmer Patrick R, Antoine Capel (2007). Application of centered differentiation and steepest descent to maximum power point tracking. IEEE Trans Ind Electron, 54(5):2539–49.

Yadav AK, Singh A, Azeem A, Rahi OP (2011). Application of simulated annealing and genetic algorithm in engineering application. International Journal of Advanced Engineering Technology, 1(2):81–5.

Yang X.-S. (2014). Nature-inspired Optimization Algorithms, Elsevier, London, UK.

Yang X.S., Deb S., Fong S. (2011). Accelerated particle swarm optimization and support vector machine for business optimization and applications, in: S. Fong (Ed.), Networked Digital Technologies. Proceedings of the Third International Conference NDT2011, Springer, Heidelberg, Germany, pp. 53–66.

Yi-Hua Liu, Jing-HsiaoChen, Jia-WeiHuang (2015). A review of maximum power point tracking techniques for use in partially shaded conditions. Renewable and Sustainable Energy Reviews, 41:436–453.

Yin F., Wang Y. N., Wei S. N. (2011). Inverse kinematic solution for robot manipulator based on Electromagnetism-like and modified DFP algorithms, *Acta Automatica Sinica*, 37:74-82.

Yu Shuhao, Zhu Shenglong, MaYan, Mao Demei (2015). A variable step size firefly algorithm for numerical optimization. Applied Mathematics and Computation, 263:214–220.

Yua S. H., Zhu S. L., Y. Ma, Mao D. M. (2015). A variable step size firefly algorithm for numerical optimization, *Applied Mathematics and Computation*, 263:214 220.

Zahedi A (2006). Solar photovoltaic (PV) energy; latest developments in the building integrated and hybrid PV systems. Renew Energy, 31:711–8.

Zhang L, Al-Amoudi A, Bai Y (2000) . Real-time maximum power point tracking for grid-connected photovoltaic systems. In:Proceedings of the 8th international conference on power electronics variable speed drives, p.124–129.

Zhang M, Wu J, Zhao H (2004). The application of slide technology in PV maximum power point tracking system. In: Proc 5th world congr intell contr automat, p. 5591–4.

Zhang Y., Duan S., Liu F., Kang Y. (2008). Comparison of p&o and hill climbing mppt methods for grid-connected pv converter,. *IEEE 3rd conference on Transaction on Industrial Electronics and Applications*,p. 804–807.

Zimmermann H-J, Tselentis G, Van Someren M, Dounias G. (2001). Advances in computational intelligence and learning: methods and applications. Dordrecht: Kluwer Academic.

## LIST OF PUBLICATIONS

1. Tan J.D., Dahari M., Koh S.P., Koay Y.Y., Abed I.A. (2016). An improved electromagnetism-like algorithm for numerical optimization. *Theoretical Computer Science*, 641: 75–84. *(ISI Listed) (Published)*
2. Tan J.D., Dahari M., Koh S.P., Koay Y.Y., Abed I.A. (2016). Analysis of the effect of search step size on the accuracy and convergence properties of electromagnetism-like mechanism algorithm. *Journal of Multiple Valued Logic and Soft Computing. (ISI Listed) (Accepted)*
3. Tan J.D., Dahari M., Koh S.P., Koay Y.Y., Abed I.A. (2016). A new experiential learning electromagnetism-like mechanism for numerical optimization. *Expert Systems with Applications. (ISI Listed) (Under review-Submitted Jan 08, 2016)*
4. Tan J.D., Dahari M., Koh S.P., Koay Y.Y., Abed I.A. (2016). Solar energy harvesting system optimization via electromagnetism-like search algorithm. *Engineering Applications of Artificial Intelligence*. *(ISI Listed) (Under review-Submitted April 16, 2016)*